Abstract

European mountain grasslands, which include also Alps, Apennines and Pyrenees, are subject to relatively fast changes in both human activities and climatic conditions. Their role in the biogeochemical cycles is still highly uncertain and unknown and, in addition, the European Mediterranean mountain areas are unique and under-represented study cases. Therefore, their knowledge can therefore introduce new avenues in the understanding of the whole grassland ecosystem.
Remote sensing techniques appear as very useful tools in assessing and predicting productivity, quantity and quality of grassland over larger areas, whit higher temporal resolutions and lower cost than traditional methods of grassland sampling.
In this study we analyzed the biometric parameters of three different land uses of the Mediterranean grassland of Amplero (Abruzzo region, Italy): meadow (managed by harvesting and grazing that is the typical management in Amplero and in Appenines areas), natural (areas to exclude all external impacts) and pasture (used for animal grazing). Aim of this study has been the evaluation of the potentiality of remote sensing in the prediction or of biometric parameters, such as biomass and its partitioning, and LAI or Net Primary Productivity (NPP) and carbon fluxes (Net Ecosystem Exchange, NEE; Gross primary productivity, GPP) of a Mediterranean grassland. For this reason, we applied the following independent approaches: agronomic destructive sampling inventory, hyperspectral radiometric measurements, satellite images processing and micrometeorological methods.
We note that different management activities cause a broad variation in biomass dynamics. Cutting/harvesting and grazing have the same effects on the ecosystem reducing the quantity of available herbage and blocking the grassland growth. The effect of management on biomass quantity and quality can be detected by hyperspectral indexes and its relationships with investigated biometric parameters. Moreover, these relationships change also as consequence of growing vegetation phase and for this reason can be performed for analyzing the vegetation phenological status and characteristics of each type of managements present in the whole grassland area of Amplero. Finally, the estimation of GPP using radiometric methods it is possible to predict this variable both continuously and locally by CNR1 radiometer both discontinuously but on a larger area by MODIS images.

Riassunto

Le praterie montane europee, che includono il territorio delle Alpi, degli Appennini e dei Pirenei, sono soggette a cambiamenti relativamente veloci legati alle attività antropiche e alle condizioni climatiche. Il loro ruolo nei cicli biogeochimici è ancora molto incerto e poco conosciuto e, in più, esistono pochi casi di studio che riguardano le praterie montane mediterranee. Lo studio delle praterie mediterranee, dunque, potrebbe introdurre nuove informazioni sullo studio dell'intero ecosistema.
Le tecniche di telerilevamento consentono di ottenere informazioni sulla produttività, sulla qualità e sulla quantità delle coperture vegetali con un'ampia risoluzione spaziale e temporale ed a costi relativamente contenuti rispetto ai metodi tradizionali, basati sui rilievi di campo.
In questo studio sono stati analizzati i parametric biometrici di tre differenti tipologie d'uso del suolo presenti nella prateria mediterranea di Amplero (Regione Abruzzo, Italia): *meadow* (sfalciato), *natural* (prateria indisturbata che non viene nè pascolata nè sfalciata) e *pasture* (pascolo) con l'obbiettivo di indagare le potenzialità del telerilevamento nel predire sia i parametri biometrici, come la biomassa, il contenuto di biomassa viva e morta e il LAI, sia la

produttività primaria netta (NPP) e i flussi di carbonio (NEE, GPP) di questo ecosistema. A tale scopo abbiamo applicato i seguenti approcci indipendenti: campionamento distruttivo, misure radiometriche iperspettrali e multispettrali, elaborazioni d'immagini da satellite e metodo micrometeorologico.
I risultati mostrano che i diversi utilizzi della prateria portano variazioni abbastanza ampie nella dinamica della biomassa della vegetazione. Il taglio, l'asportazione dell'erba e il pascolamento riducono la quantità di biomassa erbacea disponibile e bloccano la crescita della prateria. L'effetto dell'uso del suolo sulla quantità e qualità della biomassa può essere investigato utilizzando gli indici di vegetazione e le loro relazioni con i parametri biometrici misurati direttamente in campo. Queste relazioni, inoltre, sono strettamente legate alla fase di crescita della vegetazione e possono quindi essere utilizzate per analizzare lo stato fenologico della vegetazione e le caratteristiche della copertura vegetale dei diversi tipi di gestione presenti in tutta l'area di Amplero. Infine, utilizzando i metodi radiometrici è possibile predire il valore della GPP sia in maniera continua e locale con il radiometro CNR1 sia in maniera discontinua (per esempio ogni sedici giorni) ma su aree ampie con le immagini NDVI-MODIS.

DIPARTIMENTO DI SCIENZE DELL'AMBIENTE FORESTALE E DELLE SUE RISORSE

CORSO DI DOTTORATO DI RICERCA IN

ECOLOGIA FORESTALE – XX CICLO

BIOMETRIC PARAMETERS AND FLUXES ESTIMATION IN MEDITERRANEAN MOUNTAINOUS GRASSLAND WITH REMOTE SENSING TECHNIQUES

Settore Scientifico Disciplinare – AGR/05

Dottorando: Manuela Balzarolo

Firma___________________________

Coordinatore: Prof. Paolo De Angelis

Firma _______________________________

Tutore: Prof. Riccardo Valentini

Firma _______________________________

Università degli Studi della Tuscia
Dipartimento di Scienze dell'Ambiente Forestale e delle sue Risorse (DISAFRI)
Via S. Camillo de Lellis, snc 01100 Viterbo

Corso di Dottorato di Ricerca in Ecologia Forestale
Coordinatore: Prof. Paolo De Angelis

Tesi di Dottorato di Ricerca in Ecologia Forestale (XX ciclo)
di: Manuela Balzarolo

Gennaio 2008

Alla mia famiglia

Index

Scientific background of the study

During the last decades, becoming responsible of the observed global warming, greenhouse gases (GHGs) and their role in the global biogeochemical cycles changes have received a relevant institutional attention (IPCC, 2000).

Nowadays, the major challenge of the ecologists is to quantify the exchange of the radiatively active trace gases between ecosystems and atmosphere and to analyze how biotic, abiotic and anthropogenic factors control this exchange (Aubinet *et al.*, 2000). Quantification and analysis of GHG exchange are necessary to understand not only the current exchange rates, but also to make hypothesis on the more probable effects of the climate and the land use changes and on the reactivity of several ecosystems.

Globally much interest has been given to forest ecosystems instead there are only few studies focused on the GHG budget at continental scale and less on the European grasslands. For this reason the potential contribute to the global warming of European grasslands is still highly uncertain.

Grassland ecosystems, as well as happens for all the other terrestrial ecosystems, contribute actively to these exchanges; they exchange CO_2, N_2O and CH_4 between atmosphere, soil and vegetation. Moreover the GHG fluxes of grasslands are strictly linked to their management (Soussana *et al.*, 2007). The influence of the human activities on these exchanges is well described by analyzing the flux changes in response to the different grassland managements. N_2O emitted by grassland soil is mainly due to the fertilization and animal waste system while CH_4 is produced by animals at grazing. Then the management strategies to reduce the GHG emissions of grassland ecosystem must focus on the preservation of grasslands and on adaptation of their management in order to maintain their delicate equilibrium.

From an economical and political point of view the political administrations of many countries have established a framework of negotiations aimed at reducing GHGs and to combating the risks linked to the increase of CO_2 and all GHG emissions displayed by the scientific community. This forum started by the Conference of UN Environment (also known as "Earth Summit") Rio in 1992 and, at the end of the negotiations (Earth Summit in 1992; Berlin in 1995; Genève in 1996; Kyoto in 1997; La Haye in 2000 and Marrakesh in 2001), the terrestrial biosphere was considered in two sections (3.3 and 3.4 sections) of the Kyoto Protocol (available at www.unfccc.de). In particular, Section 3.3 refers to the assimilation of the sources and the sinks of GHGs “resulting from human activities directly related to land use change and forestry activities, limited to afforestation, reforestation and deforestation since 1990".

According with the Kyoto Protocol, the European Community decided to limit and reduce their emission of GHGs between 2008 and 2012 by 8% as compared to 1990 and issues related to land use, land-use change and forestry are be considered for Kyoto Protocol implementation (IPCC 2000). For this reason, significant information on the carbon sequestration of forest ecosystems across Europe (e.g. EU projects EUROFLUX, CANIF, MEDEFLU and the flux network CarboEurope) and of non-forest ecosystems (CARBOMONT and the grassland section of CarboEurope) now is available.

This study falls into the CARBOMONT project (EVK2-CT2001-00125) that aimed at the monitoring of the effects of land-use change on the carbon cycle of European mountain grasslands. For analyzing ecological, socio-economic and political background conditions at the European mountain scale, this project carried out in thirteen study sites of European member states, Switzerland and the Newly Associated States. In order to determine the effect of land use changes in these areas analyses carbon sequestration and flux partitioning in differently managed non-forest ecosystems (meadows, pastures, dwarf shrub communities and abandoned areas) was carried out. Moreover this project focus on the supporting the use of proximal and remotely sensed data for scaling-up the field data for assessing the spatial distribution of land cover, LAI, phenology status NPP and CO_2 in the complex mountain grassland. The present research activity takes place in the research of the connection between the vegetation characteristics and remote sensing applications.

Grassland ecosystem and remote sensing applications

Net primary production (NPP), the rate of biomass production per area, is an important attribute of the ecosystems (Asner *et al.*, 2003, Paruelo *et al.*, 1997). It determines, for instance, the total amount of energy available for upper trophic levels. In order to make decisions on animal movements among pastures, forage storage, stocking densities, etc., range managers need accurate estimates of biomass at the paddock level and at relatively detailed temporal resolution. Using classic agronomic methods the clipping must be conducted during the peak of pasture growth season and the sampling mast be effectuated o previously the same uncut area or on different area with the same vegetation composition and in the same ecological conditions. Therefore, these methods of grassland monitoring are limited by the small areas, number of samples, infrequent measurements and are also time-consuming and costly (Li *et al.*, 1995). Remote sensing techniques appear as very useful tools in assessing and predicting changes in structure and functioning of ecosystems. Ground level remote sensing allows rapid evaluation of vegetation properties in a non-destructive way (Gamon *et al.*, 1999, Mutanga *et*

al., 2004). Moreover, remote sensing technology from airborne and satellite platforms provide information of vegetation status and composition in large areas. Many high spectral resolution reflectance vegetation indices have been proposed with the aim of monitoring biomass, phenology and physiological conditions of plants and canopies (Peñuelas *et al.*, 1998).
Few authors have applied remote sensing techniques to the problem of CO_2 fluxes estimation in grassland mountainous landscape. The remote sensing technologies could represent a new instrument available to ecologist and alpine-crops experts to support their chooses as recently exposed by several authors. Physical and physiological parameters of vegetation can be measured using particular instruments scheduled for the *Earth Observation* (EO) of remote sensing like radiometer (Hanna *et al.*, 1999, Jakomulska *et al.*, 2003). Mutanga *et al.* (2004) showed the possibility to make successful prediction of foliar quality using field spectroradiometry for the application of the approach using airborne sensors. The relationships based on plot-level measurements can be used to guide the development of larger, regional-scale models that would utilize satellite or aircraft data.
Whiting et al (Withing *et al.*, 1992) demonstrated that Net Ecosystem Exchange (NEE) of CO_2 flux at the tundra level could be predicted successfully using a spectral vegetation index, like NDVI (Normalized Difference Vegetation Index). Filella *et al.* (Filella *et al.*, 2004) applied these techniques to Mediterranean shrubland affected by warming and drought and demonstrated that remote sensing approach is useful for assessment of seasonal and annual changes in biomass and CO_2 uptake of this ecosystems.

Motivations and objectives of the thesis

In Europe grasslands cover more than 90 million ha of agricultural area that is about 22% of the EU-25 countries and represents an important economic and environmental resource; in Italy covers about 4.38 millions ha of the agricultural territory.
Grassland productivity is affected by fast changes due to anthropogenic activities and climatic conditions. Motivated by these changes in land management and climate, as well as the scarsity of long-term data on the carbon cycling in mountain grassland ecosystem, this study aims at quantifying the productivity and fluxes of a Mediterranean mountainous grassland. The location selected for the study was the grassland of Amplero (central Italy, Abruzzo Region) where activities were carried out over meadow (managed by harvesting and grazing that is the typical management in Amplero and in Appenines areas), natural (areas to exclude all external impacts) and pasture (used for animal grazing).

By means of different methodologies following specific aims are approached:

I. Assessment of net primary productivity of the different grassland landuses and its interaction with environmental conditions;

II. Estimation of grassland biometric parameters and productivity by remote sensing techniques at several spatial and temporal resolution at ground, tower and satellite levels;

III. Comparison of several radiometric sensors and definition of the most suitable sensor for estimating NDVI;

IV. Integration of eddy fluxes and remotely sensed data, collected at several temporal and spatial resolutions, by applying the correlation techniques.

Chapter I

Introduction

1.1 Mountainous Mediterranean grassland

The knowledge of grassland ecosystem dynamics is very important. As Soussana *et al.* suggest (Soussana *et al.*, 2007), these ecosystems provide a variety of goods and services to support flora, fauna, and human populations worldwide.

Globally grasslands cover around 40 % of the ice-free terrestrial surface (White *et al.*, 2000), but their role in the carbon cycle is currently poorly understood. This is mainly due to a less availability of data (Gilmanov *et al.*, 2007) compared to the wide supply of flux measurements of forest ecosystems (Baldocchi *et al.*, 2003). In addition, the European Mediterranean mountain areas are unique and under-represented study cases. The study of Mediterranean grassland can therefore introduce new avenues in the understanding of the whole ecosystem.

European grasslands cover more than 40% (90 million ha) of agricultural area and about 22% of the EU-25 territory (EEA, 2005), representing an important economic and environmental resource. The share of grassland on the total Unit of Agricultural Area (UAA) ranges from 1% in Baleares (Spain) to almost 100% in the region of Valle d'Aosta (Italy), it is high in alpine regions and relatively low in Sweden and Finland (Figure 1). In Italy grasslands cover totally 28.17 % of UAA, consisting of 4.38 millions ha (Table 1).

The grassland landscape and its productivity are linked to several factors such as human activities (harvesting, fertilization and irrigation), animal grazing and environmental conditions (precipitation, drought and snow cover duration). Principally human activities as harvesting, mowing and grazing, in the European mountainous grassland influence grassland carbon budget impacting on CO_2 plant assimilation and ecosystem respiration (Novick *et al.*, 2004). The removal of the above-ground plant mater by harvesting and grazing changes both soil temperature and moisture and, consequently, soil respiration. Fertilization changes available nutrients and the photosynthetic activities of plants, thus affecting the whole ecosystem respiration.

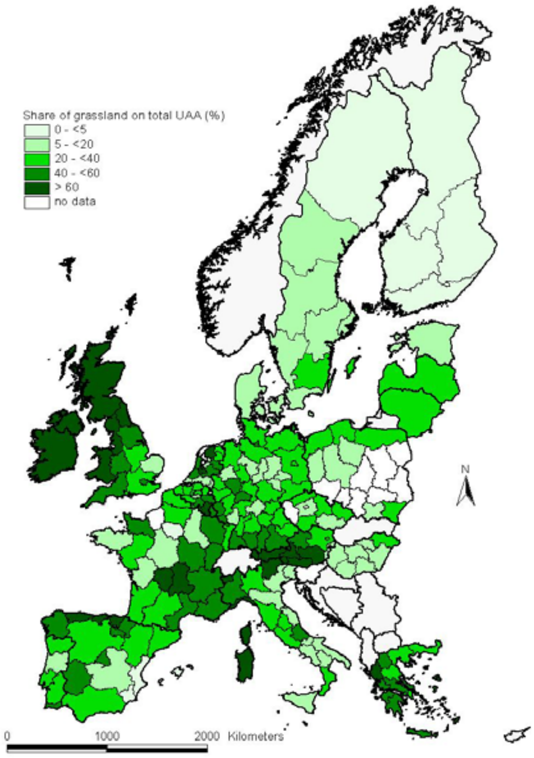

Figure 1 - Share of grassland on total UAA (in %) (data from EEA, 2005) in the European Community

Table 1 - Distribution of grassland in some European countries (in 1000 ha and % on UAA).

Country	GRASSLAND	
	in 1000 ha	in % on UAA
Finland	26.7	1.19
Greece	145.9	3.74
Denmark	186.4	6.97
Sweden	482.3	15.36
Italy	**4378.9**	**28.17**
Spain	7124.5	28.17
Germany	4969.6	29.28
France	9971.6	33.74
Portugal	1467.7	38.16
Belgium	536	38.49
Netherlands	891.9	45.75
Luxembourg	65	50.78
Austria	1917.4	56.84
UK	9905.8	60.58
Ireland	3193.4	73.04

Furthermore climatic conditions control the soil water availability and air humidity affecting CO_2 assimilation in arid, semi-arid (Hastings *et al.*, 2005) and temperate ecosystems (Baldocchi *et al.*, 1998, Novick *et al.*, 2004). For instance, leaves stomatal conductance is reduced by low soil moisture. Through its effect on enzyme kinetics, temperature is another abiotic factor influencing the assimilation of CO_2 in particular for high-latitude and high-elevation ecosystems.

European mountain grasslands, which include also Alps, Apennines and Pyrenees, are subject to relatively fast changes in both human activities and climatic conditions. The carbon cycle in the sub-arctic mountain grasslands of Europe seems to be affected by climate changes more than local human impact (IPCC *et al.*, 2000) while in the central European grasslands, also land management changes seem to affect the ecosystem structure and functionality (Cernusca *et al.*, 1999). Considering the EU agricultural politic and financing, these changes will become more important in the early future.

The climate in the Mediterranean grasslands (South Italy, Spain and Portugal) falls into the Mediterranean climate. This climate extends predominantly from 32°N to 40°S latitude in both the northern and southern hemispheres, and covers the Mediterranean basin of Europe, north Africa and west Asia, southern Australia, the southwest coast of the United States, central Chile and the Cape region of south Africa (Nahal *et al.*, 1981). The weather is characterized by warm/dry summers and mild/wet winters with rainfall occurring almost exclusively from November to February.

In the Mediterranean climate plant growth cycles depend on the rain distribution during the winter and the spring time (Xu *et al.*, 2004). The absence of precipitation during summer season gives rise to a long drought period that may have a negative effect on carbon plant assimilation and productivity caused by a reduction of photosynthetic rates and leaf surface.

In the last years, the frequency of both precipitation and drought changed dramatically in the whole Mediterranean basin. Two long term observations in the north-eastern inland of Spain and over the western Mediterranean confirmed this trend (Horcas *et al.*, 2001). Moreover, little changes or even increases of the day/night temperature differences have been highlighted in the last 130 years: daily maximum temperatures have been increased at larger rates compared to daily minimum temperatures. This differential warming rate increased during the second half of the 20th century leading a several damages on productivity of ecosystems and consequent a reduction of economical opportunities offered by different agricultural areas.

1.2 Grassland carbon stocks and distribution into pools

The importance of carbon pool assessment in terrestrial ecosystems is well known. Carbon stocks in the ecosystems are the key to understand the global carbon cycle. Generally, the long term carbon balance of grasslands has received little attention (Hui *et al.*, 2006, Jones *et al.*, 2004). Berninger *et al.* (2007, submitted) studied carbon balances and carbon stocks of 8 mountain grasslands eddy covariance sites and 22 sites with biomass data located in the European countries. Data used in this work were collected over a three-year period within the CARBOMONT project of the European Union 5th framework program (5FP). The carbon stocks in the analyzed grasslands were high and comparable to those of forest ecosystems, while carbon stocks in plant biomass is smaller (Berninger *et al.*, 2007 submitted). The carbon accumulation in the grassland ecosystems occurs mostly below the ground (Soussana *et al.*, 2004), where up to 98% of the total carbon stored can be sequestered in this compartment (Hungate *et al.*, 1997). About two-thirds of terrestrial carbon is below the ground and this pool generally has much slower turnover rates than aboveground carbon (Schlesinger *et al.*, 1977). Human activities, including harvesting of herbage, grazing and pasture management, influence the carbon stocks of grassland ecosystem. Therefore, the annual production of biomass in grassland can be large, but owing to the rapid turnover and the removals through the harvesting and grazing, the stock of aboveground biomass rarely exceeds a few ton per hectare. In addition, roots biomass and soil can accumulate large amounts of carbon but the detection of the changes of the stocks belowground is complicate. Mainly for such reason, methods based on flux measurements to assess carbon sequestrations of the grassland ecosystems are justified.

1.3 Hyperspectral proximal sensing

In the field of remote sensing the term “proximal” is used when the surface under investigation is few meters far from the detector or the spectrometer. In general proximal sensing techniques are used to validate remotely sensed data, as has been done in this study.

The term “hyperspectral” refers to those spectra made of a big number of narrow, continuously spaced spectral bands (Mutanga *et al.*, 2004) and is a synonym of spectroscopy, spectroradiometry and rarely ultraspectral (Clark *et al.*, 1999). Spectroscopy is a branch of physics concerned with the production, transmission, measurement and interpretation of electromagnetic radiation (Kumar *et al.*, 2002). Spectrometry (or spectroradiometry) derives from spectro-photometry, the “measure” of photons as a function of wavelength. Instruments used in this field are named spectroradiometers and have the same characteristic of FielSpec HH PRO® (ASD, Boulder -CO), the spectroradiometer employed in the study.

Ecological models and environmental studies require a wide range of input data, as well as data of biophysical vegetation characteristics, quality and quantity of biomass and its partitioning, leaf area index (LAI), and biochemical characteristics such as chlorophylls, carotenoids and nitrogen content. In addition to the strong necessity of high quality input data, available data from field observations are often inconsistent or totally absent. The low number of ground data necessary for both the initialization and the parameterization of models and the unknown uncertainty in their spatial distribution represent limiting factors for the application of ecological models at different scales and levels (local, regional or continental).

Quantitative remote sensing in a general, and imaging spectroscopy in a more deep level seem to be good techniques to fill the information gap explained before, to understand land-atmosphere carbon fluxes processes and to quantify and monitor plant photosynthesis needs of large areas and for long time periods (Field *et al.*, 1993). Recent studies have also been shown that biochemical and biophysical properties of vegetation can be measured with a quantifiable uncertainty that can be incorporated in the land-biosphere models (Ustin *et al.*, 2004a).

In general, the quantity of sun light that can be reflected or transmitted by leaves depends on biophysical plant properties such as the concentration of photosynthetic pigments (that capture sun light for photosynthesis), the water content, the dry plant matter and the leaf area index. During the growing season plant absorbs and reflects the solar light with different intensity. For instance, Rotondi *et al.*(2003) reported that the absorbance is reduced by pubescence, and that leaves appear more reflective after hairs have dried (Rotondi *et al.*, 2003). Ustin *et al.* confirmed that reflectance and transmittance change in predictable directions following alterations of properties of xeromorphic plant leaves (Ustin *et al.*, 2004a). In green leaves the photosynthetic pigments drive the light absorption in the visible (VIS, 400 - 700 nm) range of electromagnetic spectrum (Carter *et al.*, 1991) where there is a minimum of the absorption at 550 nm. On the contrary, elements that compound dry leaves like cellulose, lignin and other structural carbohydrates play a fundamental role in reflecting radiation in the near-infrared (NIR, NIR, 700 - 1100 nm) region, where the absorption by biochemical parties is minimal. In this range, the internal structure of leaves and the numbers of pores for water and air affect the reflectance and the absorption made by photosynthetic pigments. Indeed, if intercellular air spaces and cell sizes decrease, the reflectance, also named albedo, of the overall leaf declines. In the shortwave-infrared range (SWIR, 1100 - 2500 nm) the water content of green leaves give rise to a primary absorptions at 1450, 1940, and 2500 nm and to a secondary one at 980 nm and 1240 nm (Carter *et al.*, 1991).

In Remote Sensing vegetation indices (VIs) are calculated to quantify the rate of reflectance of a surface, like a foliar area. VIs can be obtained by simple mathematical equations starting from the reflectance values at the different wavelengths. Vegetation indices can also respond to slight changes in chlorophyll and carotenoid amounts and can thus provide an accurate estimate of seasonal changes in the photosynthetic plant activity.

The goodness of these remotely indices has been demonstrated in several scientific studies aimed to analyze biophysical properties of vegetation, biomass, Leaf Area Index (LAI), percentage of green vegetation cover, water, nitrogen and pigment contents and fluxes (Baret *et al.*, 1991, Becker *et al.*, 1988, Elvidge *et al.*, 1995, Gao *et al.*, 1996, Gianelle *et al.*, 2007, Gitelson *et al.*, 2004, Gitelson *et al.*, 2002, Huete *et al.*, 1998, Mutanga *et al.*, 2004, Pinty *et al.*, 1992, Tucker *et al.*, 1979, Turker *et al.*, 1979, Vescovo *et al.*, 2006).

The Normalized Difference Vegetation Index (NDVI) is one of the most common index; it is often proposed as a rapid, nondestructive and cost-effective means to estimate plant carbon gain over varied spatial and temporal scales (Field *et al.*, 1995). The Photosynthetic Reflectance Index (PRI), an index sensitive to changes in xanthophyll cycle pigments, was studied in depth by Gamon, Penuelas, and collaborators (Gamon *et al.*, 1992, Sims *et al.*, 1999). The Ratio Analisys of reflectance Spectra (RARS), a family of vegetation index, was developed by Chappel *et al.* in 1992, while Nagler *et al.* (Nagler *et al.*, 2000) studied the Cellulose Absorption Index (CAI).

Several studies have been shown that the relationships between vegetation indices and biomass, C/N ratio, canopy nitrogen concentration, leaf area index or water content is linear or logarithmic. The major limitation of the use of these relationships is the saturation of some indices at high values of biomass and soil background disturbance. The overlapping absorption features of plants and soils preclude direct assessment of many biogeochemical of interest. New biophysical methods that take into account the full spectral shape, including effects of one compound to the spectral absorption of another one, are needed to reduce uncertainty in their estimates. As a result, despite significant progress in understanding fundamental ecosystem processes and optical properties, more information are needed to get fully predictable quantitative methods.

1.4 Net primary productivity of grassland

Net Primary Productivity (NPP) represents the major input of carbon and energy into an ecosystem. In general, NPP is defined as the total photosynthetic gain less the respiratory losses, of vegetation per unit ground area. One of the main goal of ecosystem ecologists is the complete understanding of its spatial and temporal trends.

Nowadays, studies focused on the estimation of the NPP of grassland are few in the global existing data set. Moreover, the quality of data of NPP estimation from field biomass measurements is poor both at the spatial and the temporal scales (Scurlock *et al.*, 1998) for this reason processes of estimation, modeling of the global carbon cycle, validation and evaluation of the global NPP and carbon models are inhibited (Cramer *et al.*, 1999a, Scurlock *et al.*, 1999).
Several methods of estimation and modeling of NPP over large areas are reported in literature. Cramer *et al.*, in a study sponsored by the International Geosphere Biosphere Program (IGBP), compared the representation of NPP obtained with 17 terrestrial biosphere models (Cramer *et al.*, 1999a). Some of these models are based on complex ecological algorithms which link carbon, water and nutrient cycles, while others utilize as inputs remotely sensed data, such us satellite images (Goetz *et al.*, 1999). All models shown low productivity in dry or cold regions and high productivity in the humid tropical forests. Due to the not homogeneous and incomplete database of NPP field observations for the validation of each of these models, no one of them has been identified as the best representation of global NPP (Cramer *et al.*, 1999b).
Data obtained from satellite measurements are mainly used to provide information on vegetation conditions and to monitor changes in the leaf area index and in the canopy light absorption during the growing season. The linkage of remote sensing techniques and ecology provide a robust means to monitor short-term variations in photosynthetic capacity through limitations imposed by current light, moisture and nutrient regimes (Field *et al.*, 1995, Potter *et al.*, 1993). As shown by Sellers *et al.*, NPP of terrestrial vegetation can also be directly acquired from remotely sensed imagery through the observation of light absorption patterns (Sellers *et al.*, 1995). For this reason nowadays scientist are interested in studying the efficiency with which light absorbed by canopy is converted in dry matter or biomass.
Goward (Goward *et al.*, 1992) and Ruimy (Ruimy *et al.*, 1994) proposed that NPP could be estimated by a production efficiency approach based on the relationship between NDVI, or simple ratio (SR), and the fraction of the photosynthetic active radiation (fPAR) data (Asrar *et al.*, 1984, Baret *et al.*, 1991, Veroustraete *et al.*, 1996). This simplified approach, which employed fAPAR and radiation (or light) use efficiency (ε), has been widely used to estimate crop biomass, yield and NPP (Kumar *et al.*, 1981).
First comparison between NPP data obtained using global satellite and field measurements were carried out by the end of 2001 in the BigFoot project. From that moment global NPP at 1 km spatial resolution could be also operationally obtained starting from observations of the MODIS (Moderate Resolution Imaging Spectroradiometer) sensor (Justice *et al.*, 2002, Running *et al.*, 2004, Turner *et al.*, 2006). Since MODIS NPP is an annual value that provides a means for evaluating spatial patterns in productivity as well as inter-annual variation and long

term trends in biosphere behavior (Nemani *et al.*, 2003, Turner *et al.*, 2006), many studies employ these remotely sensed estimations as input for ecological models. However, the validation of MODIS NPP matching the 1-km resolution of the MODIS products with ground plot-scale measurements is an essential step to establish their utility (Morisette *et al.*, 2002, Turner *et al.*, 2004).

1.5 Fluxes estimation and remote sensing techniques

The direct measurements of mass and energy fluxes between vegetation and atmosphere is made by micrometeorological or eddy covariance based techniques (Aubinet *et al.*, 2000, Baldocchi *et al.*, 2003). Using these methods, it is possible to continuously monitor the net exchange of CO_2 between an ecosystem and the atmosphere (NEE), water vapor and sensible heat fluxes over a timescale range, which is typically 30 minutes.

The net exchange of CO2 between an ecosystem and the atmosphere (NEE) can be described in two alternative ways.

For a better understanding of carbon balance NEE may be defined as the difference of assimilatory uptake (A) and respiratory release (R_{leaf} + R_{root} + R_{heter}) of CO2 by the ecosystem:

$$NEP = -A + R_{leaf} + R_{root} + R_{heter}$$

Carbon can by released to the atmosphere by leaves (R_{leaf}), roots (R_{root}) and heterotrophic respiration (R_{heter}). Conventionally the positive sign denote release of carbon to the atmosphere.

Alternatively, looking at the dynamics of the total carbon stock (Ct), NEE can be calculated as:

$$NEE = NEE = \frac{\delta C}{\delta t} + E$$

where carbon is carbon density in an ecosystem, t is time, and E is the soil erosion rate. This last term of equation can be significant when there are the land use changes such as the convention from grassland to shrub land (Parizek *et al.*, 2002). In the whole study we refer to the first definition of NEE.

Carbon assimilation and allocation are principally controlled by the quantity and photosynthetic potential of above-ground plant matter, which identify the assimilation rate, and by environmental conditions that influence the photosynthetic plant activity. The photosynthetically active radiation (PPFD, 400-700 nm), providing the energy for the carboxylation of CO_2, drives the photosynthesis and is a major environmental variable that

affect/determines carbon assimilation at leaf level. In contrast, the quantity and quality of the incoming radiation affect CO_2 assimilation at canopy level. In addition, canopy structure as the foliar distribution concurs in the definition of the radiation available for photosynthesis (Gu *et al.*, 2002, De Pury and Farquhar, 1997). In optimal environmental conditions PPFD can explain s well in excess of 50 % of the variation in canopy-scale assimilation (Ruimy *et al.*, 1995).
Integrating NEE values over a given period (e.g. 30 minutes) we obtain the Net Ecosystem Productivity (NEP):

$$NEP = \int_{t_0}^{t_0+t} NEE dt$$

By definition, NEP has a positive value when the ecosystem sequesters carbon.
Quantifying the amount of carbon assimilated by photosynthesis the Gross Primary Productivity (GPP) is obtained as:

$$GPP = -\int_{t_0}^{t_0+t} (NEE - R_t - R_r - r_h) dt$$

The sum between R_t, R_r and R_h identifies the Ecosystem Respiration (R_{eco}). This index is generally calculated from temperature responses of the night-time NEE that, in the absence of the photosynthetic process, equals the CO_2 efflux to the atmosphere.
Using this method is therefore easy to sample a representative area for a studied ecosystem. On the contrary, the eddy method is limited when used for regional estimation and mapping of CO_2 fluxes, and is necessary to support this information with other data, including remotely sensed data.
Actually there are many studies aimed to integrate flux tower data and remote sensing for regional carbon budget research (Aalto *et al.*, 2004, Turner *et al.*, 2004).
As well as some recent publications highlight (Grace *et al.*, 2005, Inoue *et al.*, 2008), a new frontier of remote sensing techniques could be the analysis of biogeochemical cycles of carbon, water, and energy exchange between ecosystems and atmosphere. The integration of remote sensing and CO_2 flux data collected by eddy method could provide a more efficient mean for predicting carbon fluxes at global and regional levels. Remote sensing can also be applied at different radiometric spectral region like at optical, thermal, and microwave wavelengths; information acquired through these applications can be used together as input of ecological models (Field *et al.*, 1994). For instance, as reported above discussing about the estimation of

NPP, also for assessing GPP and predicting NEE, VI, or remotely sensed data,, approach can be employed as additional data of the landscape models (Li *et al.*, 2007, Wylie *et al.*, 2003).
The most important limitation to remote sensing and flux integration is the lack of spectral data at situ level; for this reason, the relationship between spectral indices and CO_2 flux measurements over homogenous ecosystems is not well studied (Peñuelas *et al.*, 2000). Nevertheless, NDVI, which has provided good results in predicting biophysical properties of vegetation and NPP, has also shown promising results in evaluating CO_2 fluxes and GPP estimation in grasslands and shrublands. Seen *et al.* found that there is a linear relationship between NEE and time-integrated NDVI (iNDVI) and that this relationship is influenced by their association to GPP (Seen *et al.*, 1995).
Mapping of CO_2 sources and sinks require an additional mapping of respiration since both gross productivity and ecosystem respiration do not automatically covary and respiration can be more relevant than GPP in the determination of CO_2 source and sink strengths (Valentini *et al.*, 2004). Although remotely sensed vegetation indices are more closely correlated with GPP, they can help estimate R components associated with autotrophic maintenance and growth R which are related to live biomass of the canopy (Li *et al.*, 2007) or GPP.

1.6 The study area: Amplero site

Research activities of the study were carried out in the Mediterranean mountain grassland of Amplero. This area is located in the centre of Italy, in particular in the Abruzzo region (41°54’17.8 N, 13°36’22.3 E), on a flat to gently south sloping (2-3%) area, at 884 m a.s.l. (Figure 2). The interest of this region is motivated by the lack of study case on Mediterranean mountain areas, characterized by a unique ecosystem and a strong sensitivity to global warming; additional information on their environmental mechanism will increase the general understanding of this environment and help the generation of global ecological studies and models.

In 2002, lead by the scarcity of long-term data on mountain grassland carbon cycling, European scientific community proposed the CARBOMONT project in order to quantifying pools and fluxes of this ecosystem. In June 2002 the Amplero site took place to this European network and in 2004 it was included in the CarboEurope-ip project.

Figure 2 - View of the whole grassland of the site of the Amplero, located in the Abruzzo region in the centre of Italy (41°54'17.8 N, 13°36'22.3 E).

1.6.1 Climate

According to the European climate classification (map available onhttp://dataservice.eea.europa.eu/dataservice), the climate in the Amplero area is alpine-Mediterranean (Figure 3).

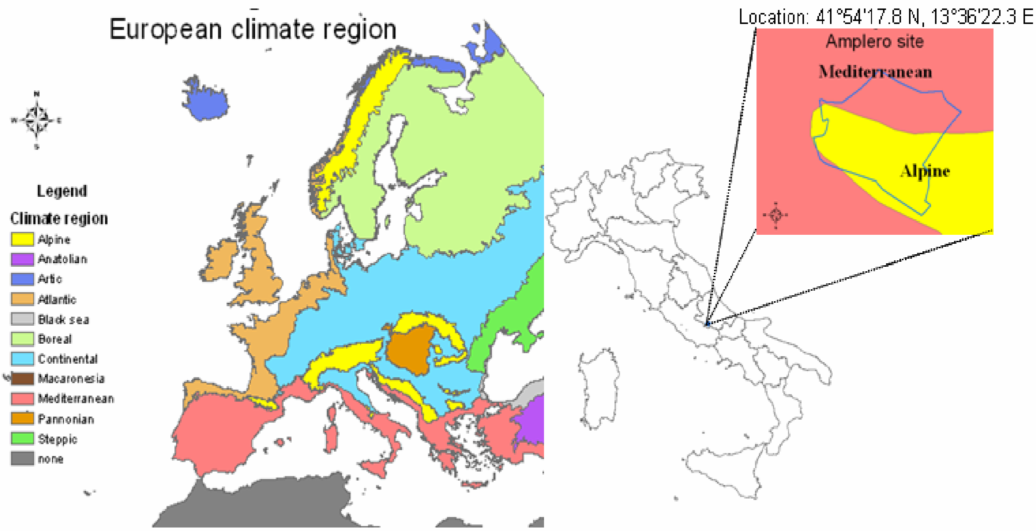

Figure 3 - Map of European climate classification.

Petriccione *et al.* (Petriccione *et al.*, 1993), it their study around the Amplero local scale, classified the climate of the site in the same way, as mountainous Mediterranean with no summer drought. Long-term mean annual precipitation is 1365 mm and annual mean temperature is 10°C (ARSSA local database).

During the time period our field campaign were carried out (2004, 2005 and 2006) the mean annual temperature was 8.5, 8.6 and 9.6 °C respectively and total annual precipitation was 1269, 681 and 742 mm, respectively (Figure 4). In particular, in 2004 and August 2006 there was a mild summer drought, while between June and September 2005 precipitation was absent, leading to a strong dry period that limited carbon grassland uptake and pasture re-growth after the cutting.

a)
b)
c)

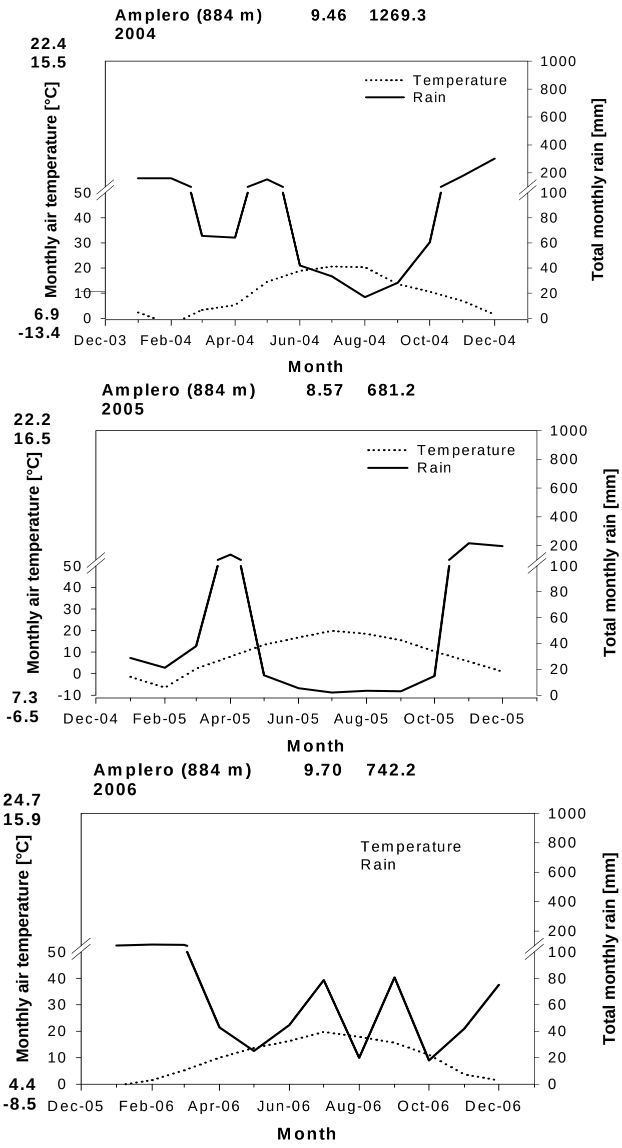

Figure 4 - Walter and Lieth diagram for 2004 (a), 2005 (b) and 2006 (c).

1.6.2 Grassland characteristics and management

Vegetation composition of the Amplero grassland was characterized during the field campaign in 2004. The study area is mainly composed of few dominant graminoids (Poa 15%), forbs (Trifolium 30%, Medicago 20%) and composites (Geranium 20%, Cerastium 20%).
The soil is poorly to a bit poorly drained, and it is defined as a Haplic Phaeozems (WRB, 2006). The humus type is Rhizomull (Green *et al.*, 1993). Soil depth is more than 1 m, and drainage ranges from poorly to imperfectly. The percentage of clays is 56% and pH is 6.5. Roots reach down to 15 cm and 90% of roots is fine.

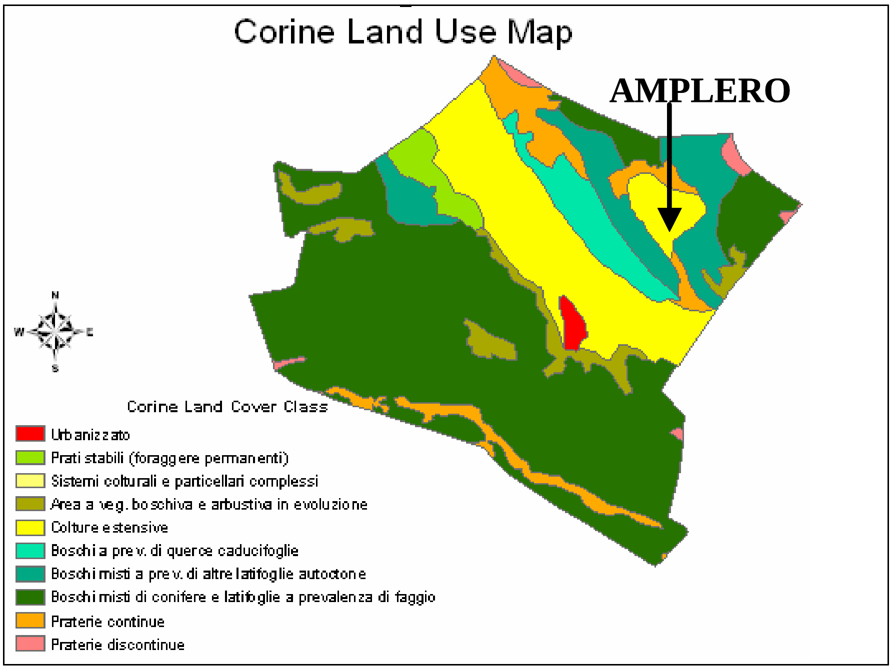

Figure 5 - Corine Land Use map (level IV)

According to the Corine Land Use classification (level IV), Amplero land use is extensive cropland; this classification includes managed grassland as well (Figure 5). Starting from the last 50 years, after been cultivated for some years, the area has been managed by a combination of cutting/harvesting and cattle grazing. The grass is nowadays cutted during the last week of June and later used for the cows, horses and donkeys grazing till the end of the year. Since grazing in the Amplero site is free it is difficult to calculate its precise impact of the area. The estimated stoking rate is around 0.3 animals per hectare each year. Comparing this value to the potential stoking rate of this pasture, it makes sense to hypnotizes that the grazing is extensive and that its effects are negligible on carbon balance.

The Amplero site is equipped with an eddy covariance tower for continuous measurements of CO_2 and H_2O. On the tower there are also all meteorological sensors for climate monitoring of the site. The entire/whole equipment (meteorological and eddy sensors) are briefly described in the material and method section (par. 2.7.2).

Chapter II

Materials and Methods

2.1 Set-up of the field work

The optimal use of radiometric measurements and of remote sensing imaging processing can be achieved through a complete and accurate set of field measurements support. For this reason, during the research study we planned to collect the following field data:

- ♣ Biometric sampling;
- ♣ Both periodic or in continuous radiometric measurements;
- ♣ Satellite image acquisitions;
- ♣ Meteorological and fluxes measurements.

During the field surveys, we analyzed three distinct grassland typologies present in the whole Amplero area (Figure 6):

- ♣ Meadow, managed by harvesting and grazing that is the typical management in Amplero;
- ♣ Natural, delimitated by fenced areas to exclude all external impacts (clipping/harvesting and grazing);
- ♣ Pasture, used for animal grazing.

Furthermore, all of our campaigns were conducted in order to evaluate the use of hyperspectral and multi-spectral sensors to retrieve biochemical and biophysical variables and fluxes. All field measurements were concentrated on two approaches: the first one, based on radiometric measurements performed to support the link between canopy reflectance and biometric parameters of the vegetation (biomass, live biomass, dead biomass, leaf area index), and the second one, performed by continuous measurements and images acquisition on vegetation to support grassland land use mapping and biometric and fluxes forecasting.

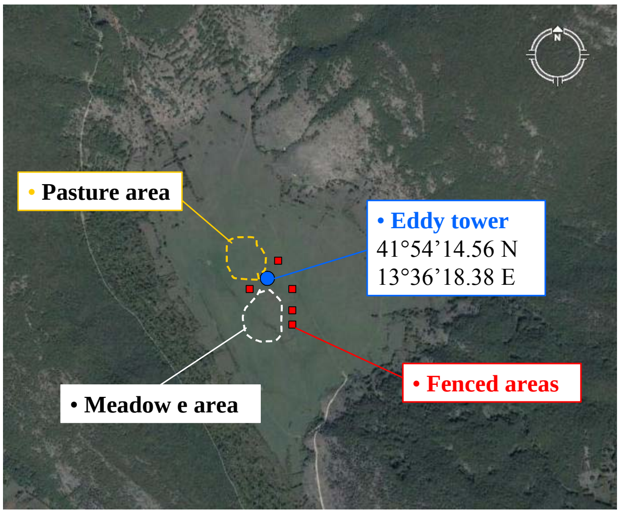

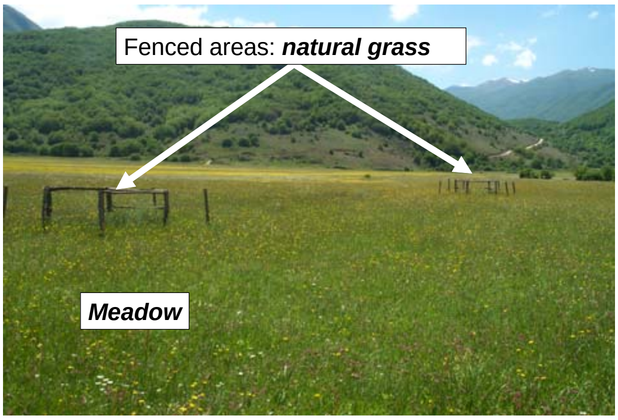

Figure 6 – In the upper part there is the satellite image of the study area of Amplero. The blue circle indicates the position of eddy station; yellow and white dashed areas represent pasture and meadow sampling areas, respectively, and red squares are fenced areas or rather natural plots. In the lower part there is a view of the fences.

2.2 Biometric measurements

In this study the aboveground biomass (AGB_{total}) refers to all collected plant material, including live biomass (AGB_{live}), dead standing biomass and litter. This latter two categories fall into a unique group, representing the total dead material on the grass (AGB_{dead}).

Operatively, the measure of the aboveground biomass of grass vegetation in the Amplero site was based on the measurements of phytomass increment during the growing season, obtained through field sampling in different small plots (Lauenroth *et al.*, 1986, Sala *et al.*, 1988). From 2004 to 2006,for each grassland typology (meadow, natural and pasture), 3 or 5 small squares of 0.30 m x 0.30 m were randomly collected at intervals of one month or less. The dry weight of the grassland biomass was determined by clipping the standing biomass at the ground level.

In order to determinate the total amount of dry matter per unit of area [g m^{-2} or t d.m. ha^{-1}], all clipped material (AGB_{total}) was sorted into the live leaves (AGB_{live}) and standing dead matter (AGB_{dead}), dried at 105°C for 48-72 h, and finally weighted. Contemporaneously to biomass sampling, the leaf area index (LAI) of live leaves part of herbaceous clipped plants was destructively estimated using leaf area meter scanner (Licor LAI-3000).
In 2004, the root biomass was sampled taking 10 cores of soil of 8.5 cm diameter, between 0-15 cm. Based on 2002-2003 results, that showed that 89% of the fine roots are located in the first 15 cm of the soil profile, samples between 15 and 30 cm had not been taken.
In order to define the carbon content of above and below ground biomass, the IPCC methodology using the default conversion factor of 0.45 (IPCC, 2003) was used, whilst the total carbon and nitrogen content of Amplero soil was carried out at the University of Florence-Italy by Dr. Chiti using a Perkin-Elmer C/H/N analyzer 2400 (Chiti *et al.*, 2007).

2.3 Assessment of NPP

We utilized data acquired from biometric measurements conducted in 2004, 2005 and 2006 to compute the net primary productivity (NPP) of the three grassland managements.
According to literature information, six algorithms are often used to estimate NPP from biomass measurements in grassland vegetation: peak live biomass, peak standing crop (live plus standing dead matter), maximum minus minimum live biomass, sum of positive increments in live biomass, sum of positive increments in live and dead plus litter, and sum of changes in live and dead biomass with adjustment from decomposition (Long *et al.*, 1992, Ni *et al.*, 2004, Scurlock *et al.*, 2002). However, each method differs in the number of inputs required to describe processes associated with biomass change over time (aboveground and belowground productivity, decomposition) and leads to different results in the assessment of NPP (Belelli Marchesini *et al.*, 2007). Moreover, certain methods may be only applied within definite biomes (Scurlock *et al.*, 2002).
Because of the high variability of inputs that each methods use to assess NPP, we chose to use two different approaches. First of all, we didn’t sampled below ground biomass (BGB) but we calculated NPP only from the field data of above ground biomass (Scurlock *et al.*, 2002), modeling below ground biomass (BGB), and implementing the existent algorithm described by Gill *et al.* (Gill *et al.*, 2002).
Among all methods reported by Scurlock (Scurlock *et al.*, 2002), we selected the following four more adapted algorithms:
Method 1 – Peak of live biomass (Long *et al.*, 1989, Singh *et al.*, 1975)

$$NPP = MAX(AGBlive)$$

Method 2 – Peak standing crop (Kucera *et al.*, 1967, Long *et al.*, 1989)

$$NPP = MAX(AGBtotal)$$

Method 3 – Maximum minus (Long *et al.*, 1989, Singh *et al.*, 1975)

$$NPP = MAX(AGBlive) - MIN(AGBlive)$$

Method 4 – Sum of positive increments (Milner *et al.*, 1968)

$$NPP = \sum(\Delta AGBtotal)$$

where AGB_{total} is the whole aboveground clipped matter and AGB_{live} is aboveground live biomass, both in g m^{-2} or t ha^{-1}.

As highlighted above, and considering that the assessment of belowground productivity (BNPP: Below-ground Net Primary Productivity) is more difficult than the estimation of aboveground productivity (ANPP: Above-ground Net Primary Productivity) (Lauenroth *et al.*, 1986), we predicted the BNPP of the Amplero site starting from the aboveground biomass (AGB_{total}) that can be roughly equivalent to ANPP and estimated from ANPP (Bradford *et al.*, 2005). Moreover, we assumed that NPP derived from all four methods could be approximated to ANPP and thus included in the estimation of BNPP. In this way, we adjusted the algorithm proposed by Gill *et al.* (Gill *et al.*, 2002) using the four different values of ANPP. We calculated BNPP using the following equation:

$$BNPP = BGB\left(\frac{liveBGB}{BGB}\right) * T_{root}$$

where:

BGB is the maximum yearly belowground biomass, in g m-2 or t ha-1;

$\frac{liveBGB}{BGB}$ is the maximum proportion of BGB that is alive during the year and it is equal to 0.6 and T_{root} is the root turnover.

Doing the same assumption made from Gill *et al.* (Gill *et al.*, 2002) and Bradford *et al.* (Bradford *et al.*, 2005), we predicted the BGB:

$$BGB_n = 0.79AGB_n - 33.3(MAT + 10) + 1289$$

where AGB_n is the value of above ground biomass obtained from each n measurement (n is varied from 1 to 4 and refers to the number of applied methods) and MAT is the mean annual temperature, in K.
Finally, according to Gill and Jackson (Gill *et al.*, 2000) we calculated root turnover from mean annual temperature:

$$T_{root} = 0.2884e^{0.046*MAT}$$

2.3.1 Statistical analysis

Doing a Kolmogorov-Smirnov test we analyzed the distribution of data set of biomass and its components and consequently the applicability of the all statistic tests, such as the t-test and the ANOVA analysis.
After that preliminary analysis by a paired t-test we investigated if the differences between the above ground biomass (AGB_{total}, AGB_{live} and AGB_{dead}) of the three grasslands typologies are significant. In this manner we tried to evaluate the amplitude of the effect on biomass and productivity of the different management activity.

2.4 Hyperspectral proximal sensing: the FieldSpec PRO® spectroradiometer

2.4.1 Radiometric sampling

The solar radiation energy transits through the atmosphere to the vegetation canopy and it is again made available to the atmosphere by reflectance and transformation of radiant energy absorbed by plants and soil into fluxes of sensible and latent heat and thermal radiation through a complicated series of bio-physiological, chemical and physical processes (Huang *et al.*, 2007).
Roughness, inhomogeneity and fragmentation of leaves influence the ideal reflection and define the scattering process of solar beams (Bolle *et al.*, 2006). The bidirectional properties of leaves

have received little investigation contrary to plant canopies; for this reason most canopy reflectance models omit these characteristics of leaves and assume that leaves are Lambertian and scatter perfectly the solar light. The specular reflection on the leaf surface, however, affects the angular distribution of light and consequently the interpretation of remote sensing data. In some situations, like remote field experiments and laboratory measurements, the bidirectional reflectance, measured in terms of HDRF (Hemispherical Directional Reflectance Factor), can be recorded using a portable spectroradiometer and measuring leaf reflectance on both a black and a white background, alternately. The limit of this method is the strong dependency on the measurement conditions. According to Martonchik *et al.*(Martonchik *et al.*, 2006):

$$HDRF(\lambda, \vartheta_{\mathrm{r}}, \phi_{\mathrm{r}}) = \frac{L_r(\lambda, \vartheta_{\mathrm{r}}, \phi_{\mathrm{r}})}{L_r^{Lam}(\lambda, \vartheta_{\mathrm{r}}, \phi_{\mathrm{r}})}$$

where:

λ is a wavelength;

ϑ_r and ϕ_r are the angles of view (zenithal and azimuthally, respectively);

L_r is the radiance reflected by the target [W sr^{-1} m^{-2}];

L_r^{Lam} is the radiance reflected by an ideal Lambertian surface [W sr^{-1} m^{-2}].

Practically, during field measurements, HDRF is estimated by measuring the total solar radiance incident on the target (Li) and dividing it by the reflected radiance upwelling from the target (Ls) in a given direction of observation (Meroni *et al.*, 2006). Omitting the dependence of radiance from the angels of view and assuming incoming radiance into the target, as incoming radiance measured of the referent panel, reflectance (ρ) of target can be calculated as:

$$\rho = \frac{L^t(\lambda)}{L^i(\lambda)}$$

where L^t is the reemitted radiance by target and L^i is the incident solar radiance, both in watts per steradian per square meter [W sr-1 m-2].

2.4.2 Radiometric characterization of the study area

The vegetation of the three different type of grassland (meadow, pasture and natural, see Figure 6) was radiometrically characterized employing the HandHeld ASD spectroradiometer (ASD Inc, Boulder, CO, USA) (Figure 7). The spectral characterization of grasses was based on *in* *situ* measurements; all spectra were collected during biometric measurements, just few minutes before the clipping and over the same square sampled plots.

The locations for the spectral characterization of the vegetation canopy were randomly sampled within the whole area of each of the three typologies. Depending on the stability of environmental condition during sunny days, five or ten spectral measurements per type of grasses were performed between 10:30 and 12:30 a.m., whereby each measurement was the average of 10 readings at the same spot. The sampling was carried out pointing at the centre of each square plot that was used in a latter stage for biomass clipping and partitioning. The spectral sampling was conducted by holding the ASD cosine optic in nadir position and supposing that the zenith and azimuth angular were approximated to zero; in addition, the distance above the ground was 150 cm, determining a field area of roughly 925 m^2. As reported by Vescovo in his PhD study (Vescovo *et al.*, 2005), this kind of optics seemed to give a better predictive power of vegetation biophysical characteristics that appeared to be related both to off-nadir direction of detected radiation and to the wider area which can be seen by the sensor.

Even if weather conditions were constant, the spectroradiometer was calibrated regularly before each reading, using an integrated Spectralon® calibration panel and doing an up reading of the total incoming radiation in order to define the L^t of the equation for reflectance calculating.

Table 2 - Technical characteristics of FieldSpec HH® spectroradiometer that was used during the field campaign.

	FieldSpec® Hand Held
Spectral Range	350-1050 nm
Spectral Resolution	1.4 nm @ 350-1050 nm
Sampling Interval	0.7 spectra/second
Optics	25° (bare head), 1°, 10°, 20° and cosine
Weight	5.7 kg or 12.55 lbs

2.4.3 Data processing of the grass spectra

Collected spectra values were first exported to ASCII files with the FieldSpec Pro® software. Single ASCII files were created for each separate spectrum. Subsequently, all data were imported into Matlab® for further processing as well as vegetation index calculation. Averages and standard deviations where computed for each reading of type of grassland and for each date, taking into account the separate measurements with a black and white background. A visual quality assessment was performed for every spectrum in order to identify incorrect spectra with which they were removed. After the quality control, all data were imported into the Matlab® software to create three referential spectral libraries containing, per each typologies of management the all and the mean reflectance spectra and the white and black background.

Table 3 - Most used vegetation indexes

ID	Algorithms	Bibliography
SR	$\mathrm{SR} = \frac{\rho_{nir}}{\rho_{\mathrm{red}}}$	(Jordan *et al.*, 1969)
NDVI	$\mathrm{NDVI} = \frac{\rho_{nir} - \rho_{red}}{\rho_{nir} + \rho_{red}}$	(Deering *et al.*, 1978, Rouse *et al.*, 1974)
Green NDVI	$\mathrm{NDVI}_{\mathrm{green}} = \frac{\rho_{nir} - \rho_{green}}{\rho_{nir} + \rho_{green}}$	(Gitelson *et al.*, 1996)
EVI	$\mathrm{EVI} = 2.5 * \left(\frac{\rho_{nir} - \rho_{red}}{\rho_{nir} + \rho_{red} + 6 * \rho_{red} - 7.5 * \rho_{blue}} \right.$	(Liu *et al.*, 1995)
GARI	$\mathrm{GARI} = \frac{\rho_{nir} - (\rho_{green} - 1 * (\rho_{blue} - \rho_{red}))}{\rho_{nir} + (\rho_{green} - 1 * (\rho_{blue} - \rho_{red}))}$	(Gitelson *et al.*, 1996)
ARVI	$\mathrm{ARVI} = \frac{\rho_{nir} - (2 * \rho_{red} - \rho_{blue})}{\rho_{nir} + (2 * \rho_{red} - \rho_{blue})}$	(Kaufman *et al.*, 1992)
VARI	$\mathrm{VARI} = \frac{\rho_{green} - \rho_{red}}{\rho_{green} + \rho_{red} - \rho_{blue}}$	(Gitelson *et al.* 2002)
WBI	$\mathrm{WBI} = \frac{\rho_{900}}{\rho_{970}}$	(Gitelson et al, 1996)

Figure 7 – Handheld spectroradiometer FieldSpec PRO® (ASD, Bulder, Colorado)

Using statistical analysis we also tested at which bands the mean reflectance spectra of the three different grassland typologies were significant different. Our research hypothesis was tested using the one-way analysis of variance. The analysis of variance was used at different sampling period such as week, month and year in order to evaluate the spectral differences for growing period of grasslands.

Considering that vegetation index calculation is a good method to remove the spectral variability due to the canopy geometry, the soil background, the sun view angles the and atmospheric conditions for estimating biophysical vegetation properties and fluxes as well as the biomass, Leaf Area Index (LAI), the percentage of green vegetation cover and the fraction of green vegetation (Baret *et al.*, 1991, Becker *et al.*, 1988, Gianelle *et al.*, 2007, Gitelson *et al.*, 2004, Gitelson *et al.*, 2002, Huete *et al.*, 1998, Pinty *et al.*, 1992, Vescovo *et al.*, 2006) most common vegetation indexes were automatically calculated in Matlab® environment. (Table 3).

We analyzed the goodness of various vegetation index as predictors of biophysical parameters using the regression techniques (Gong *et al.*, 2003). In general, for a bivariate regression model of a biophysical parameter (independent variable x) and a VI (dependent variable y), goodness-of-fit measures such as the coefficient of determination (R^2), mean squared error (MSE), and root mean squared error (RMSE) are useful to indicate the vegetation index sensitivity to the biophysical parameter. (Ji *et al.*, 2007). Moreover, the effectiveness of the regression was also evaluated using a covariance analysis.

2.5 MODerate-resolution Imaging Spectroradiometer (MODIS)

The MODerate-resolution Imaging Spectroradiometer (MODIS), that was included in the EOS (Earth Observation System) project launched on 18 December 1999, is nowadays the keystone instrument on the Terra (EOS-AM 1) and on the Aqua (EOS-PM 1) missions, and it was sent into orbit in April 2002.
MODIS scanned the Earth’s surface every 1-2 days, making observations in 36 co-registered spectral bands at moderate resolution (0.25 - 1 km); of these bands, the first seven were used for the study of vegetation and Earth’s land cover. The first two bands (red at 620-670 nm and NIR at 841-876 nm) were acquired at 0.25 Km while the five following bands (blue: 459-479 nm; green: 545-565 nm; NIR: 1230-1250 nm and SWIR: 1628-1652 nm, 2105-2155 nm) at 0.5 km (Table 4). All MODIS products are free downloadable from its web site (http://modis.gsfc.nasa.gov).

Table 4 - MODIS band amplitude.

Reflected Solar Bands			Emissive Bands
250 m	500 m	1 km	1 km
B1: 620-670nm	B3: 459-479 nm	B8: 405-420 nm	B20: 3.660-3.840 µm
B2: 841-876nm	B4: 545-565 nm	B9: 438-448 nm	B21: 3.929-3.989 µm
	B5: 1230-1250 nm	B10: 483-493 nm	B22: 3.939-3.989 µm
	B6: 1628-1652 nm	B11: 526-536 nm	B23: 4.020-4.080 µm
	B7: 2105-2155 nm	B12: 546-556 nm	B24: 4.433-4.498 µm
		B13L: 662-672 nm	B25: 4.482-4.549 µm
		B13H: 662-672 nm	B27: 6.535-6.895 µm
		B14L: 673-683 nm	B28: 7.175-7.475 µm
		B14H: 673-683 nm	B29: 8.400-8.700 µm
		B15: 743-753 nm	B30: 9.580-9.880 µm
		B16: 862-877 nm	B31: 10.780-11.280 µm
		B17: 890-920 nm	B32: 11.770-12.270 µm
		B18: 931-941 nm	B33: 13.185-13.485 µm
		B19: 915-965 nm	B34: 13.485-13.785 µm
		B26: 1.360-1.390µm	B35: 13.785-14.085 µm
			B36: 14.085-14.385 µm

2.5.1 MODIS data processing

To evaluate the comparability between values that were collected punctually at the field level by portable hyperspectral radiometer and the MODIS data acquired at satellite level with a broader wide bands and a bigger spatial resolution, spectra collected through the Field Spec Hand Held radiometer were firstly re-sampled at the different MODIS wide bands (See table above). Therefore, we directly acquired MODIS images at the same date of field surveys to scaling up the field relationship (Tab 5). We used NDVI and EVI products with a temporal resolution of 16 days and a spectral resolution of 250 m. Since images were acquired in a HDF-EOS format , they were opened and clipped using a MODIS tool provided directly from MODIS company. Images were already re-projected and atmospheric corrected.

The goodness of re-sampled MODIS vegetation indexes in predicting of grassland characteristic was tested by a the regression techniques and the covariance analysis.

The right position of the Amplero site was identified importing into images the coordinates (latitude and longitude) recorded through a portable GPS (Thales®, Mobile Mapper). To be sure that extrapolated pixel corresponded to the Amplero grassland area, we considered the mean values of NDVI and EVI calculated from a square of 9 pixels centered on the Amplero site position. At this time all field data were averaged for/to a single sampling date/value to account the intrinsic pixel spatial variability due to the spatial resolution of the MODIS sensor.

Table 5 - Number of images and days of acquisition of the 16 days/EVI-MODIS and 16 days/NDVI-MODIS data. In order to interpolated biometric and sensed data we acquired the only images that corresponded to each date of the field surveys.

	EVI-MODIS		**NDVI-MODIS**	
	N.of images	Date	N.of images	Date
2004	7	113, 129, 161, 177, 193, 209, 241	7	113, 129, 161, 177, 193, 209, 241
2005	6	129, 145, 161, 177, 193, 225	6	129, 145, 161, 177, 193, 225
2006	3	113, 161, 145	3	113, 161, 145

2.6 Continuous NDVI measurements by CNR1 Net Radiometer

In order to continuously collect NDVI of the grass of the Amplero site, in April 2005 we mounted the CNR1 spectroradiometer near to the eddy tower (Kipp & Zonen, Campbell In., Logan, UT) (Campbell *et al.*, 2000). Considering that the field of view of CNR1 pointed directly to the meadow, we used these data only for studying the properties of the meadow, the more representative typology of grassland in Amplero site.

2.6.1 Partitioning of solar radiation into wavebands and estimation of NDVIb

Data of solar radiation used for this part of work consisted in the measurements of the components (incoming and reflected) of the solar radiation and PAR (Photosynthetically Active Radiation) above the vegetation canopy at Amplero site.

The incoming and reflected PAR was measured by a two quantum sensor (SKP 215, Skye In., UK), while the components of solar radiation were measured continuously by the CNR-1 Net Radiometer (Kipp & Zonen, Campbell In., Logan, UT) with an average of 30-min. As shown in the Figure 8, the CNR1 instrument consists of two pyranometers (CM3). The CM3 that faced upward measures the incoming solar radiation whilst the other, faced downward, measured the solar radiation reflected by the surface, in our case the vegetation of the meadow (Campbell *et al.*, 2000). The radiometer is also made up of two pyrgeometers (CG3) for collecting the long wave components of the radiation (incoming and reflected thermal radiation).

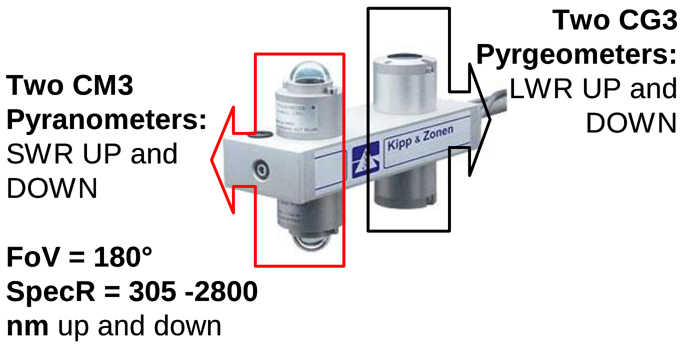

Figure 8 - Technical characteristics of CNR-1 Net Radiometer mounted on a 4 m aluminum boom above the canopy of meadow grassland at Amplero site. Two CM3 pyranometers detected the two components up and down of short wave (SWR) while the two CG3 pyrgeometers measured the two components up and down of long wave radiation (LWR). Photo took from the user instrument manual (Campbell *et al.*, 2000).

In this study, only data of the short wave radiation collected by CM3 from April 2005 to the end of 2006 were used. All radiation sensors were mounted horizontally on one end of the 4 m aluminum boom above the vegetation canopy. This position avoids the possibility of systematic error on data due to effects of the shading and of small sampled area. The field of view (FOW) of the CM3 sensors was about 150 degrees; for this reason the investigated area was a circle with a radius of about 10H (where H is the height of the sensor above the surface) (Wilson *et al.*, 2007).

Starting from the measures of incoming and outgoing PAR fluxes (mmol m_2 s_1) above the vegetation canopy we estimated the reflectance of the visible radiation (RVIS: 400–700 nm) and the reflectance of the near-infrared radiation (RNIR: 700–3000 nm) (Wilson *et al.*, 2007). RVIS was calculated by the following equation (Wilson *et al.*, 2007):

$$R_{VIS} = \frac{PAR_{out}}{PAR_{in}}$$

where PARinc and PARout, measured in mmol m_2 s_1, were the incoming and the outgoing PAR fluxes, respectively,.

According to the Weiss and Norman method (Moon *et al.*, 1940, Weiss *et al.*, 1985), the global solar radiation (SOLR) was partitioned into downward components of visible (VISin) and near-infrared (NIRin) wavebands:

$$VIS_{in} = 0.45 \cdot SOLR$$

and

$$NIR_{in} = 0.55 \cdot SOLR$$

The visible reflected upward radiation (VISout) was estimated as:

$$VIS_{out} = R_{vis} \cdot VIS_{in}$$

The near-infrared reflected upward radiation was derived as:

$$NIR_{out} = SOLR_{out} \cdot VIS_{out}$$

and

$$\mathrm{R}_{\mathrm{NIR}} = \frac{\mathrm{N}IR_{\mathrm{out}}}{\mathrm{N}IR_{\mathrm{in}}}$$

where SOLRout were the measurements of the reflected solar radiation, in W m^{-2}.

Finally we calculated the Normalized Difference Vegetation Index Broadband ($NDVI_b$):

$$\mathrm{N}DVI_b = \frac{R_{NIR} - R_{VIS}}{R_{NIR} + R_{VIS}}$$

2.6.2 Data processing of CNR1 radiometer

From all daytime field radiation CNR1 measurements we extrapolated only the data between 10:00 and 14:00 hours and during the sunny days. Extreme cloudy days were assumed to be the period where the difference between incoming solar radiation and potential radiation was more then 10%; missing data were not gap-filled in the partition of solar radiation and in the calculation of broadband NDVI ($NDVI_b$).

The performance of $NDVI_b$, derived from the CNR1 sensor was compared with NDVI calculated from FieldSpec Hand Held Spectroradiometer and the NDVI derived from MODIS acquired images.

2.7 Continuous measurements of fluxes at Amplero site

2.7.1 Theorical background

The Eddy Covariance (EC) technique has been applied on a range of different ecosystems and numerous studies have shown that grassland could be both sinks or sources of CO_2 (Flanagan *et al.*, 2002, Jaksic *et al.*, 2006, Novick *et al.*, 2004).

The eddy covariance method allow to determination of exchange rate of CO_2 across the biosphere/atmosphere interface by measuring the covariance between fluctuations in vertical wind velocity (*w*) and CO_2 mixing ratio (*c*). Mathematically this relationship has the following form:

$$F = \overline{\rho_a} \cdot \overline{w'c'}$$

and

$$c = \frac{\rho_c}{\rho_a}$$

where ρ_a is air density and ρ_c is CO_2 density. The overbars denote the time averaging (commonly between 30 or 60 minuts) and the primes represent fluctations from the mean, $x' = x - \overline{x}$. Conventionally the positive covariance sign represents net CO2 transfert into the atmosphere while a negative value represents an uptake of CO_2 from the atmosphere by the plant canopy.

Trough the equation of the conservation of the mass is possible to extend the eddy techniques to any other trace gas. In general, the conservation of a scalar is:

$$\frac{\delta\rho_s}{\delta t} + u\frac{\delta\rho_s}{\delta x} + v\frac{\delta\rho_s}{\delta y} - w\frac{\delta\rho_s}{\delta z} = D + S$$

where:

ρ_s is the scalar density;

w and *v* are the horizontal components (*u*, *y*) of the wind speed;

u is the vertical component (z) of the wind speed;

S is the sink or source term;

and D is the molecular diffusion.

Applying the Reynolds decomposition $(u = \overline{u} + u', v = \overline{v} + v', w = \overline{w} + w'$ and $\rho_s = \overline{\rho_s} + \rho_s')$, integrating along *z* direction and supposing horizontal homogeneity and negiglible flux divergence, the equation becomes:

$$\underset{\text{I}}{\int_0^{z_m} S dz} = \underset{\text{II}}{\overline{w' \rho_s'}} + \underset{\text{III}}{\int_0^{z_m} \frac{\delta \overline{\rho_s}}{\delta t} dz}$$

where:

term I is the scalar sink or source, that is the NEE in the case of CO_2;

term II is the eddy flux at height z_m of the instruments and is named as *Fc* for CO_2;

and term III is the storage below of the instruments.

2.7.2 Eddy covariance system at Amplero site

Since June 2002, the Net Ecosystem carbon Exchange (NEE) has been measured using the eddy covariance method (Baldocchi *et al.*, 2003, Baldocchi D.D. *et al.*, 1998) and following the methodology used in Euroflux project (Aubinet *et al.*, 2000).

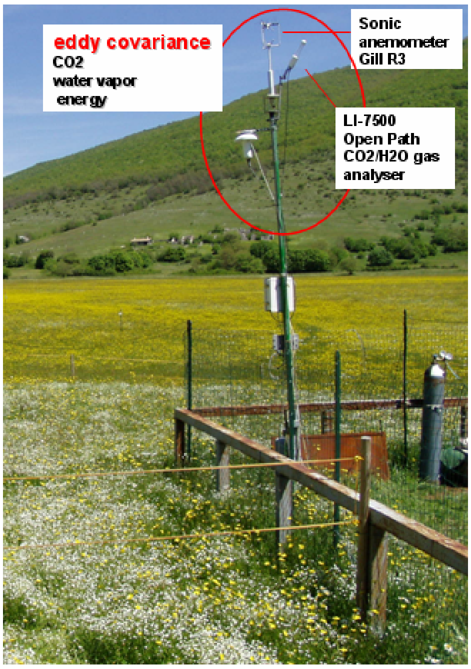

Figure 9 - Eddy covariance system of the Amplero site.

As detailed in figure Figure 9, by a three-dimensional ultra-sonic anemometer (10112R3, Gill Instrumetns, UK) and by an infra-red gas analysers (LI-7500, LiCor Inc., USA), either mounted on the top of a 4.0 m tower, the three orthogonal wind components (*u, v, w*), sonic temperature (T_s) and CO_2 and H_2O concentrations were measured. The raw data were acquired at 20 Hz and 30 min averages were saved for the post-processing in oreder to calculate carbon, water and heat fluxes.

2.7.3 Data processing

The statistical calculations on the high frequency (20 Hz) of the raw data were performed online by a MASE software (Manca *et al.*, 2003). After the transformation of instantaneous value by a linear detrending algorithm, first and second order statistical moments of the components of wind were calculated over 30 minutes times interval. Moreover, in order to align *u*-parallel to wind speed and to nullify *v*, *w* and the lateral momentum flux density ($\overline{w'c'}$) a three dimensional coordinate rotation was applied.

Computing of carbon fluxes

The flux density of CO_2 (F_c) across the atmosphere-ecosystem surface is calculated as:

$$F_c = \overline{w\rho_c} = \overline{w'\rho_c'} + \overline{w}\overline{\rho_c}$$

where ρ_c is the molecular density of CO_2.

The term $\overline{w}\overline{\rho_c}$ is the product of the mean vertical velocity and density of the carbon dioxide. Finallt Webb and Permann (Webb *et al.*, 1980) correction was applied to each flux values to account for density fluctuation effect on the vertical flux:

$$F_c = \overline{w'\rho_c'} + \frac{m_a}{m_v}\frac{\overline{\rho_c}}{\overline{\rho_a}}\overline{w'\rho_w'} + \left(1 + \frac{\overline{\rho_v}}{\rho_a}\frac{m_a}{m_v}\right)\frac{\overline{\rho_c}}{T}\overline{w'T'}$$

where:

ρ_a is dry air density

m_a is molecular weight of air;

m_v is the molecular weight of water vapour.

Net Ecosystem Exchange

Correcting F_c for the storage of CO_2 (F_{st}), that is based on the one point of the CO2 concentration measured by open-path analyzer, NEE was calcualed as:

$$NEE = F_c + F_{st}$$

and F_{st} is:

$$F_{st} = \frac{h\Delta\rho_c}{\Delta t}$$

where:

$\Delta\rho_c$ is the difference in the molar density of CO_2 between two consecutive 30 minutes averages;

h is the height of the column of the air between the soil and analyzer;

and Δt is time lag.

Despiking and gapfilling

The half-hourly NEE data were screened for the detection of anomalous values due to the sensors malfunctioning caused in particular by interference of water condensation, rain, snow or insects with the optical path of the IRGA in two steps. First, we identified all periods when the eddy covariance system would not work properly, as well as when the environmental conditions (rain, snow) were adverse or the analyzed were broken, etc. We excluded these data any further analysis.

All reaming spike after this first despiking was detected applying the median of absolute deviation about the median (MAD) according to Papale *et al.* (Papale *et al.*, 2006). This methodology use an algorithm based on the position of each half-hourly value with respect to the values just before and after that is applied to blocks of 13 days and separately for daytime and nighttime data. It is based on the double-differenced time series, using the median of absolute deviation about the median (MAD) according to the methodology we rejected the NEE values associated to low turbulence conditions.

Because of the eddy covariance method often underestimates the true NEE during periods of low turbulent mixing, lower thresholds of friction velocity (u*) was determinated using the methodology of the CarboEurope database described by Reichstein *et al.* (Reichstein *et al.*, 2005) and Papale *et al.* (Papale *et al.*, 2006).

To assess the accuracy of eddy covariance measurements we do the energy balance, we analyzed the linear regression between the sum of sensible heat (H) and latent heat (LE) versus the difference of net radiation (Rn) and soil heat flux (G) based on half hourly data:

$$H + LE = a_o + a_1(R_n - G)$$

Data gapfilling procedure was performed applying the Marginal Distribution Sampling (MDS) method (Reichstein *et al.*, 2005). The assumption of the method is that meteorological data were available without gaps and can be used for filling fluxes data. In fact, the missing values of NEE were replaced by average values under similar meteorological conditions within a time window of ±7 days. Similar meteorological conditions happen when global radiation, air temperature and VPD do not deviate by more than 50Wm^{-2}, 2.5°C and 5.0 hPa, respectively. In the case of the similar conditions do not existed within the initial time window the averaging window was increased and only Rg or simply the time of measurements as similar conditions are considered.

Fluxes partitioning

NEE was partitioned into the component of GPP using the following equation:

$$GPP = R_{eco} - NEE$$

Where the ecosystem respiration (Reco) was obtained applying the algorithm proposed by Reichstein *et al.* (2005).
The ecosystem respiration is derived as from eddy covariance data based on the exponential regression model (Lloyd *et al.*, 1994):

$$R_{eco} = R_{ref}\, e^{E_0 (1/(T_{ref} - T_0) - 1/(T - T_0))}$$

E_0 is the temperature sensitivity parameter estimated applying the regression the period of 15 days fixing the reference temperature (T_{ref}) at 10 °C and T_0 at −46.02 °C as reported in Lloyd and Taylor (1994).

2.7.4 Meteorological sensors

Starting from June 2002, meteorological and soil variables were detected at Amplero site. Precipitation was collected by an aerodynamic tipping bucket raingauge (ARG100, Environmental Measurements Ltd., Wearfield, Sunderland, UK). Air temperature and relative humidity were recorded using a temperature probe (107 probe, Campbell Scientific Ltd., Shepshed, Loughborough, UK) and a humidity probe (MP 102A, Rotronic Instruments Corp., Huntington, NY, USA), respectively. Atmospheric pressure was measured with the use of a barometer (TP800, Tecnoel s.r.l., Formello, IT).
(HFT-1.1, REBS, Radiation and Energy Balance System, Seattle, Washington, USA) were placed at about 0.05 m and 0.10 m deep in order to calculate a mean soil heat flux. All data were recorded every 30 minutes.

Chapter III

Results and Discussion

3.1 Weather conditions and biomass dynamics

The growing season ranges from April to the end of June and is roughly 90 days long. As well demonstrated, the amount of biomass of grasslands is primarily a function of timing and quantity of precipitation (Frank *et al.*, 2001, Rogler *et al.*, 1947, Xu *et al.*, 2004). While the growing season in temperate grassland is limited by summer drought, at the Amplero site, characterized by a Mediterranean climate, it mainly depends on the timing of the beginning and the end of the rainy season (Xu *et al.*, 2004).

Annual precipitation at Amplero varied from 681 mm in 2005 to 1269 mm in 2004 (Figure 10). The total long-term annual precipitation was 1365 mm and 76% of precipitation fell from October to April. Precipitation during the growing season of our measurement period (from Mach to April) was 129, 175 and 148 mm in 2004, 2005 and 2006 while the long-term average of 270 mm. Differences in the March to May precipitation amongst measured years were absent, precipitation in February, when the vegetation was in a quiescent status, were broadly different (amongst analyzed years). February rainfall recharged the soil profile affecting the availability of water of the completely growing season. During the wet season the soil moisture was higher than 30 m^{-3} m^{-3} and decrease till 20 m^{-3} m^{-3} or less in the summer dry season (Figure 11). This decline took place mildly both in 2004 and 2006 and it started early in 2006 (DoY 90 in 2004 and DoY 120 in 2006); in 2005, it took place at DoY 110 and the reduction of soil moisture was rapid. Moreover, in summer 2005 (from DoY 140 to DoY 240) precipitation was nearly totally absent and for this reason soil moisture was constantly around 20%.

From January to the end of February a pronounced variation of daily air and soil temperature took also place (Figure 12). During the first three months of 2005 the soil temperature was roughly zero degrees and the air temperature was lower than this value. This prolonged cold weather affects germination, which started in the previous autumn that was anomaly warm. After this period, a great increment of temperature caused the beginning of the growing season, characterized by low intensity growing and finally by a reduction of the amount of biomass. Consequently, we can suppose that vegetation of Amplero was active during late winter and early spring and dead during late spring and summer, assuming that the fluctuation of grassland biomass was determined by the impacts of precipitation and probably by human disturbances in some sites (Ni *et al.*, 2004).

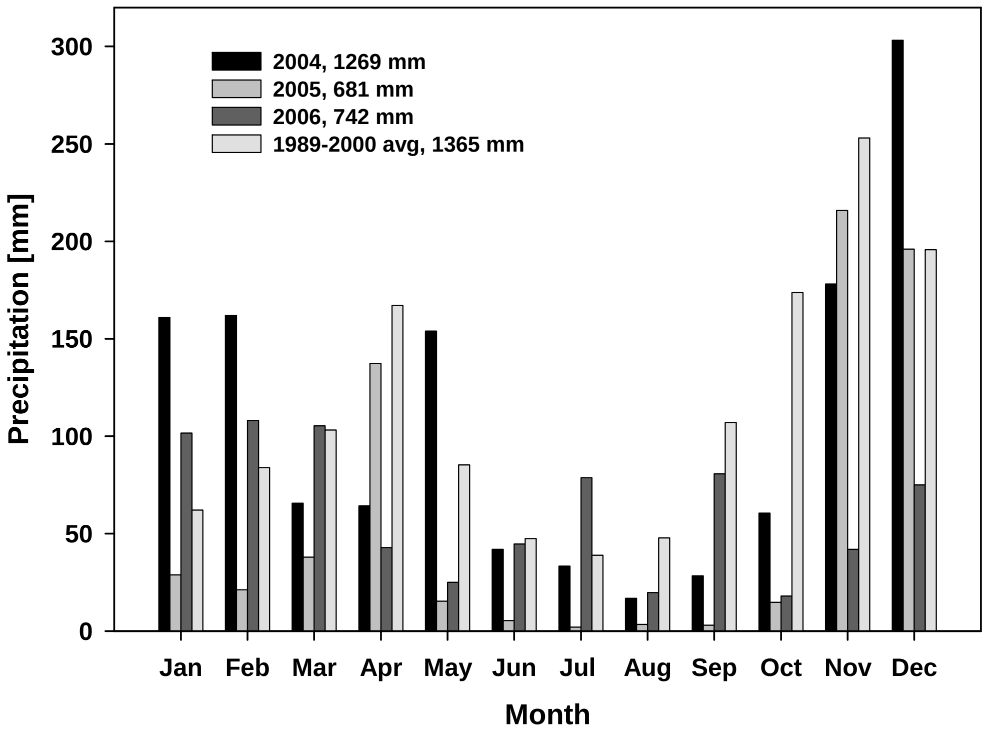

Figure 10 - Monthly total precipitation in 2004-2006. Annual and long-term average precipitation totals are shown with the bar legend.

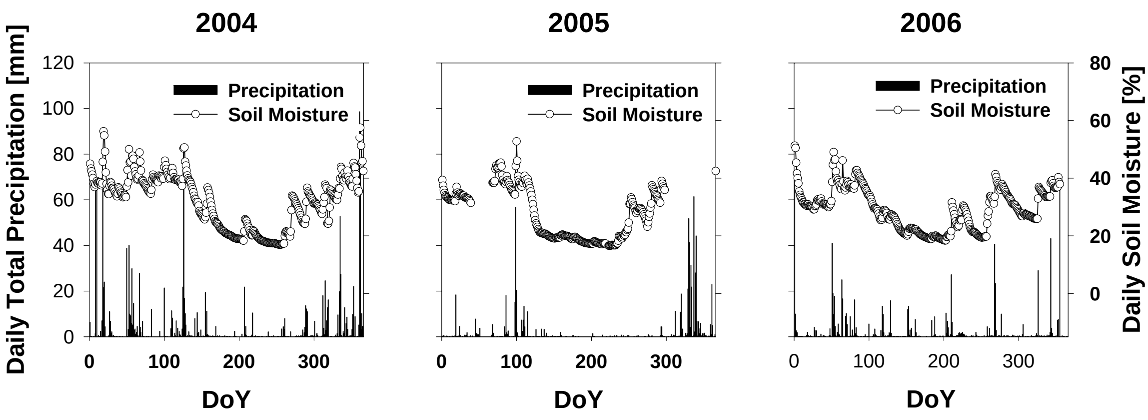

Figure 11 - Daily total precipitation and the daily percentage of soil water moisture.

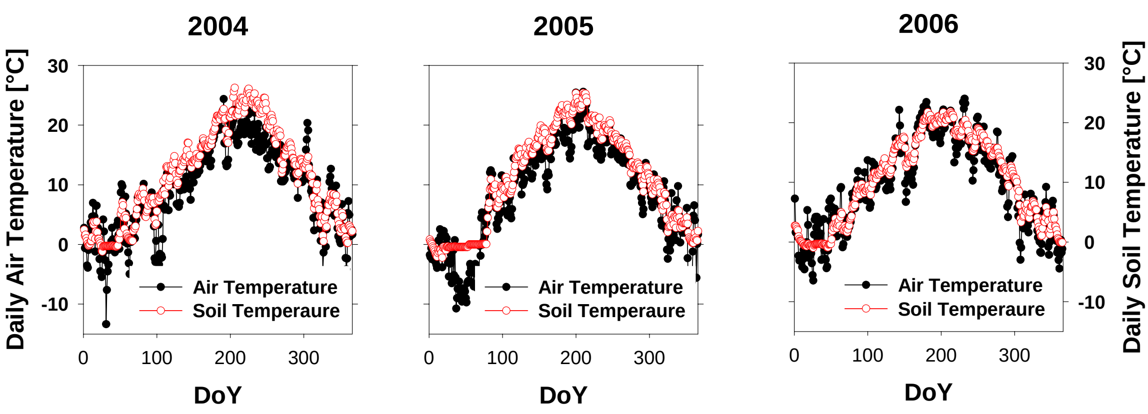

Figure 12 - Daily variation of air and soil temperature at Amplero.

Results obtained by the Pearson's correlation (showed in the Table 6) indicated that during the growing season the ABGtotal of the three grassland typologies had a negative correlation with both air and soil temperature and had positive correlation with precipitation and soil moisture. The goodness of relationships between the grassland AGB_{total} and the climate varied according to the different components of total above ground biomass. In fact, the AGB_{live} fraction correlated very well with the soil temperature but not with the air temperature. Moreover, the meadow typologies had a lower coefficient of correlation with these climatic variables.

Table 6 - Amount of the variance of the biometric parameters (R^2) explained by meteorological variables as determined by Pearson's correlation between the aboveground biomass (ABG total and live) of the grassland typologies (meadow, natural and pasture) and meteo-climatic variables during the growing season.

	MEADOW		NATURAL		PASTURE	
	ABG_{total}	AGB_{live}	ABG_{total}	AGB_{live}	ABG_{total}	AGB_{live}
Daily Air Temp.	-0.47	-0.25	-0.62	-0.22	-0.60	-0.54
p	0.04	0.19	0.03	0.28	0.02	0.03
Daily Soil Temp.	-0.62	-0.40	-0.81	-0.47	-0.71	-0.69
p	0.01	0.07	0.002	0.10	0.003	0.004
Precipitation	0.13	0.01	0.28	0.02	0.28	0.17
P	0.32	0.48	0.22	0.48	0.18	0.29
Soil Water Content	0.46	0.18	0.83	0.31	0.74	0.69
P	0.02	0.26	0.001	0.21	0.001	0.004

As expected, the mean amount of biomass changed according to the different grassland management as well as the different measured years (Table 7). Its value varied between 162.4 g DM m^{-2} to 179.9 g DM m^{-2} with an average of 172.1 g DM m^{-2} for natural grassland, between 281.2 g DM m^{-2} to 388.3 g DM m^{-2} with an average of 349.1 g DM m^{-2} for meadow, and between 156.4 g DM m^{-2} to 259.6 g DM m^{-2} with an average of 215.4 for pasture. These results were consistent with values of EU mountainous grasslands in the CARBOMONT project reported by Berninger *et al.* (100 and 1150 g of DM m^{-2} with an average of 410 g of DM m^{-2}); in that project the Amplero area was the most Southern site and one of the less productive (Berninger *et al.*, 2007, submitted).

Table 7 - Description of mean amount of above ground biomass data used in the study. All reported values are in g DM m^{-2}.

	MEADOW		NATURAL		PASTURE	
	Mean	StDev	Mean	StDev	Mean	StDev
2004	179.9	56.7	377.8	84.9	156.4	37.7
2005	162.4	66.1	281.2	107.4	259.6	9.7
2006	174.1	22.8	388.3	19.1	230.3	16.3
Mean	172.1	48.5	349.1	70.5	215.4	21.2
StDev	8.9	22.8	59.0	45.9	53.2	14.6

N. of samples	30	21	27

Through the simultaneous graphical comparison by box plots of batches of our dataset (Figure 13) we found that our data concentrated around 132.6, 366.7, and 184.2 for meadow, pasture and natural grasslands, respectively. Natural grassland had the highest above ground biomass value while meadow had the lowest one. For this two typologies values were more variable than those of the natural grassland. The position of median in the bottom end of the box of the meadow schematic plot suggested a tendency to a positive skewness. Since the median is near the middle of boxes, data distribution of natural and meadow were almost symmetrical.

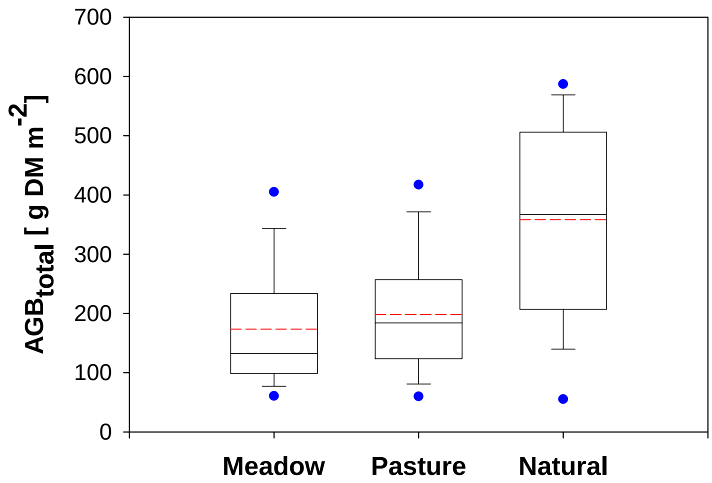

Figure 13 - Box plots that show the distribution of above ground biomass values for the three grassland typologies (meadow, pasture and natural). Each box represents the distribution of 50% of observations. Black bar inside boxes locates the median while red dash the average. Whiskers extend away from the box to the two extreme values. Blue circles refers to single observation; red dashes represent the mean values.

Results of Kolmogorov-Smirnov test (shown in Table 8) confirmed that all three datasets were normally distributed and that was therefore possible to perform all statistic tests, including t-test and the ANOVA analysis.

By a paired t-test we analyzed differences between the above ground biomass of the three grasslands typologies and we found that differences between natural and meadow and between natural and pasture were significant ($p>>0.001$); in contrast, differences between meadow and pasture were not statistically significant ($p>0.05$) (Table 9). The different management activity done during the same meteorological conditions caused a broad variation in biomass; moreover, cutting/harvesting and grazing gave the same effects of available herbage reduction and grassland growth blockage.

Table 8 - Results of the Kolmogorov-Smirnov test. The values of AGB_{total} of all three typology were normally distrusted ($p>0.05$).

	N of samples	D	P
Meadow	30	0.19	0.24
Natural	21	0.11	0.95
Pasture	26	0.11	0.93

Table 9 - Results of paired t-test. p-values higher than 0.05 indicated that differences between grassland typologies were not significant.

	d.f.	t-Student	p
Pasture – Meadow	26	-2.09	0.4
Natural – Meadow	20	-7.29	<<0.001
Natural – Pasture	20	5.25	<<0.001

Focusing on the effect of climate conditions during analyzed years, we noted a significant reduction of AGB_{total} in natural grassland ($P<<0.05$) from 2004 to 2005, and a subsequent return to values obtained in 2004 (Figure 14). Considering that this typology was undisturbed by harvesting or grazing, it was possible to hypothesize that low precipitation, high temperatures and low soil moisture during the spring-summer 2005 generate a similar decrement of mean total biomass. As expected, the AGB of meadow grassland maintained constant values, all standing biomass were exported by harvesting in all three years, and the pasture re-growth in autumn was always low (Figure 15). As concern the pasture typology, we noted that from 2004 to 2005 there was an increment of biomass for pasture and after that the AGB_{total} seamed to be constant: this trend can be attribute to a change of pasture pressure in term of stoking rate.

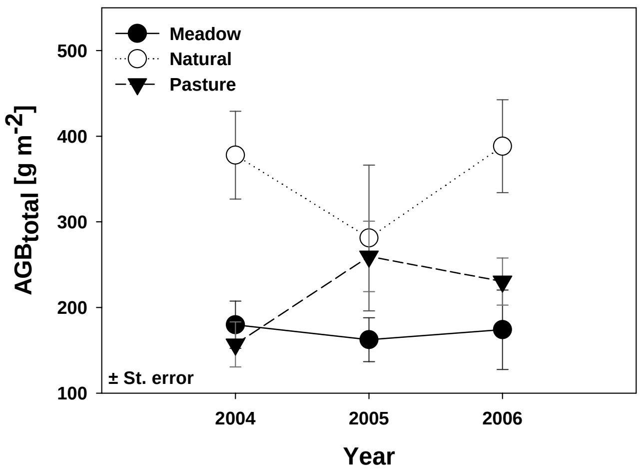

Figure 14 - Inter-annual variation of mean AGB_{total} values of the three different grassland typologies (mean ± standard deviation).

The different management activity caused a broad variation in biomass as well as a variation in the mean peak of live biomass (Ni *et al.*, 2004). Natural grassland has the highest peak of AGB_{live} (408.9 ± 86.7 g m-2), while meadow and pasture have a similar values: 218.1 ± 35.9 g m-2 and 275.1 ± 23.2 g m-2, respectively. High standard deviations in the peak biomass measurements could reflect high spatial variation mainly due to grassland composition and environmental conditions (Table 10).

The peak of live biomass in the Amplero site occurs between the middle of May and end of June (Figure 16). As shown in Table 10, the peak of live biomass sampled during different growing seasons changed among the years depending on climatic conditions, with respect of precipitation. In 2005, characterized of a very dry spring season without relevant precipitation events, vegetation of the meadow peaked at day 146 (26th May), 22 and 13 days before the peak reached in 2004 (16th June) and 2006 (7th June), respectively. The amount of the live biomass at the peak did not change. Because of the dryness during the growing season in 2005, the growth of pasture delayed its start of about four and one weeks in 2004 and 2006, respectively; generating a reduction of biomass of roughly 100 g DM m-2. Finally, the growth of pasture seamed to start about one and two weeks before in 2005 than in 2004 and 2006, with an increasing of about 70 g DM m-2 of live biomass.

Table 10 - Mean peak of live biomass in the site of Amplero, shown as g m-2, and the day of the year (DoY) in which it has been sampled in the growing season 2004, 2005 and 2006.

Peak of AGB_{live}	MEADOW			NATURAL			PASTURE		
	DoY	Mean	StDev	DoY	Mean	StDev	DoY	Mean	StDev
2004	168	219.7	23.3	132	446.3	134.8	176	243.4	2.4
2005	146	212.0	56.9	162	347.3	97.9	162	325.0	-
2006	159	222.7	27.4	159	433.0	27.4	178	257.0	44

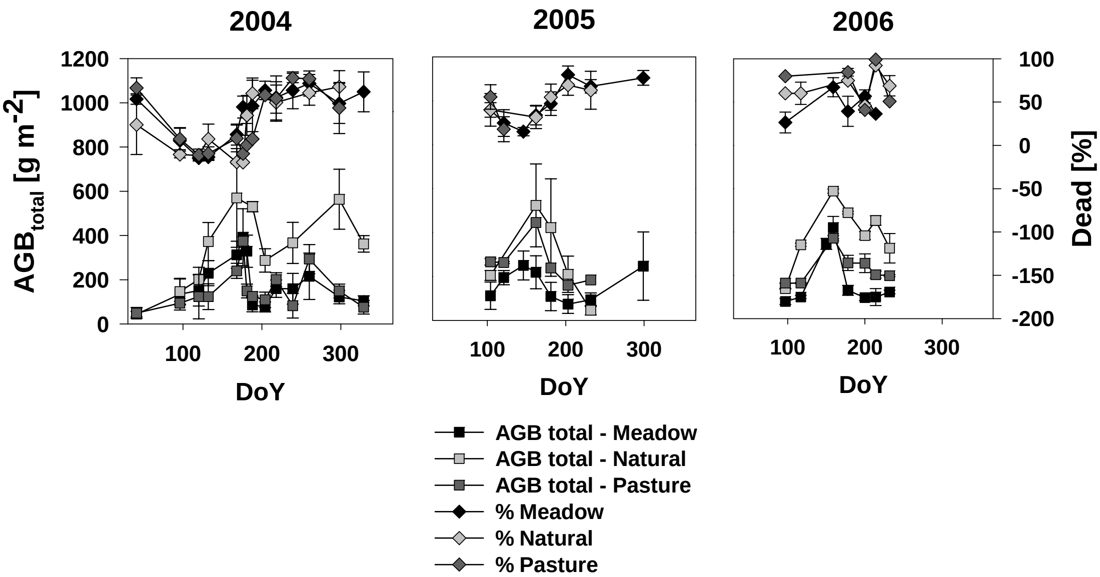

Figure 15 - Trend of above ground biomass (AGB_{total}) and of the percentage of dead matter (% dead) during the growing season 2004, 2005 and 2006 at Amplero site (black symbols: meadow; grey symbol: natural and dark grey symbols: pasture).

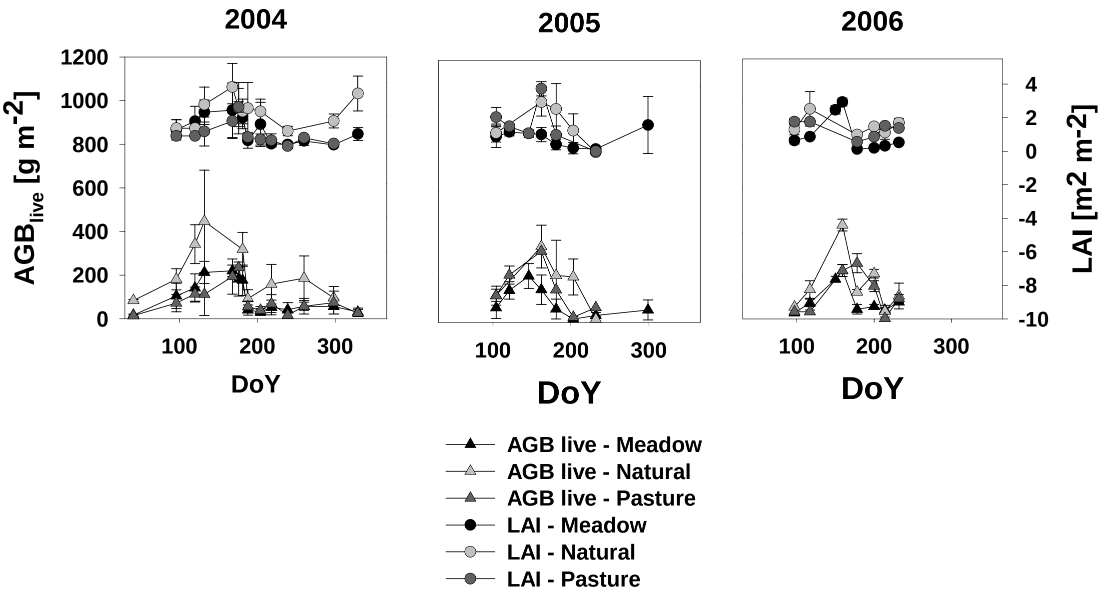

Figure 16 - Trend of live above ground biomass (AGBlive) and of leaf area index (LAI) during the growing season 2004, 2005 and 2006 at Amplero site (black symbols: meadow; grey symbol: natural and dark grey symbols: pasture).

Peak of LAI of all three typologies seamed to occur about two week after of that of live biomass. Moreover the natural plot had a higher LAI value at the peak than managed plots (meadow and pasture). This result was well confirmed in whole experiment conducted by Berninger *et al.* (Berninger *et al.*, submitted 2007).

3.2 NPP assessment

In the Figure 17 there were reported the results of the estimations of NPP and its partitioning between above NPP (ANPP) and below NPP (BNPP), obtained applying four different algorithms (see par. 2.3). Reported data are the mean values calculated on the all years of the measurements. As showed, among all applied methods there were some differences in the values of estimated NPP due to the assumptions of each method (Belelli Marchesini *et al.*, 2007, Ni *et al.*, 2004, Scurlock *et al.*, 2002). Meadow has among all methods the lower mean value of NPP (5.97 ± 0.49 t ha^{-1} y^{-1}) while natural has the higher mean value (8.61 ± 0.38 t ha^{-1} y^{-1}). Method 2 which make use of the peak of standing biomass, estimated the highest value of NPP and ANPP for all typologies. In contrast, the method of the positive increments of live biomass (Method 4) predicted the highest mean values of BNPP.

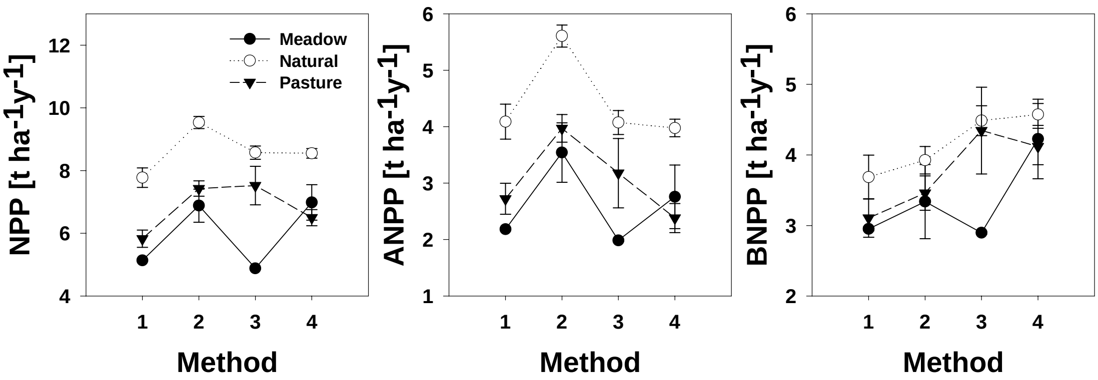

Figure 17 - Above ground (ANPP), belowground (NPP) and total NPP estimates for the three typologies of grasslands (meadow, natural and pasture) of Amplero site for each method. The values are obtained as the mean (mean ± standard deviation) of the biometric sampling overall years (2004, 2005 and 2006).

The fBNPP (Figure 18), defined as the fraction of belowground net primary productivity to total NPP varied from 0.49 ± 0.25 to 0.56 ± 0.22 across the three typologies. These results agreed with the results found by Hui and Jackons (Hui *et al.*, 2006) where the fBNPP of 12 different ecosystems ranged between 0.40 and 0.86. Finally, among all methods the lowest estimated values of fBNPP correspond to the natural grass and it can be link to different species composition of the grasses.

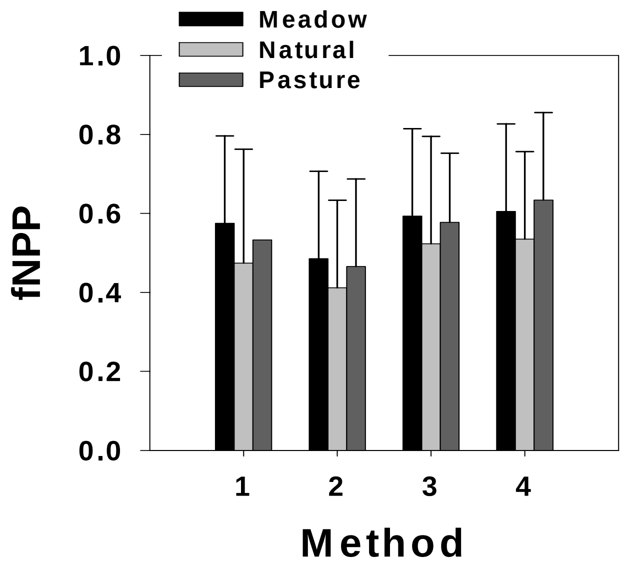

Figure 18 - fNPP estimates for the three typologies of grasslands (meadow, natural and pasture) of Amplero site. The values are obtained as the ratio of the mean BNPP and the mean NNP (mean ± error) of the all years of the biometric sampling (2004, 2005 and 2006).

In order to keep all differences between all employed algorithms and NPP estimations of the studied typologies of grasslands we did an ANOVA one-way analysis (Table 11). In particular, testing if the difference between the estimate of NPP of the meadow, natural and pasture, and each applied methods were significant, it was obtained that the values of NPP of the natural typologies were always significantly different ($p<0.05$) respect to the other two typologies. Therefore, NPP of the meadow and the pasture are comparable confirming that cutting and harvesting has the same effect on NPP. P value is a measure of the probability that the hypothesis being tested is true. In these cases our hypothesis is that all biometric parameter are not different.

Table 11 - Results of the ANOVA one way analysis for testing if the differences between NPP of the three typologies and applied methods were statistically significant. The differences were not significant only when meadow and pasture was compared (: p<0.05).**

	Meth – 1	Meth - 2	Meth - 3	Meth – 4
Meadow vs Pasture	no	no	no	no
Meadow vs Natural	yes**	yes**	yes**	yes**
Natural vs Pasture	yes**	yes**	yes**	yes**

Moreover, all values of NPP simulated using the four different algorithms for 2004, 2005 and 2006, years of the biometric measurements at Amplero site. Averaging out the four methods, as it is showed in the Figure 19, it was possible to make some consideration on the inter-annual variation of NPP from 2004 to 2006 for each typologies. NPP remained roughly constant for each type of management; there was only a weak decrease of the NPP of the meadow in the year 2005 but not significant ($p>0.05$). In addition, we can still note, as well as before, that the meadow and the pasture showed nearly the same trend.

Table 12 - NPP assessments retrieved by four algorithms at the Amplero site for the year 2004, 2005 and 2006, in t ha-1 y^{-1}.

	MEADOW			NATURAL			PASTURE		
	2004	2005	2006	2004	2005	2006	2004	2005	2006
Meth-1	5.13	5.14	5.13	8.03	7.15	8.13	5.31	6.59	5.58
Meth-2	7.34	5.62	7.68	9.62	9.13	9.84	7.11	8.13	7.04
Meth-3	4.90	4.95	4.79	8.93	9.04	7.70	6.27	7.31	8.98
Meth-4	7.91	5.22	7.83	8.88	7.54	9.23	7.61	5.78	6.10
Mean	6.72	5.26	6.77	9.14	8.57	8.92	7.00	7.07	7.37
St Dev	1.53	0.28	1.62	0.65	1.02	0.98	1.01	1.00	1.50

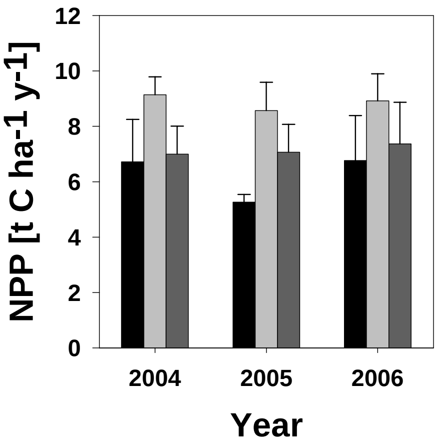

Figure 19 - Mean value of NPP retrieved by the application of the four different algorithms for the Amplero site for the years 2004, 2005 and 2006 (mean ± standard deviation). The decrement of NPP of the meadow in 2005 was not statistically significant (p>0.05).

3.3 Variation in reflectance spectrum

The high reflectance in the near infrared region (from 800 nm to 2500 nm) and low reflectance in the visible (from 550 nm to 700 nm) represent a typical spectral response of the green vegetation. The spectral trend of vegetation is a function of the compounds of the leaves, such as chlorophyll, water, dry plant matter. For this reason all changes of the physiological status of the leaves can be highlighted by its spectral signature. In the Figure 20 and 21 we reported the mean signatures of the three studied typologies of grassland for 2004 and 2005. In the Figure 22 there is the mean spectral trend of the meadow for 2006. All spectral signatures are the average of the 50 measurements (10 readings per plot) per typology per date. After the visual “cleaning” of the spectra we noted that dataset the standard error of all signatures was higher in the infrared than in the visible region. The amplitude of the error in the infrared bands it is linkable to the high sensivity to spatial distribution of vegetation. As Gitelson (Gitelson *et al.*, 2004) showed this higher sensitivity in the near infrared region has little effect on NDVI values. Ustin *et al.* related the reflectance changes to the biophysical and biochemical properties changes of plant leaves (Ustin *et al.*, 2004b). The pigment content and the proprieties of green leaves dominated the absorption of light in the visible part of the electromagnetic spectrum (400 - 700 nm), with a minimum at 550 nm (Carter *et al.*, 1991), that was clearly identifiable into the spectra collected in the spring season at Amplero site (Figure 20 and Figure 21 and Figure 22). Indeed, scanning more deeply the spectral curves the mean spectral reflectance of the vegetation of the three grassland typologies showed high reflectance in the near infrared and low reflectance in the visible at the beginning of the spectral measurements (April 29th in 2004, May 15th in 2005 and April 21st 2006). With the ongoing of the growing season the reflectance in the near infrared range decreased while increased in the visible portion of the spectrum. This change of the reflectance of the leaf was bounded to the changes in the phenological status of vegetation and to the incoming summer dryness. The effect of the pubescence was evident in a reduction of the absorbance in the visible range (400 – 700) and the leaves appeared more reflective after hairs have dried (Rotondi *et al.*, 2003). During the summer spectra increased approximately constantly from visible to near infrared (Ustin *et al.*, 2005) whit a very low shift between visible and near-infrared region. Besides considering the red-edge bands, or rather the narrow spectral region between 700-725 nm at the long-wavelength edge of the chlorophyll absorption feature, we noted that it was absent in the spectra of summer season. The position of this region was not influenced by the soil background or by the atmosphere (Baret *et al.*, 1992) and can be utilized for detecting the trace of green vegetation in the arid and semiarid region (Elvidge *et al.*, 1993).

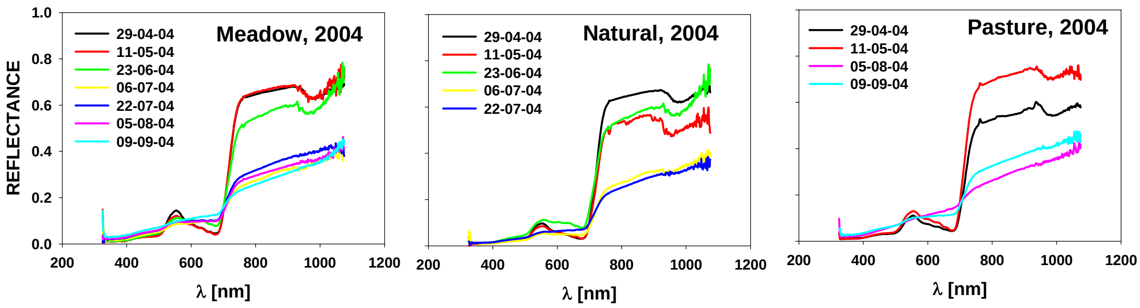

Figure 20 - Spectral signatures of the three different grassland typologies measured in 2004.

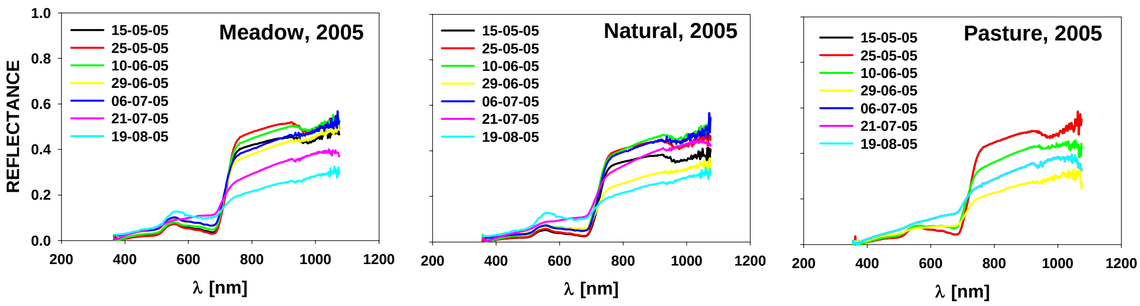

Figure 21 - Spectral signatures of the three different grassland typologies measured in 2006. Each signature was the average of the different measurements.

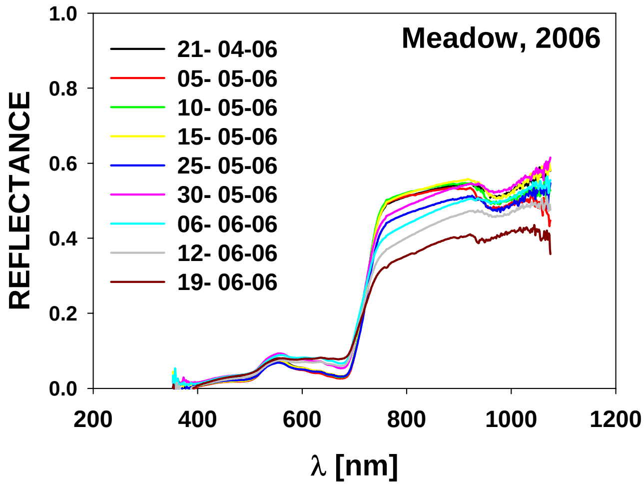

Figure 22 - Spectral signature of the meadow typology measured in 2006.

The changes in the reflectance and transmittance at around at 980 nm are dominated by the absorption of the water in the green leaves, as well happens in the whole shortwave-infrared region (SWIR, 1100 - 2500 nm) (Carter *et al.*, 1991).

3.4 Comparing the performance of the indexes in estimating biomass

As many authors reported, the shape of the relationship between the reflectance of the vegetation, and consequently between the vegetation indexes and its biophysical properties is linear or asymptotic (Gitelson *et al.*, 2004, Turker *et al.*, 1979). Therefore, supposing the linearity of the relationship between reflectance in hyperspectral bands and biomass (AGB_{total}, AGBlive, AGB_{dead}) and LAI was always linear, the regression coefficient R and R^2 were determined. Firstly all data of the three different grassland managements (meadow, natural and pasture) were putted in an only data set. The correlogram in the Figure 23 shows the correlations, in term of R^2, between the reflectance of all hyperspectral bands of the FieldSpec HH spectroradiometer (687 bands) and the biometric measurements, as well as the total, live and dead aboveground biomass and LAI. Significant correlations between the reflectance and dead biomass between 400 nm and 500 nm and between 600 nm and 680 nm (R^2 range from

0.6 to 0.8) were found. However, in this part of the electromagnetic spectrum there is no correlation with the other biometric parameters (AGB_{total}, AGB_{live} and LAI) that showed also a weak correlation in the NIR region (780 nm – 1000 nm).

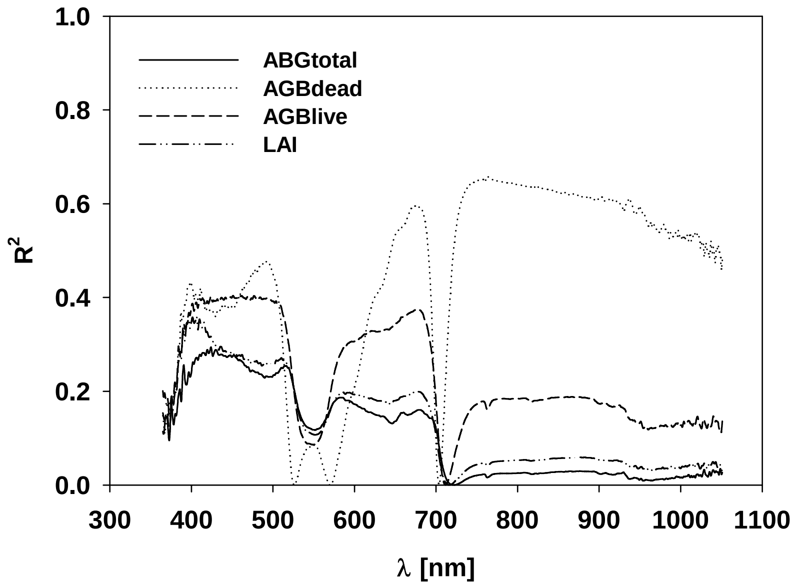

Figure 23 - Relationship between the reflectance and biophysical parameters of vegetation using the whole data set (meadow+natural+pasture).

Sharing the data into the three typologies of management (meadow, natural and pasture) and doing the same analysis as before, the meadow has always the highest values of R^2 of the correlation between the aboveground dead biomass (ABGdead) and the hyperspectral reflectance bands of the meadow were always highest (Figure 24). R^2 of the meadow ranged from 0.5 to 0.7 between 400 nm and 500 nm, reached 0.9 in the red region (between 670 nm and 700 nm) and remained constant around to 0.7 in the NIR region (between 760 nm and 900 nm). The pasture has a lower correlation than the meadow but always good. R^2 of this typology was about 0.6 in the first two spectral windows (400 nm and 500 nm and 670 nm and 700 nm) and 0.5 between 760 nm and 900 nm. Moreover, the pasture showed the lowest coefficient of correlation in the NIR region, also lower than natural grassland that has a R^2 of 0.7. Contrary to the trends of the meadow and the natural typologies, the values of R^2 of the pasture were lower than 0.2 in the whole range among 400 nm and 670 nm.

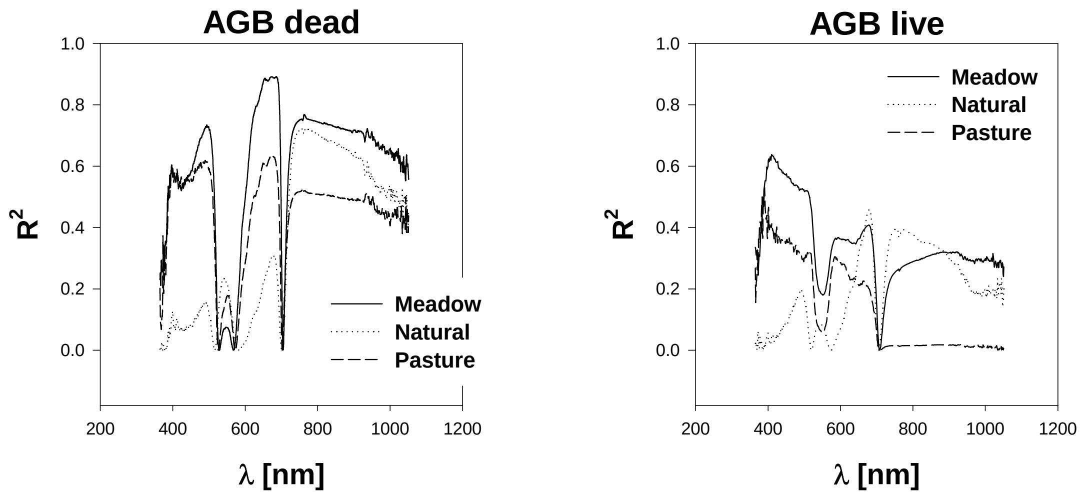

Figure 24 - Relationship between the reflectance and the biomass (AGB_{dead} and AGB_{live}) of the three distinct grassland typologies.

The correlogram in the right part of the Figure 24 highlighted the trend of the coefficient of the correlation between the live biomass and all possible combinations of the narrow bands. The shapes of the three R^2 correlation lines showed a specific trend in each spectral region. The live biomass of the natural correlated only in the red and infrared region; meadow and pasture correlated between 400 nm and 780 nm. However, the pasture did not correlate in the NIR region.

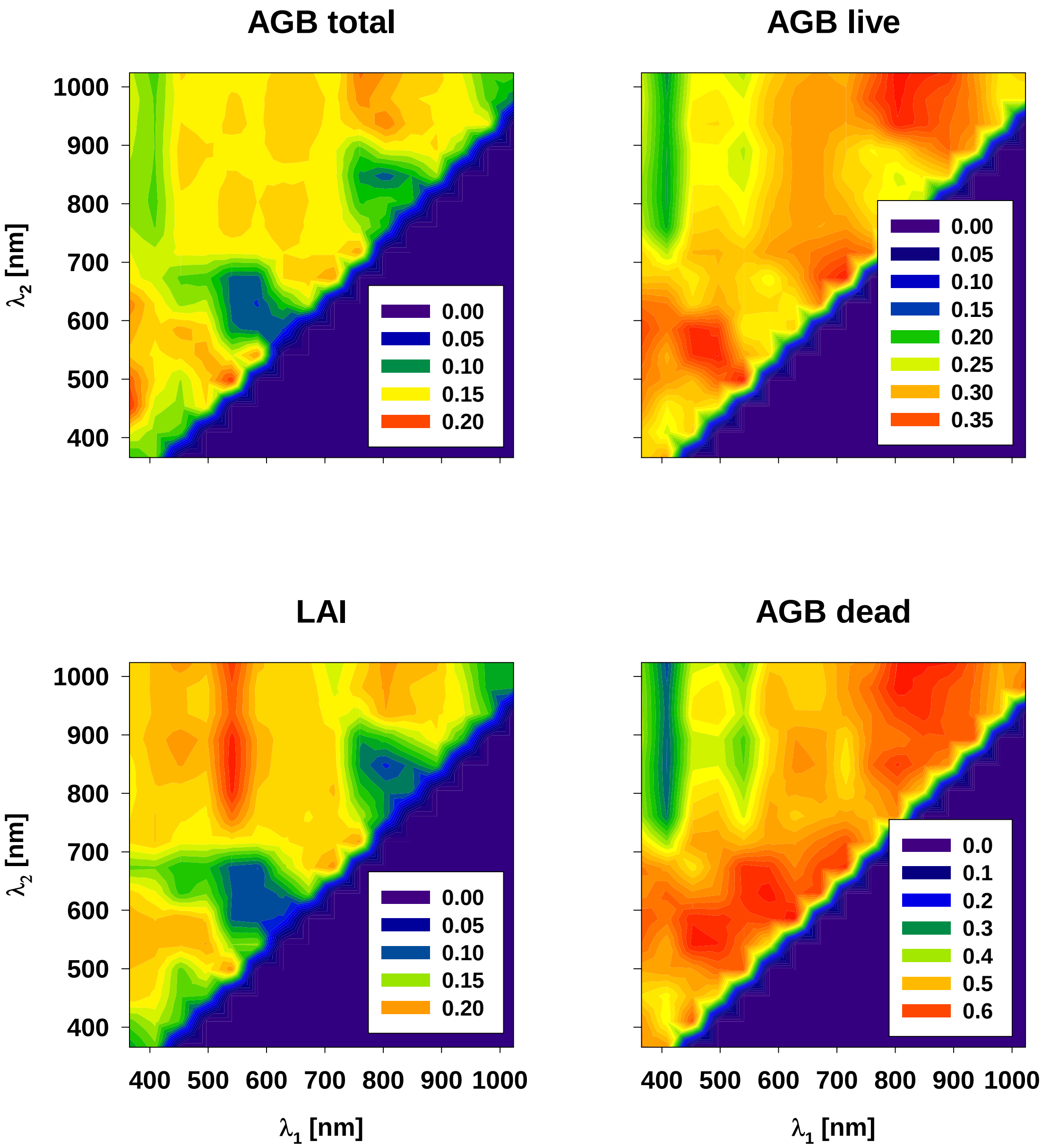

Figure 25 - The maps showing the correlation coefficient (R2) between ABG total, ABG live, LAI and AGB_{dead} and narrow bands of SR derived from all possible combinations across $\lambda 1$ (from 350 to 1050 nm) and $\lambda 2$ (from 350 to 1050 nm).

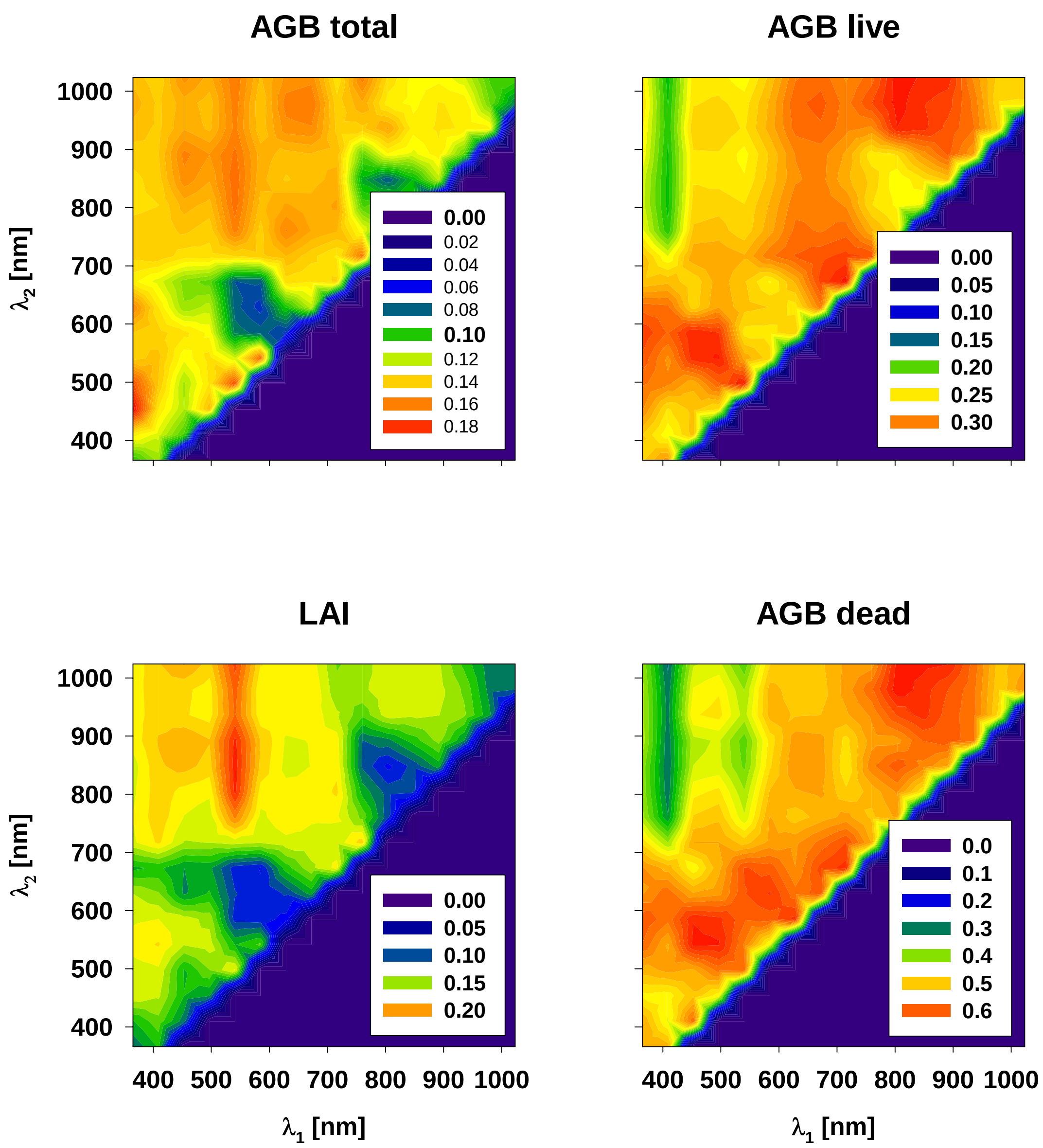

Figure 26 - The maps showing the correlation coefficient (R2) between ABG total, ABG live, LAI and AGB$_{dead}$ and narrow bands of NDVI derived from all possible combinations across λ1 (from 350 to 1050 nm) and λ2 (from 350 to 1050 nm).

Combining all narrow bands of FieldSpec HH spectroradiometer was computed 217,470 possible combinations for estimating the biometric characteristics of the vegetation. Figure 25 and 26 show the results of this analysis in form of R^2 for each combination of λ_1 (from 350 10 1050 nm) and λ_2 (from 350 10 1050 nm) using the simple ratio formula (SR=λ_1/λ_2) and the normalized difference formula (NDVI=λ_1- $\lambda_2/\lambda_1+\lambda_2$) between all combinations of λ_1 and λ_2.
Both SRs and NDVIs correlated well with the percentage of dead biomass (R^2 from 0.10 to 0.60) but not with AGB$_{total}$, live and LAI. Good correlations were obtained between the near infrared (around 800 nm) and red narrow bands (around 680 nm). Moreover, the first 15 best

combinations of bands for calculating SRs and NDVIs index were reported in the Table 13 and 14.

Table 13 - The first 15 combinations of the two bands for calculating the SR index that gave the best value of correlation (R^2) with dead biomass.

λ_1	λ_2	R^2
891	1024	0.62
847	1024	0.62
847	980	0.61
847	936	0.61
803	980	0.63
803	1024	0.62
803	848	0.60
716	673	0.60
672	673	0.59
628	585	0.63
584	629	0.63
584	673	0.60
584	585	0.60
540	673	0.61
540	629	0.60

Table 14 - The first 15 combinations of the two bands for calculating the NDVI index that gave the best value of correlation (R^2) with dead biomass.

λ_1	λ_2	R^2
891	1024	0.64
891	980	0.60
847	1024	0.65
847	980	0.63
847	936	0.63
804	980	0.65
804	1024	0.65
804	936	0.60
716	673	0.63
716	717	0.60
672	673	0.61
628	585	0.62
584	629	0.62
540	673	0.60
540	629	0.60

3.5.1 Seasonal variability of NDVI, EVI and WBI

Using the canonical equation of the most common vegetation indexes and the proposed spectral bands, we selected the best for predicting the vegetation properties of the grass at Amplero site: NDVI, EVI and WBI (Elvidge *et al.*, 1990, Tucker *et al.*, 1979).

The seasonal trend of NDVI (Figure 27) showed that all three typologies have roughly the same value at the beginning of the growing season. Natural grassland has always the highest NDVI value when the field measurements started. The ongoing of the growth of the grasslands produced a reduction of this index that is a consequence of the increment of the dry matter. Pasture showed the lowest NDVI during the summer season. In 2004, NDVI of the meadow increased after the clipping. NDVI of pasture has a distinct trend and started to fall down very soon while NDVI of the meadow and of the natural have the similar tendency and dropped later than 2005. In particular, in 2005 NDVI seams to go down about ten days later than in 2004. In 2006 for the meadow, NDVI remained constant from starting of the growing season until the senescence that became before the clipping. Therefore, the reduction of the NDVI in the meadow from May to June was due to the changes of the phenological status of vegetation and not to the management. In the Figure 28 is represented the trend of EVI index that is comparable to that of the NDVI. Finally WBI, which depends of the leaf water content (Sims *et al.*, 2003), not show significant differences between the typologies and the date (Figure 29).

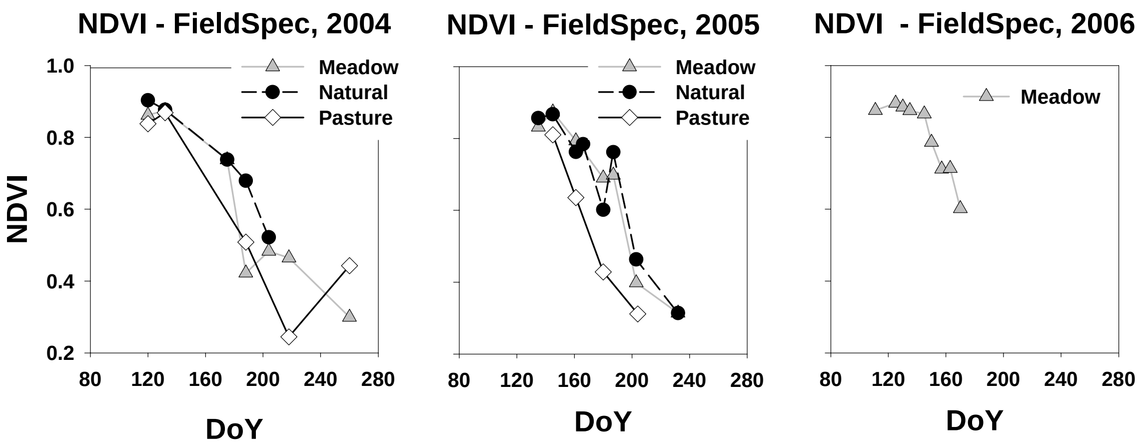

Figure 27 - Temporal trend of NDVI index of meadow, natural and pasture in 2004, 2005 and of meadow in 2006.

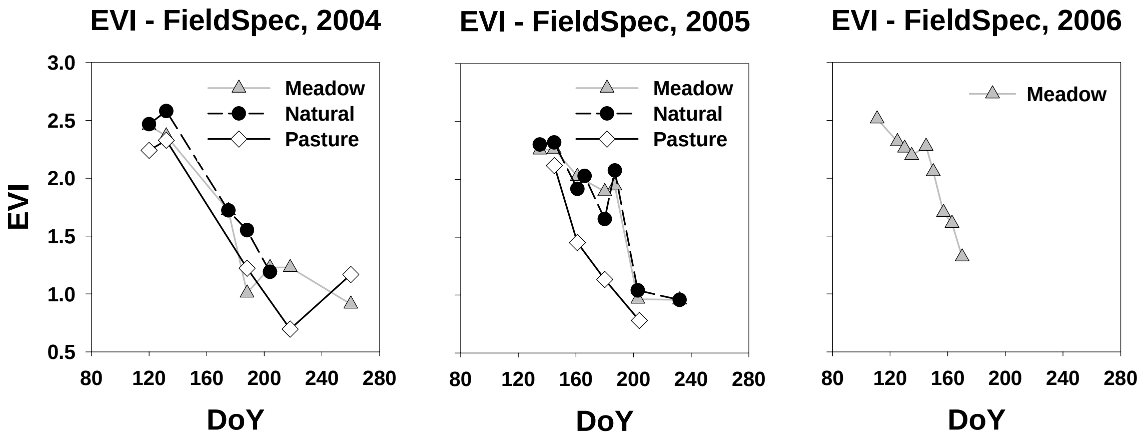

Figure 28 - Temporal trend of EVI index of meadow, natural and pasture in 2004, 2005 and of meadow in 2006.

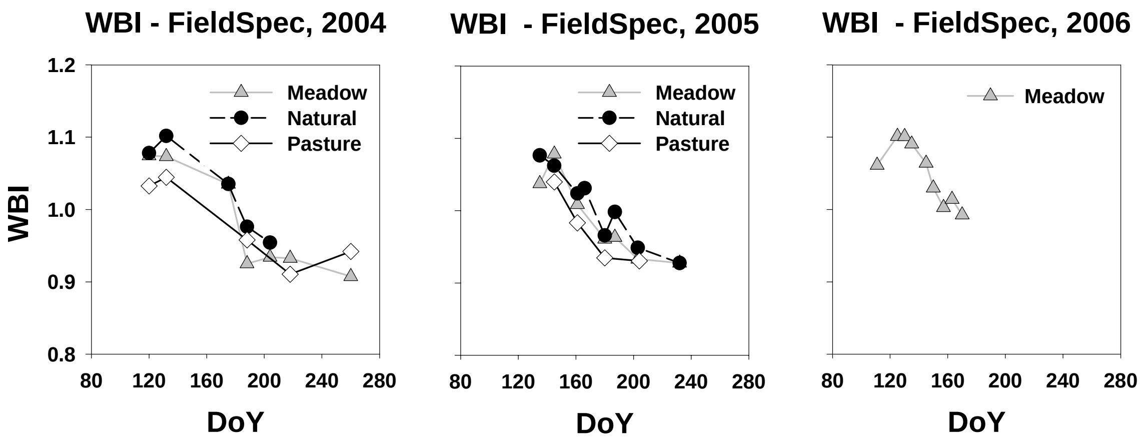

Figure 29 - Temporal trend of WBI index of meadow, natural and pasture in 2004, 2005 and of meadow in 2006.

1.6.3 **3.6 Biometric parameters and vegetation index relationship**

Table 15 and Table 16 show the results of the linear regression analysis between NDVI, SR, and WBI and EVI and all measured parameters of grass vegetation. Table 15 refers to vegetation indexes calculated directly from the FieldSpec spectra while the Table 16 refers to the vegetation indexes derived by rescaling the field spectra measurements using spectral MODIS bands. Doing these analyses all collected data were considered in a only data set.

All considered vegetation indexes (NDVI, SR, EVI and WBI) show a good and significant ($p<0.01$) relationship with % of dead biomass. Both MODIS-simulated-SR both FieldSpec-SR present the highest R^2: 0.74 and 0.71, respectively. While LAI show the lowest values of correlation probably because LAI was destructively measured.

NDVI provide a linear correlation with live biomass (AGB_{live}) as demonstrated by Mutanga (Mutanga *et al.*, 2004). WBI also showed a linear relationship with live biomass as NDVI. The low R^2 of these two last vegetation indexes are due to the fast growth and early maturation of herbage in the Mediterranean grassland.

Table 15 - Type, determination index and parameters of the linear functions used to describe the response of the vegetation hyperspectral indexes to biophysical proprieties of grasslands of Amplero site. In this analysis typologies are considered all together (: p<0.01).**

FieldSpecHH		R^2	Parameter	Coefficient	Std. Error	t	P
NDVI	AGBtotal	0.16	y_0	0.48	0.07	7.1	**
			A	0.0006	0.0002	2.29	0.03
	AGBlive	0.43	y_0	0.47	0.05	9.74	**
			A	0.0012	0.0002	5.00	**
	% Dead	0.66	y_0	0.93	0.05	18.57	**
			A	-0.007	0.0009	-7.11	**
	LAI	0.26	y_0	0.46	0.06	7.40	**
			A	0.11	0.04	3.02	**
SR	AGBtotal	n.s.	y_0	-	-	-	-
			A	-	-	-	-
	AGBlive	0.29	y_0	3.66	1.45	2.53	0.02
			A	0.03	0.007	4.25	**
	% Dead	0.74	y_0	14.87	1.08	13.75	**
				-0.17	0.02	-8.56	**
	LAI	n.s.					
EVI	AGBtotal	n.s.	y_0	-	-	-	-
			A	-	-	-	-
	AGBlive	0.39	y_0	1.20	0.14	8.69	**
			A	0.003	0.0007	4.58	**
	% Dead	0.70	y_0	2.49	0.13	19.31	**
			A	-0.02	0.002	-7.82	**
	LAI	0.16	y_0	1.27	0.18	6.85	**
			A	0.24	0.11	2.25	0.03
WBI	AGBtotal	0.16	y_0	0.95	0.019	49.28	**
			A	0.0002	0.00007	2.29	0.03
	AGBlive	0.45	y_0	0.94	0.01	66.61	**
			A	0.0004	0.00007	5.20	**
	% Dead	0.56	y_0	0.93	0.0127	73.93	**
			A	0.0004	0.00007	5.52	**
	LAI	0.26	y_0	0.94	0.02	51.69	**
			A	0.03	0.01	3.04	**

Table 16 - Type, determination index and parameters of the linear functions used to describe the response of the vegetation MODIS simulated indexes to biophysical proprieties of grasslands of Amplero site. In this analysis typologies are considered all together (: p<0.01).**

MODIS simulation		R^2	Parameter	Coefficient	Std. Error	t	P
NDVI	AGBtotal	0.17	y_0	0.56	0.05	11.16	**
			A	0.0004	0.0002	2.32	0.03
	AGBlive	0.44	y_0	0.54	0.03	15.29	**
			A	0.0009	0.0002	5.09	**
	% Dead	0.65	y_0	0.89	0.03	23.67	**
			A	-0.005	0.0007	-6.99	**
	LAI	0.27	y_0	0.54	0.05	11.80	**
			A	0.08	0.03	3.13	**
SR	AGBtotal	n.s.	y_0	-	-	-	-
			A	-	-	-	-
	AGBlive	0.33	y_0	3.96	1.06	3.74	**
			A	0.02	0.005	4.07	**
	% Dead	0.71	y_0	12.31	0.83	14.79	**
			A	-0.12	0.01	-8.07	**
	LAI	0.11	y_0	4.50	1.27	3.53	**
			A	1.34	0.73	1.82	0.08
EVI	AGBtotal	n.s.	y_0	-	-	-	-
			A	-	-	-	-
	AGBlive	0.40	y_0	1.31	0.09	13.55	**
			A	0.002	0.0005	4.65	**
	% Dead	0.66	y_0	2.19	0.09	22.80	**
			A	-0.01	0.002	7.05	**
	LAI	0.16	y_0	1.37	0.13	10.75	**
			A	0.16	0.07	2.26	0.03
WBI	AGBtotal	0.15	y_0	0.89	0.020	48.25	**
			A	0.0003	0.00006	1.23	0.09
	AGBlive	0.44	y_0	0.97	0.01	63.59	**
			A	0.0005	0.00006	4.00	**
	% Dead	0.55	y_0	0.90	0.0128	72.89	**
			A	0.0004	0.00008	5.47	**
	LAI	0.27	y_0	0.93	0.02	49.87	**
			A	0.02	0.01	3.04	**

3.6.1 Temporal variation

Dividing the data between two different growth periods, before (April-May) and after growth (June), and using the linear and exponential regression we note that there are some significant differences in estimating total biomass of the Amplero grass (Figure 30, Figure 31, Figure 32 and Figure 33).

NDVI – AGB_{total} relationship shows better R^2 after the growth and the shape of the best fit seems exponential. The absence of a relationship during the growth period could be linked to the high values of reflectance in this period and to low biomass amount in the field. The R^2 for the exponential curve was 0.54 while for linear curve was 0.49.

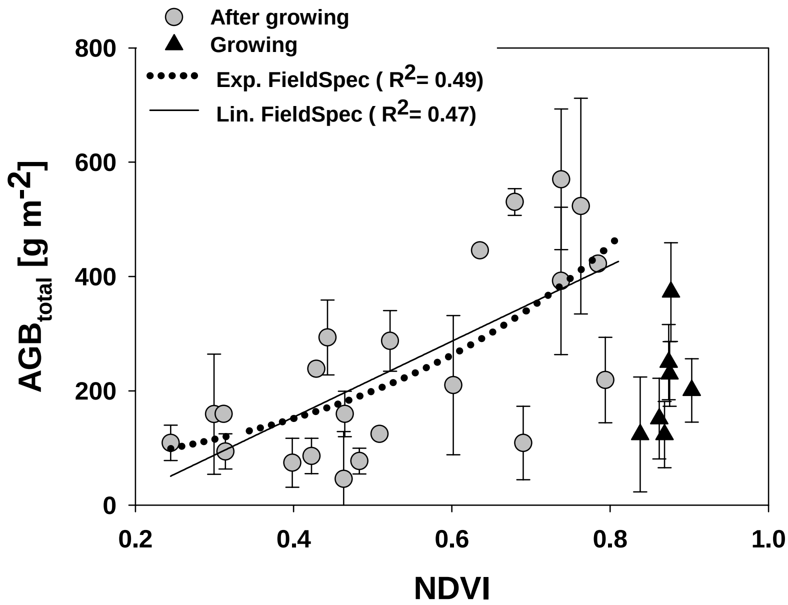

Figure 30 – Total biomass amount (AGB_{total}, mean ± standard deviation) and NDVI in Amplero site sharing data in two period of grass growing: during the growing (from April to May) and during the early senescence (from the end of May to the end of June).

Table 17 - Type, determination index and parameters of the linear functions used to describe the response of the vegetation indexes to biophysical proprieties of grasslands of Amplero site. In this analysis typologies are considered all together.

NDVI - AGB_{total}							
Period	**Type**	**R^2**	**Parameter**	**Coefficient**	**Std. Error**	**t**	**P**
Growing	*Linear*	n.s.	Y_0	-1497.43	1598.04	-0.94	0.39
			a	1957.06	1834.12	1.07	0.33
	Exponential	n.s.	a	0.24	1.91	0.13	0.90
			b	7.75	9.04	0.86	0.43
After growing	*Linear*	0.47	Y_0	-111.60	87.46	-1.28	0.22
			a	663.85	156.42	4.24	**
	Exponential	0.49	a	105.37	33.23	3.17	**
			b	0.19	0.12	1.68	0.14

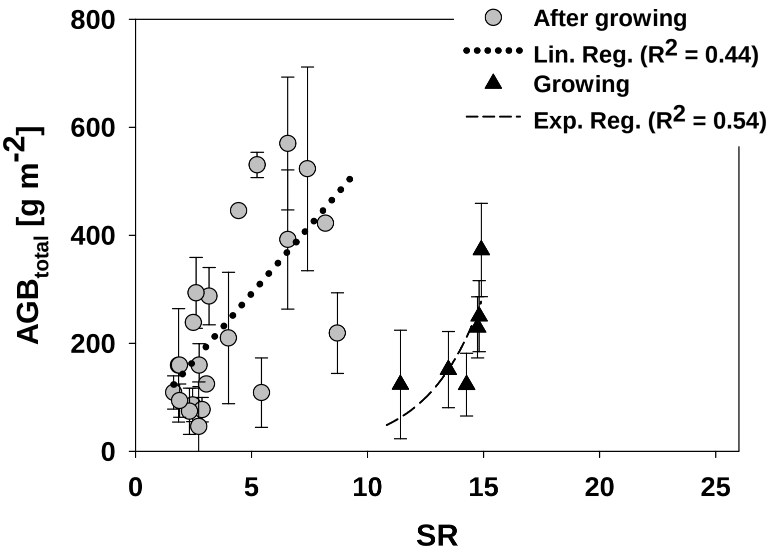

Figure 31 - Total biomass amount (AGB$_{total}$, mean ± standard deviation) and SR in Amplero site sharing data in two period of grass growing: during the growing (from April to May) and during the early senescence (from the end of May to the end of June).

Table 18 - Type, determination index and parameters of the linear functions used to describe the response of the vegetation indexes to biophysical proprieties of grasslands of Amplero site. In this analysis typologies are considered all together (: p<0.01).**

SR - AGB$_{total}$							
Period	**Type**	**R^2**	**Parameter**	**Coefficient**	**Std. Error**	**t**	**P**
Growing	*Linear*	0.42	Y_0	-447.07	382.35	-1.17	0.31
			a	47.04	47.04	1.72	0.16
	Exponential	0.54	a	0.48	1.77	0.27	0.80
			b	0.43	0.25	1.69	0.17
After growing	*Linear*	0.44	Y_0	41.22	57.44	0.72	0.48
			a	50.08	12.60	3.97	**
	Exponential	0.37	a	125.29	35.58	3.52	**
			b	0.15	0.05	3.52	**

SR seems to correlate with total above ground biomass (AGB$_{total}$) showing always the same correlation. Linear regression fits better than exponential relationship that has a better R^2 during the growing season (see Table 18 and Figure31).

EVI shows a weak exponential correlation with biomass (Figure 32 and Table 19) in each period (0.44 and 0.33, respectively).

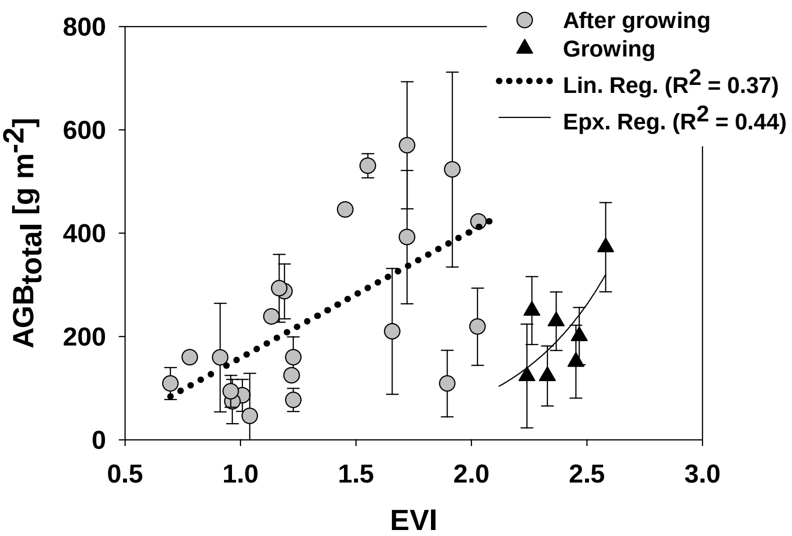

Figure 32 - Total biomass amount (AGB$_{total}$, mean ± standard deviation) and EVI in Amplero site sharing data in two period of grass growing: during the growing (from April to May) and during the early senescence (from the end of May to the end of June).

Table 19 - Type, determination index and parameters of the linear functions used to describe the response of the vegetation indexes to biophysical proprieties of grasslands of Amplero site. In this analysis typologies are considered all together (: p<0.01).**

EVI - AGB$_{total}$							
Period	**Type**	**R^2**	**Parameter**	**Coefficient**	**Std. Error**	**t**	**P**
Growing	*Linear*	n.s.	y_0	n.s.	n.s.	n.s.	n.s.
			a	n.s.3	n.s.	n.s.	n.s.
	Exponential	0.44	a	0.58	1.63	0.36	0.73
			b	2.44	1.14	2.15	0.08
After growing	*Linear*	n.s	y_0	n.s.	n.s.	n.s.	n.s.
			a	n.s.3	n.s.	n.s.	n.s.
	Exponential	0.33	a	73.85	36.81	2.01	0.06
			b	0.85	0.30	2.83	0.01

The water band index (WBI) shows a surprising exponential correlation with total biomass in each period. Correlation during growing has a value of R^2 of 0.86 while is lowest after the growth period (R^2 =0.58). This index is linked to foliar water content that in a Mediterranean ecosystem decrease from the early summer drought that starts at the beginning of the senescence of grassland, around June. Finally, WBI seems to be a most suitable index to predict total amount of biomass.

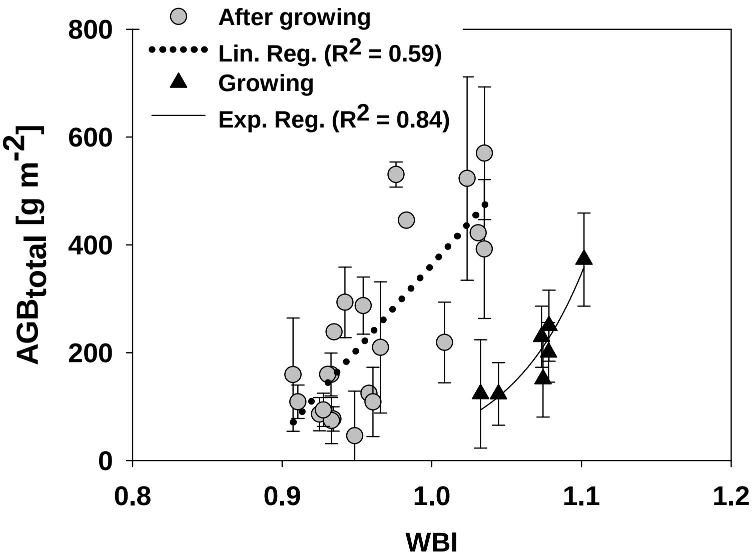

Figure 33 - Total biomass amount (AGB_{total}, mean ± standard deviation) and WBI in Amplero site sharing data in two period of grass growing: during the growth (from April to May) and during the early senescence (from the end of May to the end of June).

Table 20 - Type, determination index and parameters of the linear functions used to describe the response of the vegetation indexes to biophysical proprieties of grasslands of Amplero site. In this analysis typologies are considered all together (: p<0.01).**

WBI - AGB_{total}							
Period	**Type**	**R^2**	**Parameter**	**Coefficient**	**Std. Error**	**t**	**P**
Growing	*Linear*	ns	y_0	n.s.	n.s.	n.s.	n.s.
			a	n.s.	n.s.	n.s.	n.s.
	Exponential	0.86	a	0.0007	0.0001	0.25	0.81
			b	19.39	3.61	5.36	**
After growing	*Linear*	ns	y_0	n.s.	n.s.	n.s.	n.s.
			a	n.s.	n.s.	n.s.	n.s.
	Exponential	0.58	a	0.005	0.01	0.46	0.65
			b	11.06	2.17	5.09	**

3.6.2 Spatial variation

In the Figure 34 there is the synthesis of the analysis between vegetation indexes and biometric parameters of three typologies of grassland management.

Considering the three different typologies of grassland was carried out that natural grassland is highly correlated with the live fraction of above ground biomass (AGB_{live}) and seems to have the same values of R^2 for both linear and exponential regression. EVI showed the lowest R^2 values and the fit is better using an exponential regression curve. In contrast, NDVI, SR and WBI have a very strong linear correlation with this grassland parameter.

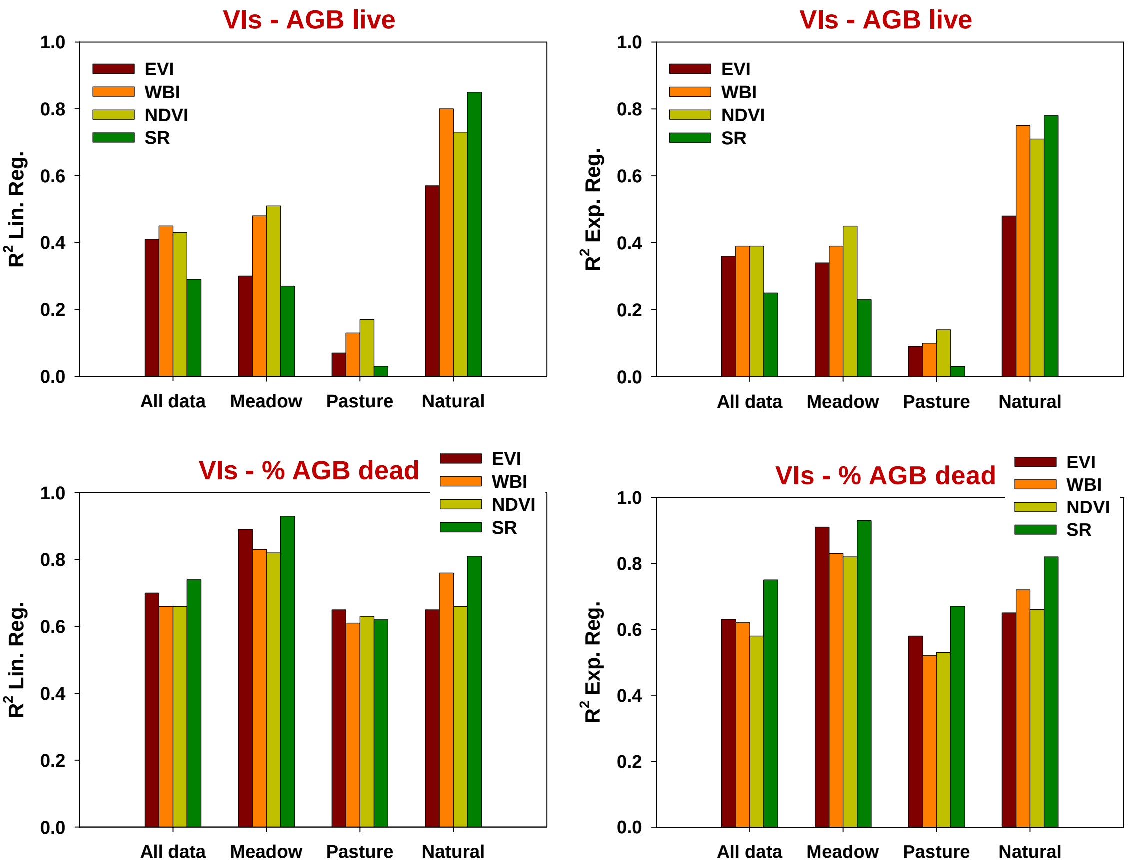

Figure 34 – Correlation coefficients (R^2) between vegetation indexes (VIs) and above ground and % of dead biomass for the managements.

Managed grasslands (meadow and pasture) present a correlation coefficient always minor of 0.60 and linear relationships seems to be better than exponential, excepted for the EVI index. Looking at the percentage of dead biomass (% AGB_{dead}) meadow shows the highest values of correlation between studied vegetation indexes and AGB_{live}. Because of meadow have the lowest values of total and live biomass and comparable to that of pasture it is possible to conclude that using this hyperspectral remote sensing these typologies are distinguishable.

Finally, the relationships showed are specific for each type of management and then this approach is a good and low cost method to estimate live and dead biomass of grassland without make destructive field measurements.

3.7 Partitioning of the solar radiation into the wavebands of CNR1

The partitioning of the solar radiation into the visible (Rvis) and near-infrared (Rnir) wavebands based on the field measurements of the incoming and the outgoing components, made by CNR1 radiometer at the Amplero site, was reported in the Figure 35. During the winter season the reflectivity showed a large scatter due to the presence of the snow and consequently a high value of albedo. All the winter values were skipped for calculating NDVI. The reflectivity of the solar radiation in the visible and in the near-infrared wavebands varied normally between 0.3 and 0.6 for the Rnir and between 0.03 and 0.15 for the Rvis during no-snowing conditions. The trend of the components of reflected radiation was strictly linked to the phenological status of vegetation.

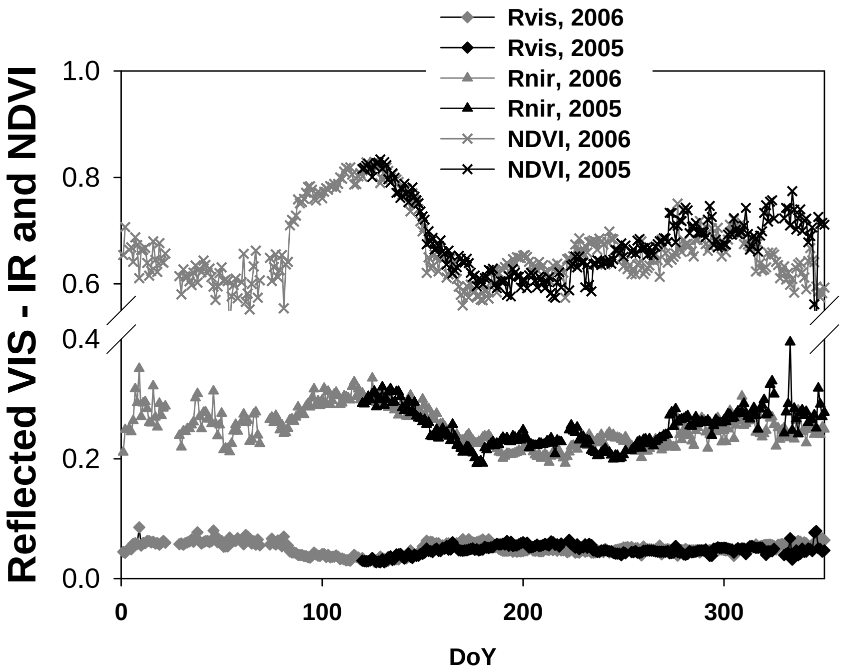

Figure 35 - Partitioning of radiation between visible (Rvis), near-infrared (NIR) and derived NDVI) from CNR1 sensor.

The normal range of reflectivity values was 0.3 - 0.6 for the VIS, 0.03–0.15 for the PAR, and 0.1–0.3 for solar radiation during non snowy conditions, with reflections lower during active vegetation growth in the summer season than in periods of low vegetation during the spring and fall (Wilson *et al.*, 2007).

Calculated NDVI using CNR1 sensor shows the same trend of the NDVI derived form FieldSpec measurements and NDVI extracted from the MODIS images (Figure 36).

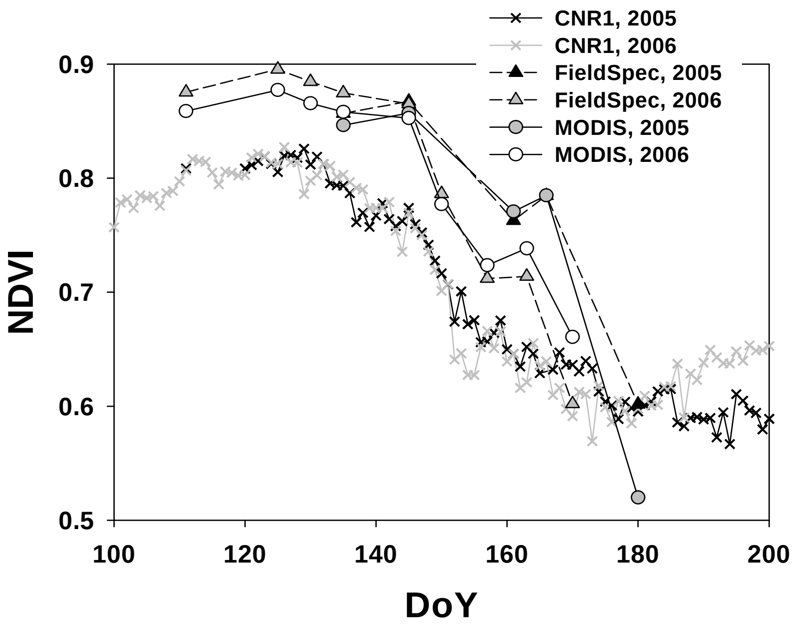

Figure 36 - Seasonal trends of NDVI calculated by CNR1, FieldSpec and MODIS sensors over the year 2005 and 2006.

The data gap is due to the different spectral wide bands for these sensors. CNR1 sensor has a broad bands for calculating NDVI, in fact this sensor measure the radiation between whole visible range between 400 nm and 700 nm while FieldSpec and MODIS use more narrow bands for computing NDVI.

Figure 37 shows the linear correlation between MODIS-NDVI and CNR-NDVI, Fieldspec-NDVI and MODIS-NDVI and Fieldspec-NDVI CNR-NDVI.

The comparison of these three methods highlighted that NDVI values are comparable because linear trends are visible (Figure 37). The slope of the relationship indicated the goodness of the comparison and the presence of eventual systematic differences. The best agreement appears when comparing MODIS with Fieldspec, but the lowest dispersion is achieved between MODIS and CNR1.

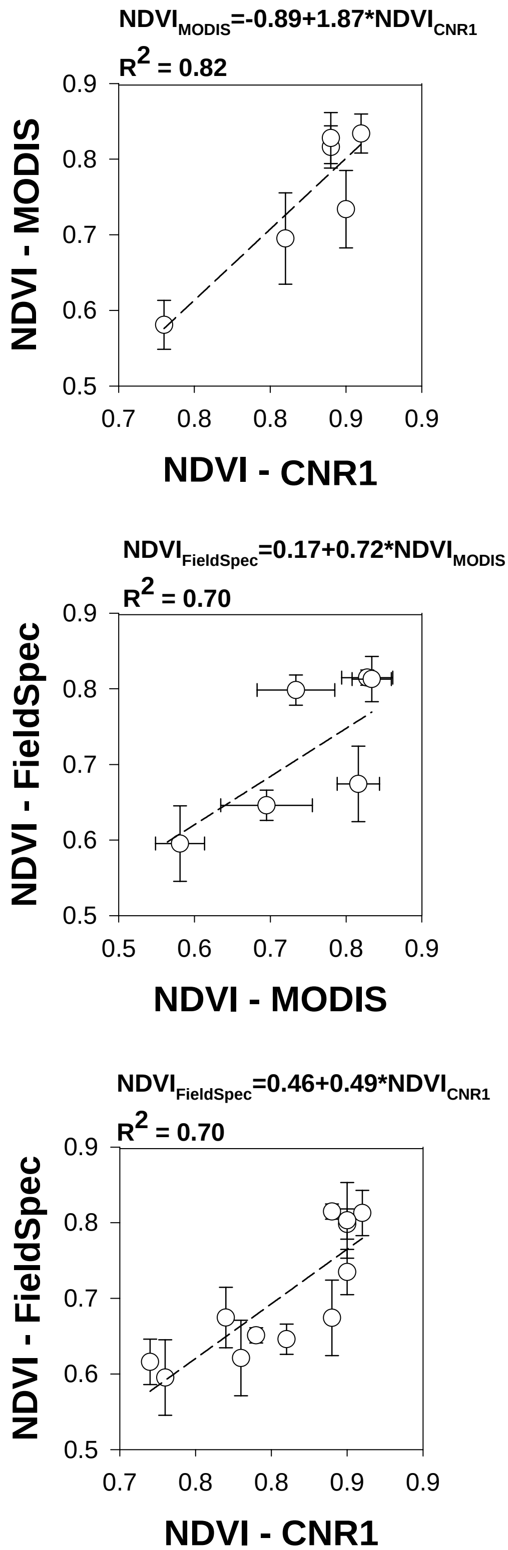

Figure 37 – Comparison of NDVI calculated from FielSpec, CNR1 and MODIS sensors.

3.8 NPP estimation from remote data

Analyzing the relationship with the NPP, at the peak, and several vegetation indexes, calculated from the spectral field measurements, we noted that the most suitable index in predicting NPP is NDVI (Table 21). In fact, NDVI correlate whit all NPP values derived from all applied methods. NDVI shows the best values of the correlation whit Method 2 (max of the total biomass) (R^2=0.90, Figure 38). Moreover, the estimated parameters for all methods are statistically significant ($p \leq 0.05$, see Table 22). In contrast, SR shows a relation (R^2=0.57) only with Method 1 (max of the live biomass) while EVI (Figure 39) correlate with Method 1 and Method 3 (difference between max and min of total biomass) (R^2: 0.50 and 0.48 respectively) but the estimated parameters is not statistically significant ($p>0.05$, see Table 23). For this reason we estimated NPP at tower (CNR1) and MODIS level applying the relationship with only NDVI and NPP (figure 40). In particular, we used the following relationship: NPP=15.75-11.21*NDVI where NDVI corresponds to MODIS-NDVI or CNR1-NDVI rescaled values. MODIS and CNR1 were rescaled by the following relations:

for MODIS data: $NDVI_{fs}$=0.17+o.72*$NDVI_{MODIS}$ (R^2=0.70)
for CNR1 data: $NDVI_{fs}$=0.46+0.49*$NDVI_{CNR1}$ (R^2=0.70)

where NDVIfs, NDVIMODIS and NDVICNR1 are NDVI from FieldSpec, MODIS and CNR1 respectevly (Figure 37).

Table 21 - Correlation coefficients of linear regression functions ($NPP_{method}=y_0+a*VI$, where VI is the employed vegetation index in the relation) used to describe the response of NDVI, SR and EVI index to NPP assessed by the four different methods at Amplero site.

R^2 values			
Method	NDVI at peak	SR at peak	EVI at peak
1	0.70	0.57	0.50
2	0.90	0.13	0.16
3	0.55	0.13	0.48
4	0.69	n.s.	n.s.

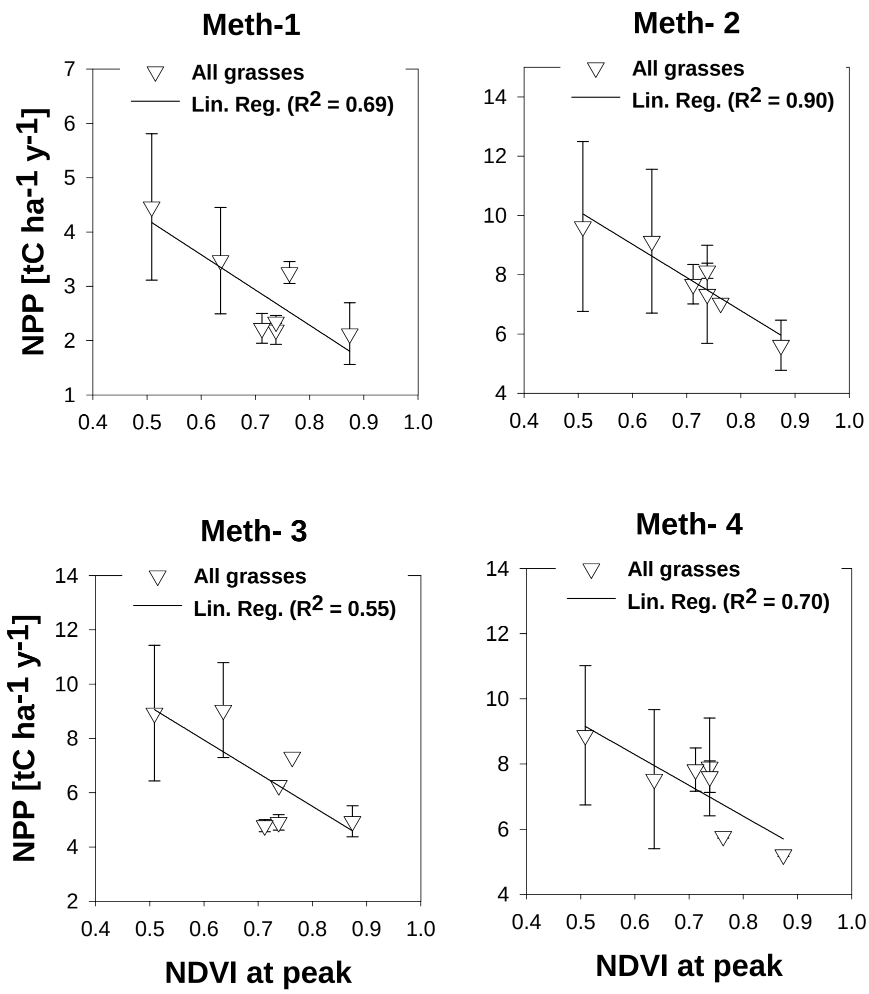

Figure 38 - Linear regression between NPP (mean ± standard deviation), retrieved from the four different method and NDVI values ($NPP_{method}=y_0+a*NDVI$). The value of NDVI corresponds to their value at the peak of the grassland productivity.

Table 22 - Parameters of the linear functions ($NPP_{method}=y_0+a*NDVI$) used to describe the response of NDVI index (at the peak of growth) to NPP assessed by the four different methods at Amplero site.

	NPP versus NDVI				
	R^2	y_0	p	a	P
Meth-1	0.69	7.47	<<0.01	-6.49	0.02
Meth-2	0.90	15.75	<<0.01	-11.21	<<0.01
Meth-3	0.55	15.27	0.05	-12.21	<<0.01
Meth-4	0.70	13.96	<<0.01	-9.45	0.01

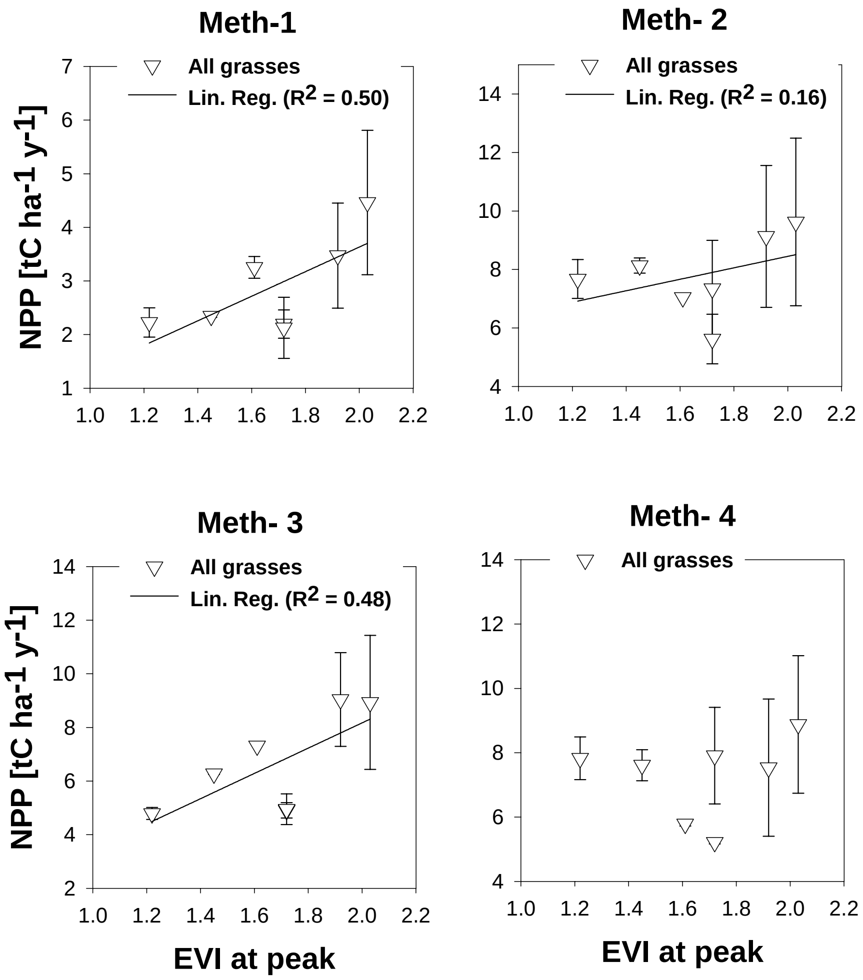

Figure 39 - Linear regression between NPP (mean ± standard deviation) and EVI index ($NPP_{method}=y_0+a*EVI$), retrieved from the four different method and EVI values. The value of EVI corresponds to their value at the peak of grassland productivity.

Table 21 - Parameters of the linear functions ($NPP_{method}=y_0+a*EVI$) used to describe the response of EVI index (at the peak of growth) to NPP assessed by the four different methods at Amplero site.

NPP versus EVI					
Method	R^2	y_0	p	a	p
1	0.50	-0.95	0.60	2.29	0.07
2	0.16	4.53	0.24	1.96	0.37
3	0.48	-1.26	0.75	4.71	0.08
4	0.02	6.00	0.15	0.75	0.73

Using rescaled-NDVI data of CNR1 and MODIS annual NPP seems to be overestimated (Figure40) by a relatively small amount of carbon, ranging from 0.49 t C ha^{-2} yr^{-1} to 1.53 t C ha^{-2} yr^{-1} maximum. The overestimation of NPP increases with the ongoing of the season (Figure 41); there is a good prediction overall growing season for all studied year (2004, 2005 and 2006) but not after the senescence and cutting of the herbage, that take place always at the end of June (doy 170).

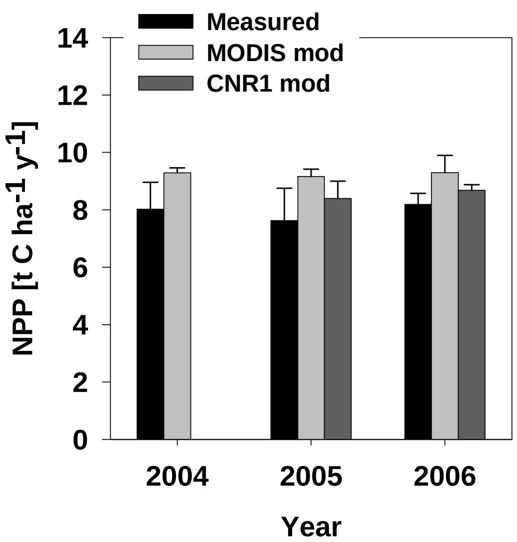

Figure 40 - Modeled NPP (mean ± standard deviation) from ground spectral relationship relationships.

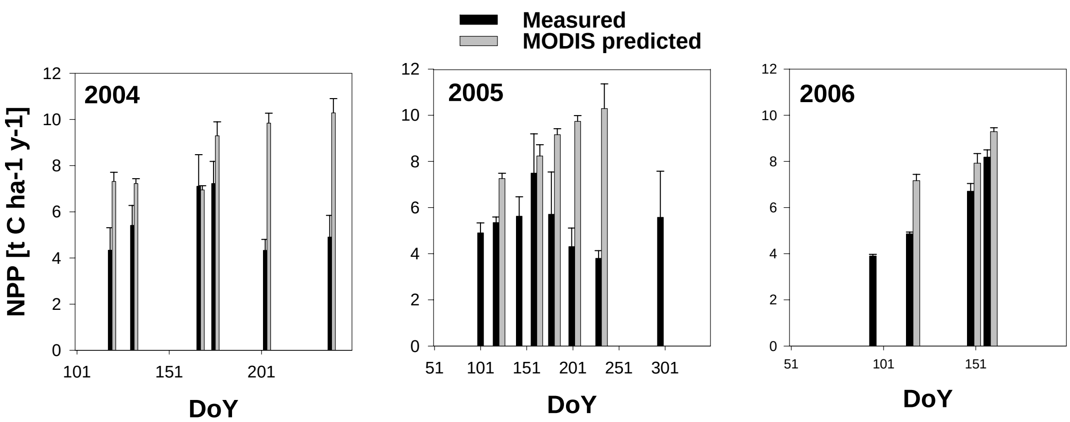

Figure 41 – Seasonal trend of modeled MODIS-NPP (mean ± standard deviation) of Amplero site for the year 2004, 2005 and 2006.

We can conclude that this method is useful to estimate the grassland total NPP over all year when the growth of vegetation is not limited by any abiotic factor as grazing, harvesting or drought. Then this method can be applied to evaluate the increment of biomass during the growth season where above ground NPP (ANPP) is equal to below ground NPP.

3.9 Carbon dioxide fluxes over Amplero grassland

3.9.1 Evaluation of eddy measurements

In order to assess the accuracy of eddy covariance measurements, half-hourly data were used for calculating a surface energy budget from April to September, period of field campaign, for all year of the interest (Figure 42).

There was a relative strong correlation between the sum of sensible heat (H) and latent heat (LE) and available energy that is the difference between the net radiation (Rn) and soil heat flux (G).

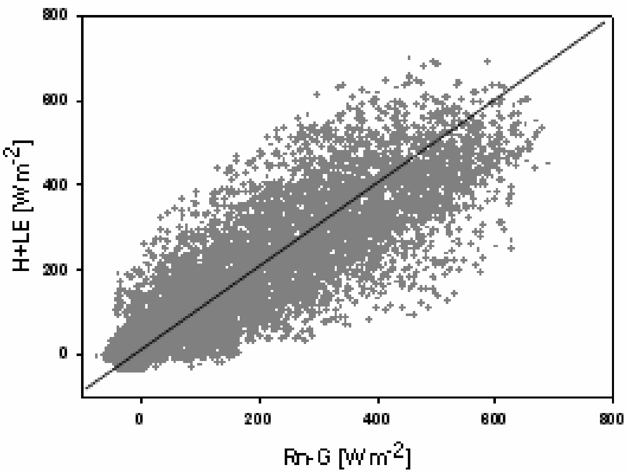

Figure 42 – Energy balance closure at Amplero site between April to September for 2005 and 2006. The line is the 1:1 slope of the panel.

We obteined a R^2 higher than 0.80 grouping all data of the three different growing season. The parameters of the relationship $H+LE = a_0 + a_1(Rn+G)$ retrieved from the linear regression from the plot in the Figure 41 are: a_1 =0.82 and a_2 =2.25. The a_1 value, which is the slope of the regression line, indicates the degree of closure of the energy balance (82%).

The slope of the relations indicated that the eddy covariance measurements underestimated sensible or/and latent heat fluxes whit a medium loss of 18% due to methodological or instrumental lacks.

3.9.2 Carbon balance and correlated radiation fluxes

The photosynthetic rates differ for the studied years (Figure 43). Considering half-hourly NEE values, the most negative average NEE among all years (2005 and 2006) is -5.07 µmol m^{-2} s^{-1}, observed in 2005 while the lowest is -2.01 µmol m^{-2} s^{-1} in 2006. These trends are typical for Mediterranean grassland ecosystems with a water deficit during the growing season and a prolonged drought during summer (Xu *et al.*, 2004).

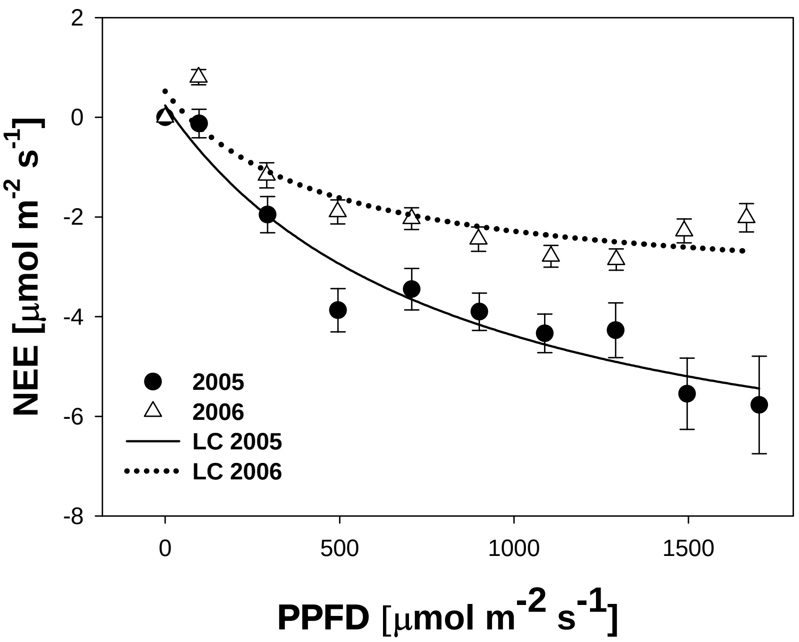

Figure 43 - Light curve (LC) response of Amplero grassland for 2004, 2005 and 2006.

Table 22 - Light curve response parameters of Amplero grassland.

	R^2	Y_0	As	A
2005	0.94	0.24	8.42	0.01
2006	0.82	0.53	4.07	0.01

PPFD explains more than 90 % of the variability in NEE in spring and autumn, when soil water availability was high, but not during the summer drought. This is very clear in studied years when the rainfall and then soil water content were not limiting (annual precipitation 681 and 742 in 2005 and 2006, respectively, see par.3.1). The fraction of variability in NEE explained by PPFD varies markedly during the growing season (Wohlfahrt *et al.*, 2008) as reported in Figure 44. The uppermost panels of Figure 44 reports the R^2 values of the correlation between NEE and PPFD using the Ruimy *et al.* (1995) equation (light curve response) and fitted on weekly time windows. The fraction of variability in NEE explained by PPFD was also affected by management, decreasing in response to mowing or grazing (Wohlfahrt, 2008). Alpine meadows were not affected by summer drought while in the Mediterranean mountainous grassland the effect of clipping/harvesting or grazing is added to that of summer drought and then not clearly distinguishable.

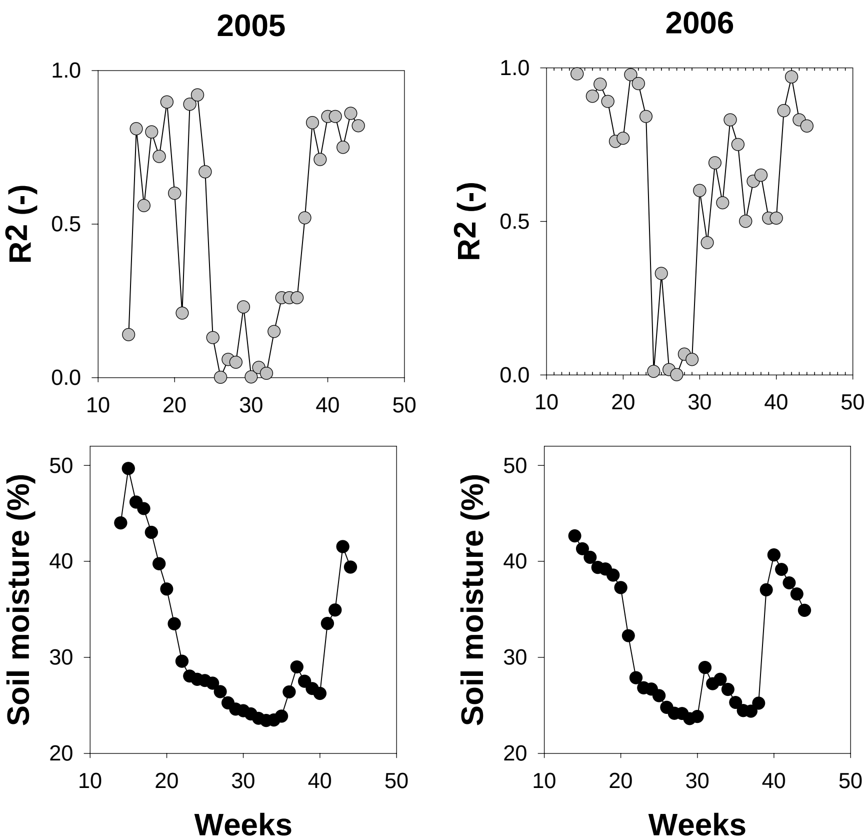

Figure 44 - Weekly values (2005 and 2006) of the correlation coefficient (R^2) for PPFD versus NEE (weekly light response curve), and weekly soil water content (RSWC).

The large differences in maximum weekly coefficient of light curve seem to be not accompanied by proportionally higher respiration rates as showed in Figure 45 and 46.

Maximum of daily NEE takes place later in 2006 than in 2005 when occurs roughly 3 weeks before. Moreover, maximum absorption of NEE has similar mean values in the two years.

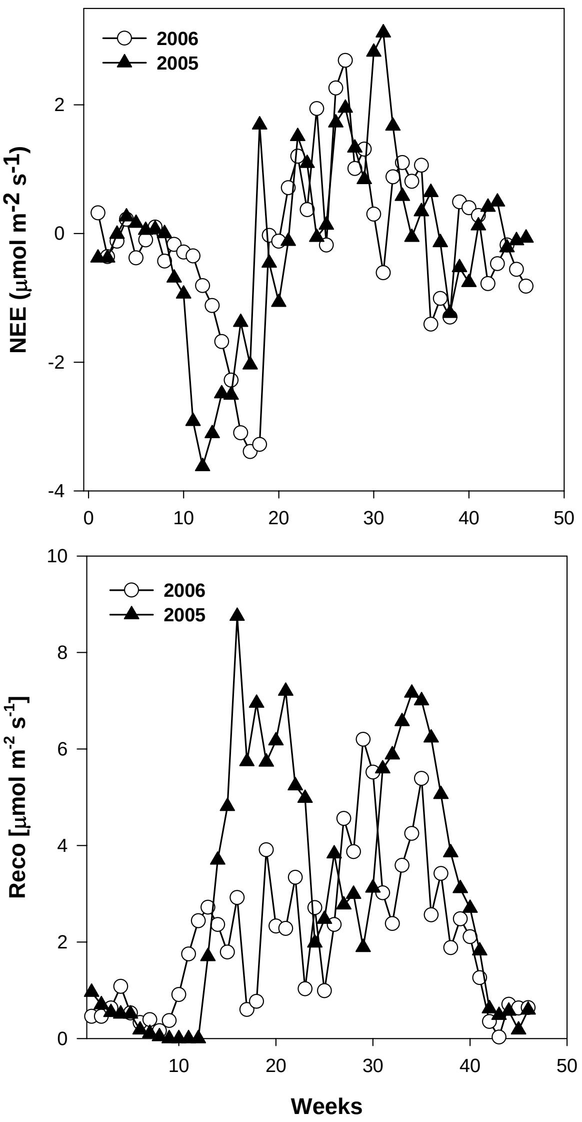

Figure 45 – Weekly mean trends of NEE and Reco (in μmol m_{-2} s^{-1}) for 2005 and 2006

Ecosystem respiration is always nearly to zero at the beginning of the season when snow felt down and the soil was frozen. The respiration rate in 2005 is larger than in 2006 mainly from March until the cutting period that corresponds to the maturity of grass. In 2006 respiration peaks in August reflects the rapid increase of soil moisture due to summer sporadic rainfall. This respiration pattern is typical of the Mediterranean ecosystems where soil temperature stimulates respiration in not water limited conditions (Figure 47) until the developing of drought inhibits the temperature effect on the rise of respiration rates.

Finally in these two years Amplero grassland is a weak sink of carbon (Table 23 and Figure 46), as happens for the most part of European grasslands.

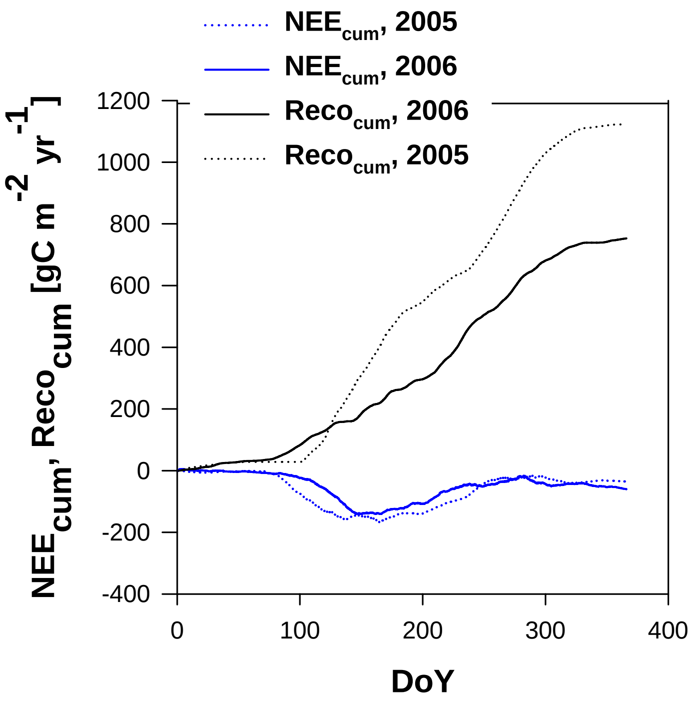

Figure 46 – Weekly mean trends of NEE and Reco (in μmol m_{-2} s^{-1}) for 2005 and 2006

Table 23 – NEE, Reco, GPP cumulated values (in g C m^{-2} yr^{-1}) overall year and over spring-summer period (from April to August) of 2005 and 2006.

	NEE	Reco	GPP
2005	-34.6	1125.2	1159.8
2006	-60.6	753.2	813.8
2005 (April-August)	-14.2	656.2	670.4
2006 (April-August)	-32.8	427.8	460.6

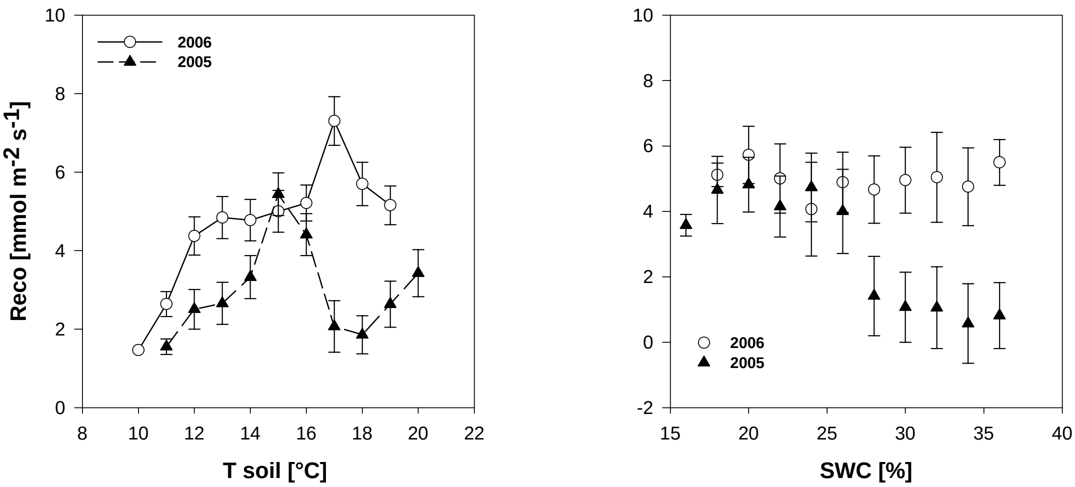

Figure 47 – Response of R_{eco} (in μmol m_{-2} s^{-1}) to soil temperature and SWC classes from April to August of 2005 and 2006.

3.9.3 NEE and GPP estimation from NDVI

Because of CNR1 radiometer acquired continuously NDVI values, this sensors was selected for predicting CO_2 in term of daily Net Ecosystem Exchange (here indicated as NEE). Daily data collected by CNR1 from April to August in 2005 and 2006 was analyzed. Over all the studied periods only the relation between NDVI-CNR1 and NEE showed a good R^2 value (0.62). The goodness of this relationship is already confirmed by considering the growing season period from April to June of 2005 (Figure 48). This relation, in fact, can explain 60 % of the variation of NDVI in 2005 while only 29 in 2006 and its shapes are linear and have the following equations:

$NEE_{2005}=13.35 - 20.28*NDVI_{CNR1}$ $(R^2=0.60, p<<0.01)$

$NEE_{2006}=9.12 - 13.80*NDVI_{CNR1}$ $(R^2=0.29, p<<0.01)$

The limitation on this application of NDVI in 2006 could be linked to the effect of the low values of R_{eco} during the growing season and to its fast changes (see Figure 45) in response to the precipitation in late summer that introduce an error in estimating NEE. Moreover, by eddy technique, R_{eco} is computed by nighttime CO_2 fluxes assuming that all fluxes during the night contribute the whole respiration without discrimination between autotrophic and heterotrophic respiration that happens also during the daytime. For this reason, the correct way to link radiometric measurements and photosynthetic fluxes and to minimize the effect of ecosystem respiration on CO_2 exchanges is the estimation of gross primary productivity (GPP) that is the difference between NEE and R_{eco}.

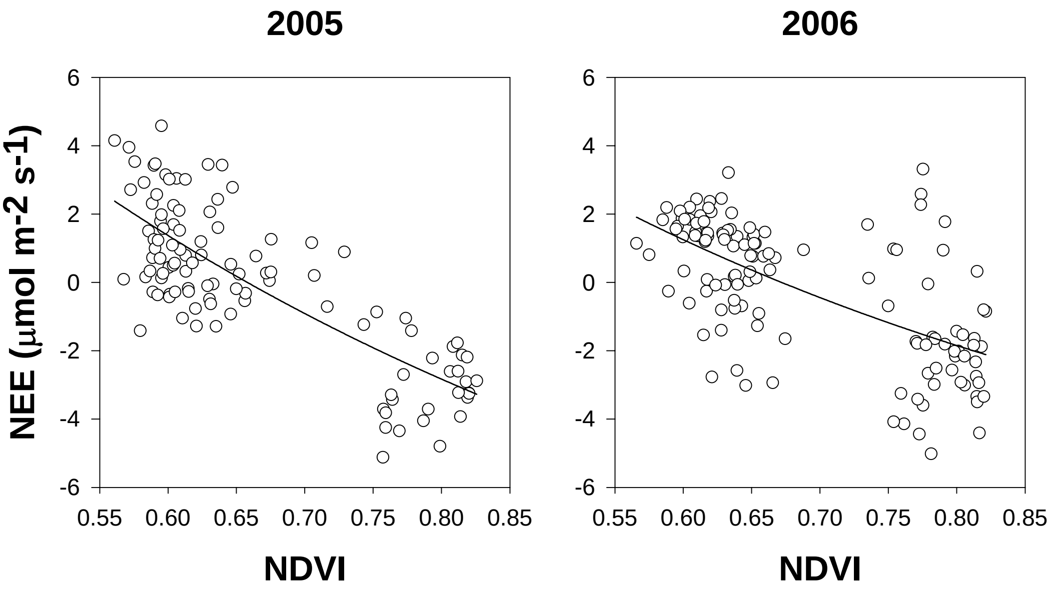

Figure 48 - Shape of correlation between several NDVI and mean daily GPP. The black circles represent FieldSpec-NDVI, azure are MODIS-NDVI and green are CRN1-NDVI.

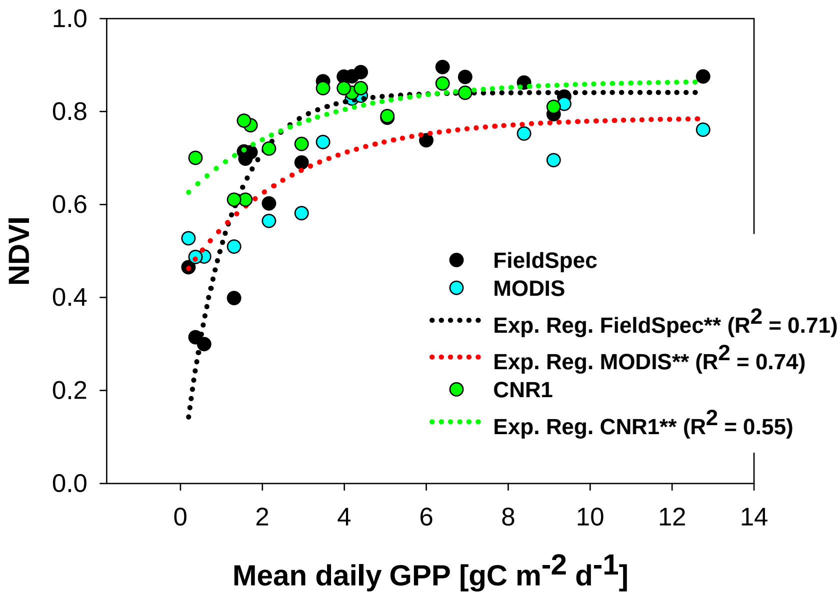

Figure 49 - Shape of correlation between several NDVI and mean daily GPP. The black circles represent FieldSpec-NDVI, azure are MODIS-NDVI and green are CRN1-NDVI.

Overall periods of measurements, there are not significant relationships between daily mean NDVI and GPP but this relation become more consistent considering only daily data of NEE taken during the date of spectral field surveys (Figure 49). Moreover using NDVI derived from MODIS images and from CNR1 the relation is also good (R^2 value of 0.74, 0.74 and 0.55 for FieldSpec, MODIS and CNR1, respectively). The shapes of the relationships are exponential and saturate between 4 g C m^{-2} d^{-1} and 5 g C m^{-2} d^{-1}.

Approaching the estimation of GPP using radiometric methods it is possible to predict this variable both continuously by CNR1 radiometer and over a large area by MODIS images. Therefore, acquiring daily MODIS images of reflectance it is possible to investigate contemporaneously spatial and temporal variation of GPP improve the information on grassland ecosystems, in particular in all those areas that are impractically and where is not possible to mount an eddy tower. In order to evaluate the potentiality of this method it would be great to apply it in the areas where there are some topographic limitation as the presence of mountain that affect the acquisition of sensor images.

Chapter IV
Conclusions

Different management activities, done during the same meteorological conditions, cause a broad variation in biomass dymamics. Cutting/harvesting and grazing have the same effects on the ecosystem reducing the quantity of available herbage and blocking the grassland growth. In this study we analyzed the biometric parameter of three different landuses: meadow (managed by harvesting and grazing that is the typical management in Amplero and in Appenines areas), natural (areas to exclude all external impacts) and pasture (used for animal grazing).
Aim of this study has been the characterization of biometric parameters, NPP and carbon fluxes using the following independent approaches: agronomic destructive sampling inventory, hyperspectral radiometric measurements, satellite images processing and micrometeorological methods.

Natural grassland has the highest peak of AGB_{live} (408.9 ± 86.7 g m^{-2}), while meadow and pasture have a similar and lower values, 218.1 ± 35.9 g m^{-2} and 275.1 ± 23.2 g m^{-2}, respectively. Therefore, NPP of the meadow and the pasture can be comparable confirming that cutting and harvesting have the same effect on NPP.

With the ongoing of the growing season, the reflectance in the near infrared range decreases while increases in the visible portion of the spectrum due to the changes in the phenological status of vegetation and to the incoming summer drought, that is typical in Mediterranean areas. NDVI, SR, EVI and WBI, both from MODIS and from FieldSpec bands, provide a reliable estimation of percentage of dead biomass over all the spring-summer season, while only SR and WBI correlate with the live biomass content. Moreover, it is demonstrated that these relationships are strictly dependent on grassland land uses and for this reason can be performed for distinguishing the vegetation phenological status and characteristics of each type of managements present in the whole grassland area of Amplero. In particular, the relationship between the live part of aboveground biomass can be used to separate different managements.

Finally, WBI show a significant exponential correlation with total biomass both during growing and senescence of grasslands. Consequently, this approach is a good and low cost method to estimate live and dead biomass of grassland without make destructive field measurements.

Simple NPP-model here proposed, based on the direct estimation of NPP from NDVI, is useful to estimate the grassland total NPP over all year when the growth of vegetation is not limited by any abiotic factor as grazing, harvesting or drought and can be applied to evaluate the increment of biomass during the growing season

Approaching the estimation of GPP using radiometric methods it is possible to predict this variable both continuously and locally by CNR1 radiometer both discontinuously but on a larger area by MODIS images. Therefore, acquiring daily MODIS images of reflectance it is possible to investigate contemporaneously spatial and temporal variation of GPP and to improve the information on grassland ecosystems, in particular in those areas that are impractically and where is not possible to install an eddy tower.

Bibliography

Aalto, T., Ciais, Ph., Chevillard, A., Moulin,C. (2004) Optimal determination of the parameters controlling biospheric CO2 fluxes over Europe using eddy covariance fluxes and satellite NDVI measurements. *Tellus,* **56 (B),** 93–104.

Asner, G.P., Scurlock, J. M. O., Hicke, A. J. (2003) Global synthesis of leaf area index observations: implications for ecological and remote sensing studies. *Global Ecology & Biogeography,* **12,** 191–205.

Asrar, J.K., Hipps, L.E., Kanemasu, E.T. (1984) Estimating absorbed photosynthetic radiation and leaf area index from spectral reflectance in wheat. *Agronomy J.,* **76,** 300-306.

Aubinet, M., Grelle, A., Ibrom, A., Rannik, Ü., Moncrieff, J., Foken, T., Kowalski, A.S., Martin, P.H., Berbigier, P., Bernhofer, C., Clement, R., Elbers, J., Granier, A., Grünwald, T., Morgenstern, K., Pilegaard, K., Rebmann, C., Snijders, W., Valentini, R., Vesala, T. (2000) Estimates of the annual net carbon and water exchange of forests: the EUROFLUX methodology. *Advances in Ecological Research,* **30,** 113-175.

Baldocchi, D. (2003) Assessing the eddy covariance technique for evaluating carbon dioxide exchange rates of ecosystems: past, present and future. *Global Change Biology,* **9,** 479-492.

Baldocchi D.D., H.B.B., Mayers T.D. (1998) Measuring biosphere-atmosphere exchange of biologically related gases with micrometeorological methods. *Ecology,* **69,** 1331-1340.

Baldocchi, D.D., Hicks, B.B., Mayers, T.D. (1998) Measuring biosphere-atmosphere exchange of biologically related gases with micrometeorological methods. *Ecology,* **69,** 1331-1340.

Baret, F., & Guyot, G. (1991) Potentials and limits of vegetation indices for LAI and APAR assessment. *Remote Sensing of Environment,* **35,** 161 − 173.

Baret, F., Jacquemoud, S., Guyot, G., Leprieur, C. (1992) Modeled analysis of the biophysical nature of spectral shifts and comparison with information content of broad bands. *Remote Sensing of Environment,* **41,** 133-142.

Becker, F., & Choudhury, B. J. (1988) Relative sensitivity of normalized difference vegetation index (NDVI) and microwave polarization difference index (MPDI) for vegetation and desertification monitoring. *Remote Sensing of Environment,* **24,** 297 − 311.

Belelli Marchesini, L.P., D., Reichstein, R., Vuichard, N., Tchebakova, N., Valentini, R. (2007) Carbon balance assessment of a natural steppe of southern Siberia by multiple constraint approach. *Biogeosciences,* **4,** 581–595.

Berninger, F., Gianelle, D., Bahn, M., Wohlfahrt, G., Susiluoto, S., Campbell, C., Anderson, M., Sutton, M., Christensen, T., Garcia-Pausas, J., Gimeno, C., Sanz, M-J., Dore, S., Rogiers, N., Furger, M., Eugster, W., Balzarolo, M., Sebastia, T., Tenhunen, J., Stazewski, T., Cernusca, A. (2007, submitted) Management and site effects on carbon balances of European mountain grassland ecosystems. *Ecosystems*.

Bolle, H.-J.E., M., Koslowsky, D., Maselli, F., Melia Miralles, J., Menenti, M., Olesen, F.-S., Petkov, L., Rasool, S.I., Van de Griend, A. (Eds.) (2006) Mediterranean Land-surface Processes Assessed from Space. Series: Regional Climate Studies. Radiative processes of the surface-atmosphere system, pp. 137 - 189. *Springer, New York*.

Bradford, J.B., Hicke, J.A., Lauenroth, W.K. (2005) The relative importance of light-use efficiency modifications from environmental conditions and cultivation for estimation of large-scale net primary productivity. *Remote Sensing of Environment,* **96,** 246 – 255.

Campbell, I. (2000) CNR1 Radiomater, Instruction manual. *Campbell Scientific, Logan, Utah*.

Carter, G.A. (1991) Primary and secondary effects of water content on the spectral reflectance of leaves. *Am. J. Bot.,* **78,** 916-924.

Cernusca, A., Tappeiner, U., Bayfield, N. (1999) *Land-Use changes in European Mountain Ecosystems. ECOMONT – Concept and results.* Ed. Blackwell, Berlin.

Chiti, T. (2007) Soil organic matter characterization of alpine forests, grasslands, and mediterranean forests of italy, by the use of ^{13}C NMR spectroscopy and isotopes C analysis. *Phd thesis, University of Florence, Italy*.

Clark, R.N. (1999) *Spectroscopy of rocks and minerals, and principles of spectroscopy. In Manual of Remote Sensing: Remote Sensing for Earth Sciences.* Ed. A.N. Rencz, New York, pp. 3-58.

Cramer, W., D.W. Kicklighter, A. Bondeau III, G. Churkina, B. Nemry. A., Ruimy. A. Schloss, J. Kaduk, et al. (1999a) Comparing global models of terrestrial net primary productivity (NPP): Overview and key results. *Global Change Biology,* **5 (Supplement),** 1–15.

Cramer, W., Field., C.B. (1999b) Comparing global models of terrestrial net primary productivity (NPP): Introduction. . *Global Change Biology,* **5 (Supplement)**.

Deering, D.W. (1978) Rangeland reflectance characteristics measured by aircraft and spacecraft sensors. . *PhD Thesis, Texas A&M Univ. College Station, Texas, USA.*

Elvidge, C.D., Chen, Z. K. (1995) Comparison of broad-band and narrow-band red and near-infrared vegetation indices. *Remote Sensing of Environment,* **54,** 38-48.

Elvidge, C.D., Chen, Z.K., Groeneveld, D.P. (1993) Detection of trace quantities of green vegetation in 1990 AVIRIS data. *Remote Sensing of Environment,* **44,** 271-279.

Elvidge, C.L. (1990) Visible and NIR reflectance characteristics of dry plant materials. *International Journal of Remote Sensing,* **2,** 1775-1795.

Field, C.B., and J.R. Ehleringer (1993) *Questions of scale. In Scaling Physiological Processes: Leaf to Globe.* . Ed Ehleringer, J.R. & Field, C.B., Academic Press, San Diego, pp. 1-4.

Field, C.B., Gamon, J.A., Peñuelas, J. (1994) *Remote sensing of terrestrial photosynthesis. In Ecophysiology of Photosynthesis, Ecological Studies.* Ed by Schulze E.D., Caldwell MM, pp. 511-527.

Field, C.B., Randerson, J. T., Malmstrom, C. M. (1995) Global net primary production: Combining ecology and remote sensing. *Remote Sensing of Environment,* **51,** 74– 88.

Filella, I., Penuelas J., Llorens L., Estiarte M. (2004) Reflectance assessment of seasonal and annual changes in biomass and CO_2 uptake of a Mediterranean shrubland submitted to experimental warming and drought. *Remote Sensing of Environment,* **90,** 308–318.

Flanagan, L.B., Wever, L. A., Carlson, P. J. (2002) Seasonal and interannual variation in carbon dioxide exchange and carbon balance in a northern temperate grassland. *Global Change Biology,* **8,** 599-615.

Frank, A.B., Dugas, W.A. (2001) Carbon dioxide fluxes over a northern, semiarid, mixed-grass prairie. *Agricultural and Forest Meteorology,* **108,** 317–326.

Gamon, J.A., Penuelas, J., Field, C.B. (1992) A narrow-waveband spectral index that tracks diurnal changes in photosynthetic efficiency. *Remote Sensing of Environment,* **41,** 35-44.

Gamon, J.A., Qiu, H. (1999) *Ecological applications of remote sensing at multiple scales. In F. I. Pugnaire and F. Valladares (Eds.), Handbook of Functional Plant Ecology.* pp. 805–846. New York: Marcel Dekkerm.

Gao, B.-C. (1996) NDWI - A normalized difference water index for remote sensing of vegetation liquid water from space. *Remote Sensing of Environment,* **58,** 257-266.

Gianelle, D., Vescovo, L. (2007) The determination of GR in grasslands using spectral reflectance. Methods and ground measurements. *International Journal of Remote Sensing,* **28,** 931 - 942.

Gill, R.A., Jackson, R. B. (2000) Global patterns of root turnover for terrestrial ecosystems. *New Phytologist,* **147,** 13 – 31.

Gill, R.A., Kelly, R. H., Parton, W. J., Day, K. A., Jackson, R. B., Morgan, J. A., Scurlock, J. M. O., Tieszen, L. L., Castle, J. V., Ojima, D. S., Zhang, X. S. (2002) Using simple environmental variables to estimate belowground productivity in grasslands. *Global Ecology & Biogeography,* **11,** 79–86.

Gilmanov, T.G., Soussana, J.-F., Aires, L., Allard, V., Ammann, C., Balzarolo, M., Barcza, Z., Bernhofer, C., Campbell, C. L., Cernusca, A., Cescatti, A., Clifton-Brown, K. J., Dirks, M., Dore, S., Eugster, W., Fuhrer, J., Gimeno, C., Gruenwald, T., Haszpra, L., Hensen, A., Ibrom, I., Jacobs, A.F.G., Jones, M. B., Lanigan, G., Laurila, T., Lohila, A., Manca, G., Marcolla, B., Nagy, Z., Pilegaard, K., Pinter, K., Pio, C., Raschi, A., Rogiers, N., Sanz, M. J., Stefani, P., Sutton, M., Tuba, Z., Valentini, R., Williams, M. L., Wohlfahrt, G (2007) Partitioning European grassland net ecosystem CO2 exchange into gross primary productivity and ecosystem respiration using light response function analysis. *Agriculture, Ecosystems and Environment,* **121,** 93-120.

Gitelson, A.A. (2004) Wide dynamic range vegetation index for remote quantification of biophysical characteristics of vegetation. *Journal of Plant Physiology,* **161,** 165 − 173.

Gitelson, A.A., Kaufman, Y.J., Merzlyak, M. N. (1996) Use of a green channel in remote sensing of global vegetation from EOS-MODIS. *Remote Sensing of Environment,* 289–298.

Gitelson, A.A., Kaufman, Y. J., Stark, R., Rundquist, D. (2002) Novel algorithms for remote estimation of vegetation fraction. *Remote Sensing of Environment,* **80,** 76−87.

Goetz, S.J., Prince, S.D. , Goward, S.N., Thawley, M.M., Small., J. (1999) Satellite remote sensing of primary production: an improved production efficiency modeling approach. *Ecological Modeling,* **122,** 239–255.

Gong, P., Pu, R., Biging, G. S., Larrieu, M. R. (2003) Estimation of forest leaf area index using vegetation indices derived from hyperion hyperspectral data. *IEEE Transactions on Geoscience and Remote Sensing,* **40,** 1355 − 1362.

Goward, S.N., & Huemmrich, K. F. (1992) Vegetation canopy PAR absorbance and the normalized difference vegetation index: as assessment using the SAIL model
Remote Sensing of Environment, **39,** 119– 140.

Grace, J. (2005) *Role of forest biomes in the global carbon balance. In The carbon balance of forest biomes. Ed by H. Griffiths, & P. G. Jarvis.*, Taylor & Francis Group,New York , pp. 19−46.

Hanna, M.M., Steyn-Ross, D.A., Steyn-Ross, M (1999) Estimating Biomass for New Zealand Pasture Using Optical Remote Sensing Techniques. *Geocarto International,* **14 (3)**.

Hastings, S.J., Oechel,W.C., Muhlia-Melo, A. (2005) Diurnal, seasonal and annual variation in the net ecosystem CO2 exchange of a desert shrub community (Sarcocaulescent) in Baja California, Mexico. *Global Change Biology,* **11,** 927–939.

Horcas, R., Rasilla, D., Fernández, F. (2001) *Temperature variations and trends in the Segura River Basin. An exploratory analysis, in Detecting and Modelling Regional Climate Change, pp. 133-142.* Brunet M.and López D. (Eds), Springer-Verlag, Berlin.

Huang, D., Knyazikhin, Y., Dickinson, R. E., Rautiainen, M., Stenberg, P., Disney, M., Lewis, P., Cescatti, A., Tian, Y., Verhoef, W., Martonchik, J. V., Myneni, R. B. (2007) Canopy spectral invariants for remote sensing and model applications. *Remote Sensing of Environment,* **106,** 106-122.

Huete, A.R. (1998) A soil-adjusted vegetation index (SAVI). *Remote Sensing of Environment,* **25,** 295 − 309.

Hui, D., Jackson, R. B. (2006) Geographical and interannual variability in biomass partitioning in grassland ecosystems: a synthesis of field data. *New Phytologist,* **169,** 85–93.

Hungate, B.A., Holland, E.A., Jackson, R.B., Chapin, F.C. III, Mooney, H.A., Field, C.B. (1997) The fate of carbon in grasslands under carbon dioxide enrichment. *Nature,* **388,** 576 – 579.

Inoue, Y., Peñuelas, J., Miyata, A., Mano, M. (2008) Normalized difference spectral indices for estimating photosynthetic efficiency and capacity at a canopy scale derived from hyperspectral and CO2 flux measurements in rice. *Remote Sensing of Environment,* **112,** 156–172.

IPCC (2000) Good Practice Guidance and Uncertainty Management in Greenhouse Gases Inventories. *Cambridge University Press, Cambridge, UK,.*

Jakomulska, A. (2003) *Field remote sensing techniques for mountains vegetation investigation. In Proceedings 3rd EARSeL Workshop On Imaging Spectroscopy* DLR, Oberpfaffenhofen, Germany. pp.483-491.

Jaksic, V., Kiely, G., Albertson, J., Oren, R., Katul, G., Leahy, P., Byrne, K. A. (2006) Net ecosystem exchange of grassland in contrasting wet and dry years. *Agricultural and Forest Meteorology,* **139,** 323–334.

Ji, L., Peters, A. J. (2007) Performance evaluation of spectral vegetation indices using a statistical sensitivity function. *Remote Sensing of Environment*, **106**.

Jones, M.B., Donnelly, A. (2004) Carbon sequestration in temperate grassland ecosystems and the influence of management, climate and elevated CO2. *New Phytologist,* **164,** 423-439.

Jordan, C.F. (1969) Derivation of leaf-area index from quality of light on the forest floor. *Ecolgy,* **50,** 663–666.

Justice, C.O., Townshend, J. R. G., Vermote, E. F., Masuoka, E., Wolfe, R. E., Saleous, N., et al. (2002) An overview of MODIS Land data processing and product status. *Remote Sensing of Environment,* **83,** 3−15.

Kaufman, Y.J., Tanré, D. (1992) Atmospherically resistant vegetation index (ARVI) for EOS-MODIS. *IEEE Transactions on Geoscience and Remote Sensing,* **30,** 261-270.

Kucera, D.L., Dahlman, R. C., Koelling, R. (1967) Total energy productivity and turnover on an cncrgy basis for tall grass prairie. *Ecolgy,* **48,** 536 - 541.

Kumar, L., Schmidt, K., Dury, S., Skidmore, A. (2002) *Imaging spectrometry. Basic principles and prospective applications. In Imaging spectrometry and vegetation science: earth and environmental science.* Ed Springer, Netherlands, pp. 111-115.

Kumar, M., Monteith, J.L. (1981) *Remote sensing of crop growth. Plants and the day light spectrum.* Ed. by Smith H., Academic Press, pp. 133-144.

Lauenroth, W.K., Hunt, H.W., Swift, D.M., Singh, J.S. (1986) Reply to Vogt et al. . *Ecology,* **67,** 580–582.

Li, J., Ren , J., Chen, Q. (1995) The research prospective of grassland resource dynamic monitoring, estimating and management by remote sensing technology. *Grassland of China,* **87(3),** 35-39.

Li, Z., Yu, G., Xiao, X., Li, Y., Zhao, X., Ren, C., Zhang, L., Fu, Y. (2007) Modeling gross primary production of alpine ecosystems in the Tibetan Plateau using MODIS images and climate data. *Remote Sensing of Environment,* **107,** 510-519.

Liu, H.Q., Huete, A. R., (1995) A feedback based modification of the NDVI to minimize canopy background and atmospheric noise. *IEEE Transactions on Geoscience and Remote Sensing,* **33,** 457-465.

Lloyd, J., Taylor, J. A. (1994) On the temperature dependence of soil respiration. *Functional Ecology,* **8,** 315-323.

Long, S.P., Garcia Moya, E., Imbamba, S.K., Kamnalrut, A., Piedade, M.T.F., Scurlock, J.M.O., Shen, Y.K., Hall, D.O. (1989) Primary productivity of natural grass ecosystems of the tropics: a reappraisal. *Plant and Soil,* **115,** 155 - 166.

Long, S.P., Jones, M.B., Roberts, M.J. (1992) *Primary Productivity of Grass Ecosystems of the Tropics and Sub-tropics.* London.

Manca, G. (2003) Analisi dei flussi di carbonio di una cronosequenza di cerro (Quercus cerris L.) dell'Italia centrale attraverso la tecnica della correlazione turbolenta. *PhD thesis, University of Viterbo, Italy*.

Martonchik, J.V., Bruegge, C. J., Strahler, A. H (2006) A review of reflectance nomenclature used in remote sensing. *Remote Sensing Reviews,* **19,** 9 − 20.

Meroni, M., Colombo, R. (2006) Leaf level detection of solar induced chlorophyll fluorescence by means of a subnanometer resolution spectroradiometer. *Remote Sensing of Environment,* **103,** 438 – 448.

Milner, C., Hughes, R.E. (1968) *Methods for the Measurement of the Primary Production of Grassland. IBP Handbook No.6.* Blackwell, Oxford.

Moon, P. (1940) Proposed standard solar radiation curves for engineering use. *J. Franklin Inst.,* **11,** 583 – 617.

Morisette, J.T., Privette, J. L., Justice, C. O. (2002) A framework for thvalidation of MODIS land products. *Remote Sensing of Environment,* **83,** 77−96.

Mutanga, O. (2004) Hyperspectral remote sensing of tropical grass quality and quantity. *Phd thesis, University of Wageningen, Netherlands*

Nagler, P.L., Daughtry, C.S.T., Goward, S.N. (2000) Plant litter and soil reflectance. *Remote Sensing of Environment,* **71,** 207-215.

Nahal, I. (1981) *The Mediterranean climate from a biological viewpoint. In Ecosystems of the World 11. Mediterranean Type Shrublands.* Ed. by Di Castri, F., Goodall, W., Specht, R.L., Elsevier Scientific Publishing Co., Amsterdam, pp. 63–72.

Nemani, R.R., Keeling, C. D., Hashimoto, H., Jolly, W. M., Piper, S. C., et al. (2003) Climate-driven increases in global terrestrial net primary production from 1982 to 1999. *Science,* **300,** 1560−1563.

Ni, J. (2004) Estimating net primary productivity of grasslands from field biomass measurements in temperate northern China. *Plant Ecology,* **174,** 217–234.

Novick, K.A., Stoy, P. C., Katul, G. G., Ellsworth, D. S., Siqueira, M. B. S., Juang, J., Oren, R. (2004) Carbon dioxide and water vapor exchange in a warm temperate grassland. *Oecologia,* **138,** 259–274.

Papale, D., Reichstein, M., Canfora, E., Aubinet, M., Bernhofer, C., Longdoz, B., Kutsch, W., Rambal, S.. Valentini, R., Vesala, T., Yakir, D. (2006) Towards a more harmonized processing of eddy covariance CO2 fluxes: alogorithms and uncertainty estimation. *Biogeosciences,* **3,** 571–583.

Parizek, B., Rostagno, C. M., & Sottini, R. (2002) Soil erosion as affected by shrub encroachment in northeastern Patagonia. *Journal of Range Management,* **55,** 43– 48.

Paruelo, J.M., Epstein, H. E., Lauenroth, W. K., Burke, I. C. (1997) ANPP estimatres from NDVI for the Central grassland region of the United States. *Ecology,* **78,** 953–958.

Peñuelas, J., Filella, I. (1998) Visible and near-infrared reflectance techniques for diagnosing plant physiological status. *Trends in Plant Science,* **3,** 151–156.

Peñuelas, J., Inoue, Y. (2000) Reflectance assessment of canopy CO2 uptake. *Int. J. Remote Sens.,* **21,** 3353−3356.

Petriccione, B., Greco, S., Tammaro, F. (1993) La vegetazione del progettato parco archeologico-naturalistico della Valle di Amplero e della Vallelonga (AQ). *Micologia e vegetazione mediterranea.* **VIII,** 137-160.

Pinty, B., Verstraete, M. M. (1992) GEMI: A non-linear index to monitor global vegetation from satellites. *Vegetatio,* **101,** 15 − 20.

Potter, C.S., Randerson, J. T., Field, C. B., Matson, P. A., Vitousek, P. M., Mooney, H. A., et al. (1993) Terrestrial ecosystem production: a process model based on global satellite and surface data. *Global Biogeochemical Cycles,* **7,** 811- 841.

Reichstein, M., Falge, E., Baldocchi, D., Papale, D., Aubinet, M., Berbigier, P., Bernhofer, Buchmann, N., Gilmanov, T., Granier, A., Gr¨unwald, T., Havr´ankov´a, K., Ilvesniemi, H., Janous, D., Knohl, A., Laurila, T., Lohila, A., Loustau, D., Matteucci, G., Meyers, T., Miglietta, F., Ourcival, J., Pumpanen, J., Rambal, S., Rotenberg, E., Sanz, M., Tenhunen, T., Seufert, G., Vaccari, F., Vesala, T., Yakir, D., and Valentini, R. (2005) On the separation of net ecosystem exchange into assimilation and ecosystem respiration: review and improved algorithm. *Global Change Biology,* **11,** 1424–1439.

Rogler, G.A., Haas, H. J. (1947) Range production as related to soil moisture and precipitation on the Northern Great Plains. *Agronomy Journal,* **39,** 378-389.

Rotondi, A., Rossi, F., Asunis, C., Cesaraccio, C. (2003) Leaf xeromorphic adaptions of some plants of a coastal Mediterranean macchia ecosystem. *J. Mediterranean Ecol.,* **4,** 25-35.

Rouse, J.W., Haas, R.H., Schell,Jr., J.A., D.W. Deering (1974) *Monitoring vegetation systems in the Great Plains with ERTS. p. 309-317. In Proc. ERTS-1 Symp., 3rd, Greenbelt, MD. 10-15 Dec. 1973. Vol. 1. NASA SP-351. NASA, Washington, DC.* .

Ruimy, A., Saugier, B., Dedieu, G. (1994) Methodology for the estimation of terrestrial net primary production from remotely sensed data. *Journal of Geophysical Research,* **99,** 5263– 5283.

Running, S.W., Nemani, R. R., Heinsch, F. A., Zhao, M., Reeves, M., Hashimoto, H. (2004) A continuous satellite-derived measure of global terrestrial production. *Bioscience,* **54,** 547−560.

Sala, O.E., Biondi, M.E., Lauenroth, W.K. (1988) Bias in estimates of primary production: an analytical solution. *Ecological Modelling,* **44,** 43–55.

Schlesinger, W. (1977) Carbon balance in terrestrial detritus. *Annual Review of Ecology and Systematics,* **8,** 51 - 81.

Scurlock, J.M.O., Cramer W., Olson R.J., Parton W.J. and Prince S.D. (1999) Terrestrial NPP: towards a consistent data set for global model evaluation. *Ecological Applications,* **9,** 913-919.

Scurlock, J.M.O., Hall, D. O. (1998) The global carbon sink: a grassland perspective. *Global Change Biology,* **4,** 229–233.

Scurlock, J.M.O., Johnson, K., Olson, R. J. (2002) Estimating net primary productivity from grassland biomass dynamics measurements. *Global Change Biology,* **8,** 736-753.

Sellers, P.J., Meeson, B. W., Hall, F. G., Asrar, G., Murphy, R. E., Schiffer, R. A., et al. (1995) Remote sensing of the land surface for studies of global change: models–algorithms–experiments. *Remote Sensing of Environment,* **51,** 3 – 26.

Sims, D.A., Gamon, J.A. (1999) Estimating anthocyanin, chlorophyll, and carotenoid concentrations using hyperspectral reflectance. *Poster, Ecol. Soc. Ann. Meeting*.

Sims, D.A., Gamon, J.A. (2003) Estimation of vegetation water content and photosynthetic tissue area from spectral reflectance: a comparison of indices based on liquid water and chlorophyll absorption. *Remote Sensing of Environment,* **84,** 526-537.

Singh, J.S., Lauenroth, W.K., Sernhorst, R.K. (1975) Review and assessment of various techniques for estimating net aerial primary production in grasslands from harvest data. *Botanical Review,* **41,** 181 - 232.

Soussana, J.-F. (2007) The greenhouse gas balance of grasslands in Europe. *Agriculture, Ecosystems and Environment,* **121,** 1–4.

Soussana, J.-F., Loiseau, P., Vuichard, N., Ceschia, E., Balesdent, J., Chevallier, T., Arrouays, D. (2004) Carbon cycling and sequestration opportunities in temperate grasslands. *Soil Use and Management,* **20,** 219-230.

Tucker, C.J. (1979) Red and photographic infrared linear combinations for monitoring vegetation. *Remote Sensing of Environment,* **8,** 127-150.

Turker, C.J. (1979) Red and photographic infrared linear combinations for monitoring vegetation. *Remote Sensing of Environment,* **8,** 127-150.

Turner, D.P., Ollinger, S., Smith, M. L., Krankina, O., Gregory, M. (2004) Scaling net primary production to a MODIS footprint in support of Earth Observing System Product Validation. *International Journal of Remote Sensing,* **25,** 1961−1979.

Turner, D.P., Ritts, W. D., Cohen W. B., Gower, S. T., Running, S. W., Zhao, M., Costa, M. H., Kirschbaum, A. A., Ham, J. M. , Saleska, S. R., Ahl, D. E. (2006) Evaluation of MODIS NPP and GPP products across multiple biomes. *Remote Sensing of Environment,* **102,** 282–292.

Ustin, S.L., Jacquemoud, S., Palacios-Orueta, A., Li, L., Whiting, M.L. (2005) Remote sensing based assessment of biophysical indicators for land degradation and desertification.

Ustin, S.L., Roberts, D.A., Gamon, J.A., Asner, G.P., Green, R.O. (2004a) Using Imaging spectroscopy to study ecosystem processes and properties. *Bioscience,* **54,** 523-534.

Ustin, S.L., Roberts, D.A., Gamon, J.A., Asner, G.P., Green, R.O. (2004b) Using Imaging spectroscopy to study ecosystem processes and properties. *Bioscience,* **54,** 523-534.

Valentini, R., Matteucci, G., Dolman, A.J., Schulze, E.-D.,Rebman, C.,Moors , E.J., Granier, A., Gross, P., Jensen, N.O., Pilegaard, K., Lindroth, A., Grelle, A., Bernhofer, C., Grünwald, T., Aubinet, M., Ceulemans, R., Kowalski, A.S. , T. Vesala, et al. (2004) Respiration as the main determinant of carbon balance in European forests. *Nature,* **404,** 861–865.

Veroustraete, F., Patyn, J., Myneni, R. B. (1996) Estimating net ecosystem exchange of carbon using the normalized difference vegetation index and an ecosystem model. *Remote Sensing of Environment,* **58(1),** 115–130.

Vescovo, L. (2005) Remote sensing and grassland biophysical parameters estimation: a scaling up approach. *Phd thesis, University of Padua, Italy.*

Vescovo, L., Gianelle, D. (2006) Mapping the green herbage ratio of grasslands using both aerial and satellite-derived spectral reflectance. *Agriculture, Ecosystems and Environment,* **115,** 141–149.

Webb, E.K., Pearman, G.I., Leuning, R. (1980) Correction of flux measurements for density effects due to heat and water vapour transfer. *Quart J Roy Meteorol Soc.,* **106,** 85-100.

Weiss, A., Norman, J. (1985) Partitioning solar radiation into direct and diffuse, visible and near-infrared components. *Agricultural and Forest Meteorology,* **34,** 205 – 213.

Wilson, T.B., Meyers, T.P. (2007) Determining vegetation indices from solar and photosynthetically active radiation fluxes. *Agricultural and Forest Meteorology,* **144** 160–179.

Withing, G.J., Bartlett, D.S., Fan, S., Bawkin, P. S., and Wofsy, S. C. (1992) Biosphere/atmosphere CO_2 exchange in tundra ecosystems: community characteristics and relationships with multispectral surface reflectance. *Journal of Geophysical Research,* **97,** 16671 – 16680.

Wohlfahrt, G., Anderson-Dunn, M., Bahn, M., Balzarolo, M., Berninger, F., Campbell, C., Carrara, A., Cescatti, A., Christensen, T., Dore, S., Eugster W., Friborg T., Furger M., Gianelle D., Gimeno C., Hargreaves K., Hari P., Haslwanter A., Johansson T., Marcolla B., Milford C., Nagy Z., Nemitz, E., Rogiers, N., Sanz, M.J., Siegwolf, R.T.W., Susiluoto, S., Sutton, M., Tuba, Z., Ugolini, F., Valentini, R., Zorer, R., Cernusca, A. (2008) Biotic, abiotic and management controls on the net ecosystem CO2 exchange of European mountain grasslands. *Ecosystems, in press.*

Wylie, B.K., Johnson, D. A., Laca, E., Saliendra, N. Z., Gilmanov, T. G., Reed, B. C., Tieszen, L. L., Worstell B. B. (2003) Calibration of remotely sensed, coarse resolution NDVI to CO2 fluxes in a sagebrush–steppe ecosystem. *Remote Sensing of Environment,* **85** 243-255.

Xu, L., Baldocchi, D.D. (2004) Seasonal variation in carbon dioxide exchange over a Mediterranean annual grassland in California. *Agricultural and Forest Meteorology,* **1232,** 79-96.

Acknowledgements

I would like to thank Prof. Riccardo Valentini who has given me the possibility to do this PhD and improve my knowledge in the ecosystem science without giving up my background on Remote Sensing.

I extend my gratitude also to Prof. Paolo De Angelis, the advisor of the PhD course, for his kind assistance.

I would like also to thank all the people of the laboratory of the Forest Ecology who helped me during these three years of my research work. Special thanks to Dario Papale for urging me into Matlab programming world (Now I easily elaborate my data!).

I cannot forget the precious technical assistance of Renato Zompanti when I started this work, the constant informatics baking of Massimo Celestini and the help of Annarita Rossi and Alessandra Settimi on the administrative issues. I extend my gratitude also to Cristina Monteverdi and Monia Santini to our friendship that is beyond our work.

I extend my gratitude to my father and my sisters because with their support I realized this work and to all people who soften my permanence in Viterbo: Alessio, Alessandra, Luca, Nicolas, Lucia and Tommaso and last but not least thank to Nicola!